UNIVERSIDAD AUTÓNOMA DEL ESTADO DE MÉXICO

FACULTAD DE QUÍMICA

"ELECTROCOAGULACIÓN DE AGUAS RESIDUALES EN UN REACTOR EN FLUJO CONTINÚO"

TESIS

PRESENTA:

VIOLETA MARICRUZ GARCÍA OROZCO

DIRIGIDO POR:

DRA. GABRIELA ROA MORALES

DRA. IVONNE LINARES HERNÁNDEZ

DRA. REYNA NATIVIDAD RANGEL

AGOSTO DEL 2020

El presente trabajo de investigación se realizó en el Laboratorio de Ciencias Ambientales y el de Ingeniería del Centro Conjunto de Investigación en Química Sustentable CCIQS UAEM-UNAM a través del Proyecto.

Proyecto de la UAEM con el número 4986/2020CIB y 4967/2020 CIB

En el área de **"Calidad Ambiental"**.

En la línea de investigación **"Prevención, Control y efectos de la contaminación"**.

El presente trabajo fue registrado con el título **Electrocoagulación de aguas residuales en un reactor en flujo continúo,** ante la Secretaría de Investigación y Estudios Avanzados de la Universidad Autónoma del Estado de México con el número **DCAAM-0618**.

AGRADECIMIENTOS

A la Universidad Autónoma del Estado de México, Facultad de Química, al laboratorio de Ciencias Ambientales del Centro Conjunto de Investigación en Química Sustentable UAEM-UNAM y al Consejo Nacional de Ciencia y Tecnología (CONACYT), por el apoyo económico de la beca de manutención para estudio de posgrado bajo el CVU 626446.

A la UAEM por el apoyo al proyecto mediante los fondos de 4986/2020CIB y 4967/2020 CIB

DEDICATORIA

INDICE GENERAL

ÍNDICE DE FIGURAS

ÍNDICE DE TABLAS

RESUMEN

Aguas residuales industriales de una fábrica de chocolate que tenía las siguientes condiciones; pH ácido (4.38), con un alto contenido de materia orgánica como Demanda Química de Oxígeno (DQO) de 9566 mg/L, Demanda Bioquímica de Oxígeno (DBO_5) de 4666.97 mg/L, Índice de Biodegradabilidad (IB) de 0.49 y carbono orgánico total (COT) de 1318.7 mg/L, se trató por electrocoagulación en batch. La muestra de agua residual presenta importante contenido de nitrógeno y fósforo que podrían causar eutrofi
zación si se descarga sin tratamiento previo. En este proyecto, se propone un tratamiento por electrocoagulación solar fotovoltaica para tratar las aguas residuales utilizando aluminio, cobre y zinc como materiales anódicos. Se estudió el efecto del pH (4.38 y 7), la densidad de corriente (1.781 mA/cm^2 y 0.356 mA/cm^2) a los 60 minutos de tiempo de tratamiento. El sistema de aluminio exhibió los mejores resultados para parámetros orgánicos: la DQO logró una eficiencia de eliminación del 50%, reduciendo la DBO_5 al 39%. El IB aumentó considerablemente de 0.49 a 0.59 y el TOC disminuyó solo 26.65%. El sistema de cobre también mostró un comportamiento aceptable en la eliminación orgánica al 43% de DQO, 53% de DBO_5, 30.7% de COT y el IB fue 0.4. Y el sistema de zinc fue ligeramente menos eficiente que el cobre y el aluminio, donde la eliminación alcanzada fue de 39% DQO, 30% BOD_5 y 19% COT. El IB muestra un aumento a 0.56, mejorando la biodegradabilidad de las aguas residuales. La cuantificación y caracterización del lodo se llevó a cabo mediante Microscopía Electrónica de Barrido (SEM) y Espectroscopía de dispersión de energía (EDS). Los ahorros de energía se efectuaron utilizando un panel solar, sin embargo, se calcularon los costos asociados con el consumo energético. La Espectroscopía Infrarroja (IR) y la espectroscopía de fluorescencia demostraron la eliminación de materia orgánica y nitrogenada.

En una segunda etapa, se probó un reactor electroquímico de columna de flujo descendente, los experimentos previos mostraron que los electrodos de aluminio eliminaron una mayor concentración de DQO y materia inorgánica de un agua residual de la industria del chocolate. Las variables estudiadas fueron corriente eléctrica 1.58 A (781mA/cm^2) y 3.16 A (562 mA/cm^2) y caudal volumétrico (*Q)* (0.060 L/s y 0.032 L/s). Se encontró que el efecto conjunto de ambas variables es importante en la eliminación de DQO. El volumen de aguas residuales procesadas fue

de 6 L. La corriente continua se proporcionó desde un panel solar. La carga entregada al sistema fue regulada por un controlador de energía. Por lo tanto, la corriente eléctrica fue constante durante todo el tratamiento y esto lleva a ahorrar energía. Se observó que después de los primeros 5 minutos de tratamiento, se eliminaron 51% de DQO y 80% de color a 0.06 L/s y 3.16 A. En estas condiciones, también se eliminaron los sólidos en suspensión. Se concluye que una de las ventajas del reactor en columna de flujo descendente es que el hidrógeno producido se retiene en el sistema sin presurizarlo. Los datos resultantes fueron ajustados por un modelo Behnajady-Modirshahla - Ghanbery (BMG).

Durante la estadía en Universidad de Castilla-La Mancha (UCLM), se trabajó con el desempeño de un electrolizador, para tratar un desecho de clopiralida. El electrolizador equipado con electrodo que constan del mismo revestimiento de Diamante Dopado con Boro (DDB) depositado en diferentes sustratos (Si, Ta y Nb). Los resultados exponen grandes diferencias a pesar de usar el mismo recubrimiento. Se lograron tasas de eliminación más rápidas con electrodos Ta- y Nb-BDD. La cantidad de energía requerida para lograr la misma eficiencia de eliminación mostró grandes diferencias. Se eliminaron hasta 1.95 mg/Wh de plaguicida cuando se usó sustrato de Si, en comparación con 2.14 mg/Wh eliminados con Ta. Además, la cantidad y la fuerza de los oxidantes generados también fueron bastante diferentes. Se necesitaron 86.78 mmol de oxidantes para eliminar un gramo de plaguicida con Ta-BDD y 30.57 mmol con Si-BDD. Por lo tanto, la resistencia del electrodo es un aspecto importante que debe considerarse para obtener un diseño adecuado de sistemas de almacenamiento de energía que permitan la alimentación fotovoltaica ecológica de las tecnologías electroquímicas que utilizan baterías convencionales como refuerzo para garantizar un funcionamiento continúo.

ABSTRACT

An industrial wastewater from a chocolate factory with an acid pH (4.38), with a high content of organic matter of (COD = 9566 mg/L), Biochemical oxygen demand (BOD_5) of 4666.97 mg/L, biodegradability index (BI) of 0.49 and *Total organic carbon (*TOC) of 1318.7 mg/L, was treated by electrocoagulation in batch. The wastewater sample present important nitrogen and phosphorous content that could cause eutrophication if discharge without previous treatment. A solar-photovoltaic electrocoagulation was proposed to treat the wastewater using aluminium, copper and zinc as anodic materials. The effect of pH (4.38 and 7), current density (1.781 mA/cm^2 and 0.356 mA/cm^2) at 60 min treatment time was studied. The Aluminium system exhibited the best results for organic parameters: COD achieving 50% removal efficiency, reducing BOD_5 to 39%. The BI was increased considerably from 0.49 to 0.59 and TOC was diminished only 26.65%. Copper system also showed an acceptable behaviour in the organic removal to 43% COD, 53% BOD_5, 30.7% TOC and the BI was 0.4. And the Zinc system was slightly less efficient than copper and aluminium, where the removal achieved was 39% COD, 30% BOD_5, and 19% TOC. The BI shows an increase to 0.56, improving the biodegradability of wastewater. The quantification and characterization of sludge was carried out using Scanning Electron Microscopy (SEM) and Energy Dispersive Spectroscopy (EDS). Energy savings were reduced using a solar panel, however, energy costs associated with the use of energy were calculated. Infrared Spectroscopy (IR) and Fluorescence Spectroscopy proved the removal of organic and nitrogenous matter.

In a second stage, a down flow column electrochemical reactor was tested, previous experiments showed that the aluminium electrodes removed a higher concentration of COD and inorganic matter from the wastewater of the chocolate industry. The studied variables were electrical current 1.58 A (781mA/cm^2) and 3.16 A (562 mA/cm^2) and volumetric flowrate (0.060 L/s and 0.032 L/s). The joint effect of both variables was found to be important on COD removal. The processed wastewater volume was 6 L. The direct current was provided from a solar panel. The delivered charge to the system was regulated by an energy controller. Therefore, the electrical current was constant throughout the whole treatment and this leads to save energy. It was found that after the first 5 minutes of treatment, 51 COD% and 80% color were removed at 0.06 L/s and 3.16 A. Under these conditions the suspended solids were also removed. It was also concluded that one of the

advantages of the assessed reactor is that the produced hydrogen is retained in the system without pressurizing the system. The resulting data were fitted by a Behnajady-Modirshahla – Ghanbery Model (BMG).

During the stay at Universidad de Castilla-La Mancha (UCLM), we worked with the performance of an electrolyzer, used to treat a clopyralid waste the Electrolyzer was equipped with electrodes consisting of the same boron-doped diamond (BDD) coating deposited on different substrate (Si, Ta and Nb). The results expose great differences despite using the same coating. Faster removal rates were attained with Ta- and Nb-BDD electrodes. The amount of energy required to attain the same removal efficiency showed great differences. Up to 1.95 mg/Wh of pesticide were removed when using Si, compared to 2.14 mg/Wh removed with Ta. Furthermore, the quantity and strength of the generated oxidants were also quite different. 86.78 mmol of oxidants were needed to remove a gram of pesticide with Ta-BDD and 30.57 mmol with Si-BDD. Therefore, the electrode resistance is an important aspect that must be considered in order to get a suitable design of energy storage systems that allow the green photovoltaic powering of electrochemical technologies using conventional batteries as a booster to ensure continuous operation.

INTRODUCCIÓN

La industria alimenticia utiliza grandes cantidades de agua para la limpieza, envasar, fabricar, almacenar y manipular los alimentos, esto genera aguas residuales (Liu, 2014), que contienen contaminantes orgánicos, nutrientes y recursos energéticos (Kim, Nakhla and Keleman, 2019). La industria chocolatera produce una gran cantidad de sus productos donde en 2015 realizaron ventas mundiales de más de US $ 101 mil millones (Konstantas *et al.*, 2018). Para aguas residuales provenientes de esta industria generalmente se utilizan procesos biológicos, cuya principal desventaja es el tiempo de tratamiento, el costo energético de los aireadores y su baja eficiencia ante la presencia de compuestos refractarios (Esparza-Soto *et al.*, 2019).

En este sentido los métodos electroquímicos, específicamente la electrocoagulación (EC) permite el tratamiento de agua residual que contiene una alta concentración de materia orgánica y sólidos en suspensión, porque combina flotación, coagulación y la electroquímica de compuestos contaminantes (Moussa *et al.*, 2017). Para el tratamiento de EC se necesita un ánodo y un cátodo para llevar a cabo el tratamiento, al energizarlos el ánodo funciona como un electrodo de sacrificio que produce la electrodisolución in situ, proporcionando al sistema el agente coagulante. Los electrodos utilizados en la actualidad para este tratamiento son de aluminio, cobre, magnesio, hierro, zinc y acero inoxidable (Prajapati *et al.*, 2016; Elnenay *et al.*, 2017; Hu *et al.*, 2017; Tanner *et al.*, 2018) y en contacto con las aguas residuales conduce a productos provenientes de la hidrólisis (especies hidroxometálicas) que son efectivos en la desestabilización de contaminantes. A su vez se produce la reducción de agua en el cátodo formando burbujas de gas de hidrógeno e iones de hidróxido. Esto aumenta el pH en la solución y produce lodo en la superficie del agua y esto facilita su eliminación (Dura and Breslin, 2019).

La presente investigación desarrolló un tratamiento de electrocoagulación con diferentes materiales electrodicos (Al, Cu y Zn) energizados mediante energía fotovoltaica en batch, posteriormente se realizó la electrocoagulación con electrodos de aluminio en una columna de flujo descendente (en batch con recirculación y en continúo), produciendo una alta remoción de color, turbidez, DQO y al utilizar energía fotovoltaica se produce un ahorro de energía.

De ese modo en el capítulo I, se aborda el marco conceptual donde se presenta la afectación que produce el agua residual proveniente de una industria chocolatera, se analizan los tratamientos electroquímicos para buscar una solución a este problema, pero en especial la electrocoagulación y los beneficios que se obtienen al utilizar energía solar.

El capítulo II, presenta la justificación de la presente investigación, los objetivos y la hipótesis que ésta pretende alcanzar.

En el capítulo III, se hace referencia a la metodología utilizada en el trabajo, así como las estrategias experimentales y las técnicas utilizadas.

El capítulo IV, presenta los resultados y la discusión obtenidos en la evaluación del tratamiento de electrocoagulación con electrodos de aluminio, cobre y zinc en un reactor en batch y utilizando una columna de flujo descendente en batch con recirculación con electrodos de aluminio, los dos casos con energía fotovoltaica. Por otra parte, se realizó un análisis con electrodos DDB, depositado en diferentes sustratos (Si, Ta y Nb) para la remoción de plaguicida (clopiralida).

Finalmente, en el capítulo V, se presentan las conclusiones generales, abordando las ventajas y desventaja de los procesos evaluados.

CAPÍTULO 1. ANTECEDENTES

1. Contaminación del agua

1.1. El agua en el mundo

El agua dulce es necesaria para la paz, el desarrollo sostenible, la seguridad y el bienestar humano, se utiliza en la sociedad, en el medio ambiente y para su economía.
Para que exista vida en el planeta es indispensable de ríos, ecosistemas, los acuíferos y los lagos a su vez producen beneficios como el agua potable, la industria y el agua para la alimentación (Programa de las Naciones Unidas para el Medio Ambiente, 2017). De esto depende nuestro presente y futuro, en la alimentación y nutrición. La reducción del agua dulce y la escasez de agua son un problema para el desarrollo sostenible, esto va más en aumento por el crecimiento de la población mundial, debido al aumento de su nivel de vida, al cambio de las dietas y a por último a que se intensifiquen los cambios climáticos (FOA, 2019).

El agua es muy necesaria por esa razón existe una gran demanda mundial que se va aumentando 1% anualmente aproximadamente, esto depende del desarrollo económico, incremento de la población y el consumo. La necesidad de este recurso es notoria en la industria y el uso doméstico, la cual se eleva más rápido en estos dos sectores que en la agricultura. Aunque este último sector es el principal consumidor en el mundo. Los países con mayor demanda son aquellos que tienen economías emergentes o en desarrollo (UNESCO, 2018).

Este recurso es escaso en el mundo por varias razones entre las más importantes se encuentra la contaminación, sequía y uso descontrolados(ACNUR, 2019). Existen más de 2000 millones de personas que no cuentan con este recurso ni al saneamiento básico de ella, esto fue proclamado por la ONU, los que sufren de estas condiciones son personas de bajos recursos y representantes de grupos étnicos, ellos la recolectan a 30 minutos, utilizan pozos, manantiales no protegidos y fuente de agua superficial. Existen 10 países que aproximadamente su 20% de la población donde el servicio del agua es limitado de los cuales ocho se encuentran en África subsahariana y dos en Oceanía (ONU-OMS, 2018).

1.1.1. Lugares sin acceso al servicio de agua en México

En el 2019 con el Censo Nacional de gobiernos municipales y demarcaciones de la Ciudad de México realizado por el INEGI, existen dos mil 463 municipios de estos 25 no cuenta con el servicio de agua de la red pública en los que se encuentran Chiapas (con cuatro), Guerrero (Con tres), en el Estado de México (con uno), Oaxaca (con nueve), Puebla (con cinco) y Veracruz (con tres), también hay miles de localidades que no cuentan con este servicio al interior de los municipios (EXCELSIOR, 2020).

1.1.2. Calidad y contaminación del agua en México

Si no se cuenta con una buena calidad de agua mediante su saneamiento se expone a la población a problemas de salud como el cólera, disentería, otras diarreas, fiebre tifoidea, hepatitis A y la poliomielitis (OMS, 2019).

En México, en 2018 con respecto a los datos obtenidos por el CONAGUA donde se realizó un estudio a la red de agua superficial y a la red de agua subterránea. La red de agua superficial está compuesta por 3774 sitios de los cuales solo el 41.2% cuentan con buena calidad y de la red de agua subterránea compuesta por 1187 sitios de estos solo el 41.5% cuentan con buena calidad (CONAGUA, 2018a).

En el 2015 el INEGI en el censo Nacional de Gobiernos Municipales dentro del Módulo ambiental de agua potable y saneamiento reportó la cantidad de puntos de descarga de aguas residuales municipales sin tratamiento, Figura 1 (INEGI, 2015).

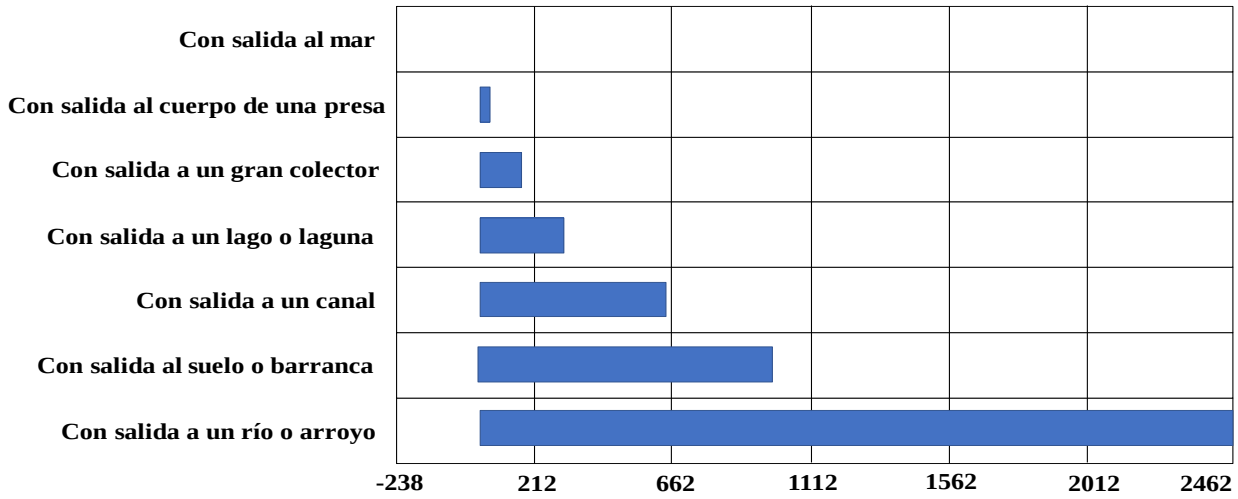

Figura 1. Cantidad de sitios de descarga de aguas residuales municipales sin tratamiento

En 2016 CONAGUA publicó resultados obtenidos desde el 2012 acerca de la calidad de la zona centro del país, sobre el Valle del Mezquital de las aguas subterráneas del acuífero. En los resultados se encontró la presencia de estreptococos fecales, coliformes totales y coliformes fecales, también cuentan con concentraciones altas de jabones y detergentes, por último, cuentan con concentraciones de arsénico, sodio, sulfatos y nitratos (Oswald, 2018).

El ser humano vierte 8 millones de toneladas de plástico cada año a los océanos**,** provocando un riesgo a la vida marina y su misma vida, produciendo una afectación en los ecosistemas naturales, contaminándolos y produciéndoles un daño irreparable (Conagua, 2018b)**.**

1.1.2.1. Industria chocolatera

Cuando se manipulan, fabrican, envasan, almacenan alimentos y se realiza la limpieza se generan aguas residuales (Liu, 2014), además los desechos de alimentos son ricos en contaminantes orgánicos, nutrientes y recursos energéticos, para su eliminación se usan tratamientos biológicos muy frecuentemente (Kim, Nakhla and Keleman, 2019).

En el 2015 se reportaron ventas mundiales de chocolate estimadas en más de US $ 101 mil millones donde se producen postres y refrigerios (Konstantas *et al.*, 2018). En estos productos se encuentra

el chocolate con leche que tiene una amplia variedad, existen productos con mayor contenido de leche, azúcar, emulsionantes, tensioactivos sólidos de cacao y grasa de la manteca de cacao 30-40% (Francis and Ramalingam, 2019; Kiumarsi *et al.*, 2020).

Las aguas residuales provenientes de una industria chocolatera carecen de compuestos peligrosos esto las hace no tóxicas, pero contienen un alto contenido de Sólidos Totales (ST), grasa, sulfatos, cloruros, fluoruros, fósforo, nitrógeno total, DBO_5, DQO y tensoactivos (Recanati, Marveggio and Dotelli, 2018). Estas concentraciones son provocadas por las grasas saturadas, polifenoles, metilxantinas, aldehídos, pirroles, mezclas de fosfolípidos, cetonas, alcoholes alifáticos, triglicéridos líquidos de manteca de cacao, glicolípidos, compuestos volátiles di y tri-terpenos, esteroles, furanos y flavonoides procedentes de la fabricación de chocolate (Patil *et al.*, 2009; Kim *et al.*, 2017; Kindlein, Elts and Briesen, 2018; Magalhães *et al.*, 2018; Toker *et al.*, 2018; Khuntia, Janardhana and Chanakya, 2020).

La industria del chocolate genera un impacto ambiental porque el agua dulce contiene de 0.87 a 0.64 g de fósforo eq/kg lo cual genera eutrofización (Konstantas *et al.*, 2018), esto produce floraciones profundas de algas, crecimiento excesivo de plantas acuáticas, aspectos estéticos negativos y desoxigenación del agua (Omwene, Kobya and Can, 2018). El impacto negativo es del 57 al 72% relacionado con leche en polvo, azúcar, harina y manteca de cacao. El chocolate con leche produce una ecotoxicidad más alta del agua dulce (133g 1.4 – DCB eq/kg), esto es ocasionado principalmente por las materias primas utilizadas (91% –96%), con más de la mitad asociada con el cultivo cacao, la leche en polvo (19% –21%) y el azúcar (11%) también tienen contribuciones notables. La ecotoxicidad del agua dulce se remonta a las liberaciones de cobre, zinc y fósforo, así como a los plaguicidas utilizados en la agricultura (Konstantas *et al.*, 2018). En 2017 se dio a conocer que existe contaminación en el cacao crudo por metales pesados (cadmio Cd, plomo Pb, níquel Ni) (Kruszewski and Obiedziński, 2018).

1.2. Normatividad

En México existen Normas Oficiales Mexicanas, que se deben seguir para descargas aguas residuales:

- NOM-001-SEMARNAT-1996; que establece los límites máximos permisibles de contaminantes en las descargas de aguas residuales en aguas y bienes nacionales (SEMARNAT, 1996a).

- NOM-002-SEMARNAT-1996; que establece lo límites máximos permisibles de contaminantes en las descargas de aguas residuales a los sistemas de alcantarillado urbano o municipal (SEMARNAT, 1996b).

- NOM-003-SEMARNAT-1997; que establece los límites máximos permisibles de contaminantes para las aguas residuales tratadas que se reúsen en servicios al público (SEMARNAT 1997; Ramos 2010).

Para tener una buena calidad de agua y cumplir con las NOM anteriores, se le realizan diferentes tratamientos al agua residual.

1.3. Tratamiento de aguas residuales

La calidad de las aguas residuales se mejora mediante su tratamiento, que consiste en aplicar sistemas primarios, secundarios y terciarios (física, química o biológica) como se muestra en la Figura 2, estos se aplican dependiendo de la calidad en la que se encuentra el agua residual (Zhang *et al.*, 2020).

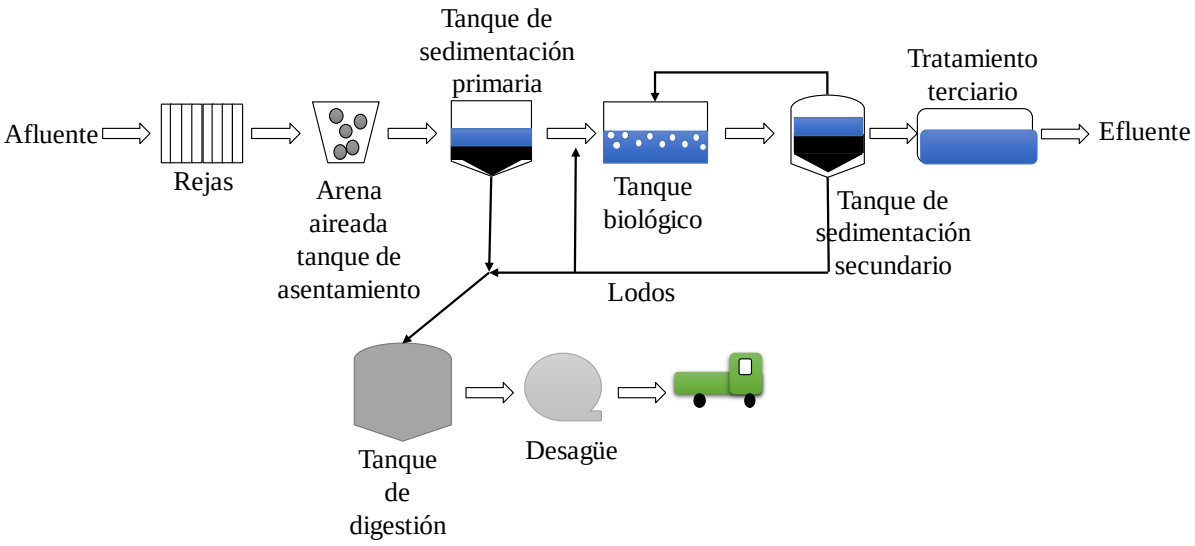

Figura 2. Implementación de los diferentes tratamientos de agua (Zhang *et al.*, 2020)

Para realizar un tratamiento de aguas residuales, se hace su recolección y envía a una planta de tratamiento donde se someten las aguas a diversos procesos. La mayoría de las plantas tratadoras tratan grandes volúmenes, por esa razón los procesos se llevan a cabo en flujo continúo (Mareddy, 2017).

1.3.1. Tratamiento primario

El tratamiento primario es el tratamiento de aguas residuales municipales que separa físicamente los sólidos grandes (escombros grandes, como ramas y llantas) del agua residual mediante una rejilla metálica. El siguiente paso es utilizar la pantalla en movimiento para filtra elementos pequeños como pañales y botellas, después de pasar por esta y de un breve tiempo de residencia (τ) en un tanque de arena provocan que la arena y la grava se asienten. El agua residual con una corriente se bombea al tanque de sedimentación primario (tanque de sedimentación o clarificador), en este se lleva a cabo la suspensión de aproximadamente la mitad de los sólidos orgánicos que se depositan en el fondo en forma de lodo (lodo primario). Esto no elimina eficientemente a los patógenos microbianos del efluente en el proceso primario (Gerba and Pepper, 2019).

Recientemente es utilizada la flotación por aire disuelto que elimina los sólidos en suspensión de las aguas residuales para la sedimentación primaria. Las burbujas de aire resultantes que se forman

son unidas a las partículas de flóculo y a los sólidos en suspensión. Para producir los flóculos por lo regular se agregan coagulantes a las aguas residuales antes del tanque flotación por aire disuelto. Ellos eliminan los sólidos suspendidos más rápidamente que la sedimentación primaria convencional (Gerba and Pepper, 2019). En la Figura 3 se muestran tratamientos físicos (Ameta, 2018).

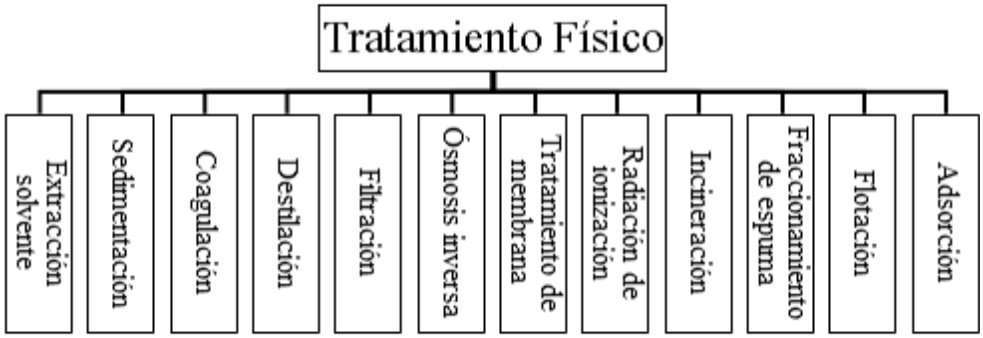

Figura 3. Tratamientos Físicos que se utilizan para la eliminación de solidos suspendidos que se encuentran en aguas residuales (Ameta, 2018)

1.3.2. Tratamiento secundario

El tratamiento secundario (tratamiento biológico) de aguas residuales pueden ser aerobios y anaerobios, eliminan los compuestos orgánicos solubles y los sólidos en suspensión que no fueron removidos con el tratamiento primario. Los tratamientos biológicos pueden eliminar 85-90% de DBO_5 y Sólidos Suspendidos Totales en una solución (SST). También son capaces de proporcionar una eliminación de nutrientes y compuestos orgánicos (Qasim and Zhu, 2017). En la Figura 4 se muestran tratamientos biológicos (Ameta, 2018).

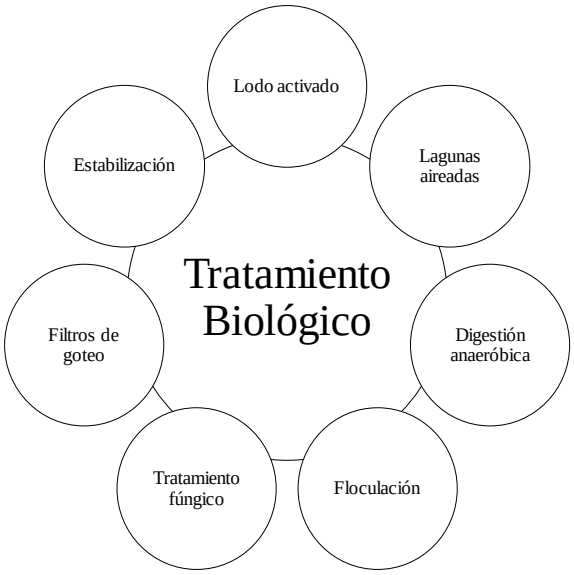

Figura 4. Tratamientos Biológicos o Secundarios para aguas residuales (Ameta, 2018)

1.3.3. Tratamiento terciario

El tratamiento terciario es también una técnica que mejora la calidad del agua después de un tratamiento de aguas residuales tradicional por lo regular se aplica en países industrializados para ayudar con la descomposición microbiológica, enzimática y la biodegradación, favorece la eliminación de sustancias orgánicas e inorgánicas residuales y en algunos casos sustancias refractarias (Muralikrishna and Manickam, 2017). También se han utilizado para la eliminación de diversos contaminantes de las aguas residuales. En estos tratamientos se encuentra los procesos avanzados de oxidación como la ozonización, Fenton y foto-Fenton, los procesos de H_2O_2 / UV, etc. (Ramalho, 2013), en la Figura 5 se muestran ejemplos de tratamientos químicos (Ameta, 2018).

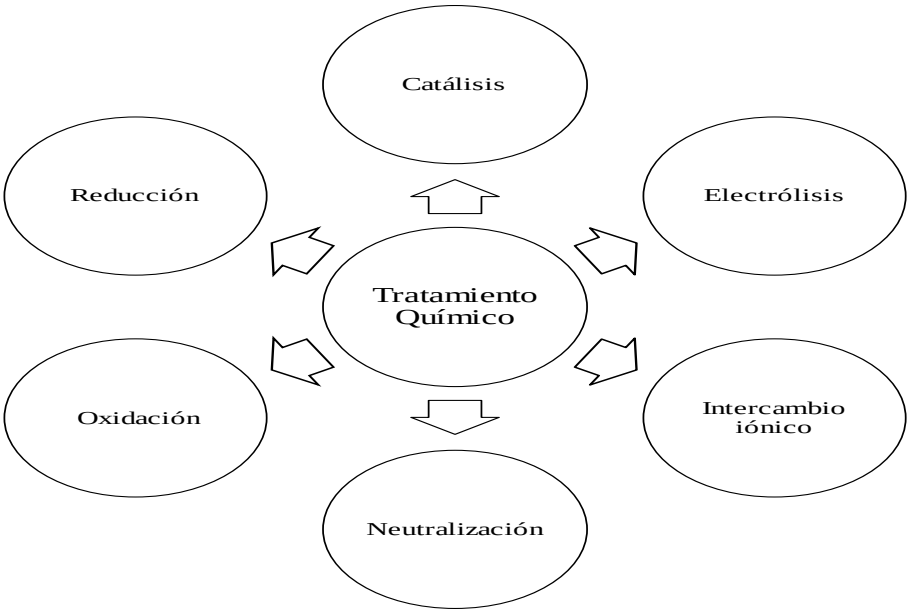

Figura 5. Tratamientos Químicos o Terciarios para aguas residuales (Ameta, 2018)

1.4. Procesos de oxidación avanzada (POAs)

La industrialización y la contaminación ambiental han permitido desarrollar tecnologías de tratamiento avanzadas, higiénicas y respetuosas con el medio ambiente. La mayoría de los procesos que realizan para mejorar la calidad del agua, sin embargo, tienen de limitación sus fuentes de energía (Ameta, 2018).

En los últimos 25 años, se está desarrollando una gran cantidad de procesos de oxidación avanzados (POAs), que incluyen tecnologías químicas, electroquímicas, fotoquímicas y fotoelectroquímicas (Brillas, 2020). Los POAs, están enfocados al tratamiento de aguas residuales que contienen contaminantes orgánicos, tóxicos, refractarios, no biodegradables, contaminantes emergentes como toxinas, plaguicidas, colorantes y contaminantes nocivos, etc. (Ma *et al.*, 2020;Ameta, 2018; Li *et al.*, 2019), presentes en aguas de origen municipal, aguas residuales textiles, aguas residuales de curtidoras, lixiviados de vertederos, aguas residuales farmacéuticas, efluente de refinería de petróleo, en especial las aguas residuales compuestas, de mataderos, de bodegas, de autolavados, etc.(Babu *et al.*, 2019).

La remoción es mediante la generación *in situ* de oxidantes potentes y no selectivos como el ozono (O_3), y los radicales superóxido (O_2^- •) hidroperoxilo (HO_2•) y sulfato (SO_4^- •) (Pirsaheb, Hossaini and Janjani, 2020; Wang and Zhuan, 2020), estos tratamientos generalmente usan los radicales hidroxilos (•OH) por su alto poder de oxidación (Hama Aziz, 2019). El tratamiento de agua se lleva a cabo a temperatura y presión cercanas a la temperatura ambiente que implican la generación de •OH en cantidad suficiente para llegar a descontaminar el agua (Gautam, Kumar and Lokhandwala, 2019). Con los •OH se oxidan la mayoría de los compuestos orgánicos sin tener en cuenta ninguna restricción de clases o grupos específicos de los compuestos (Cai *et al.*, 2020). El mecanismo de producción de •OH depende en gran medida de la técnica utilizada de los POAs (Ma *et al.*, 2020) y llegan a la mineralización completa de contaminantes, esto ocurre de forma no selectiva. Los contaminantes orgánicos los remueven por deshidrogenación, reacción redox y reacciones de hidroxilación (Babu *et al.*, 2019).

La combinación de los POAs, se realiza para ayudar a maximizar la producción de •OH y esto puede proporcionar una mayor eficiencia de degradación, que los procesos individuales (Hama Aziz, 2019). Estas combinaciones son importantes para evitar la aparición de especies refractarias y para producir mejor rendimiento de estos procesos (Mazivila *et al.*, 2019). En la Figura 6 se muestran diferentes POAs que utilizan •OH para la remoción de contaminantes, la velocidad de reacción entre •HO y moléculas orgánicas generalmente alcanza 10^6-10^9 $mol^{-1}s^{-1}$(Li *et al.*, 2019).

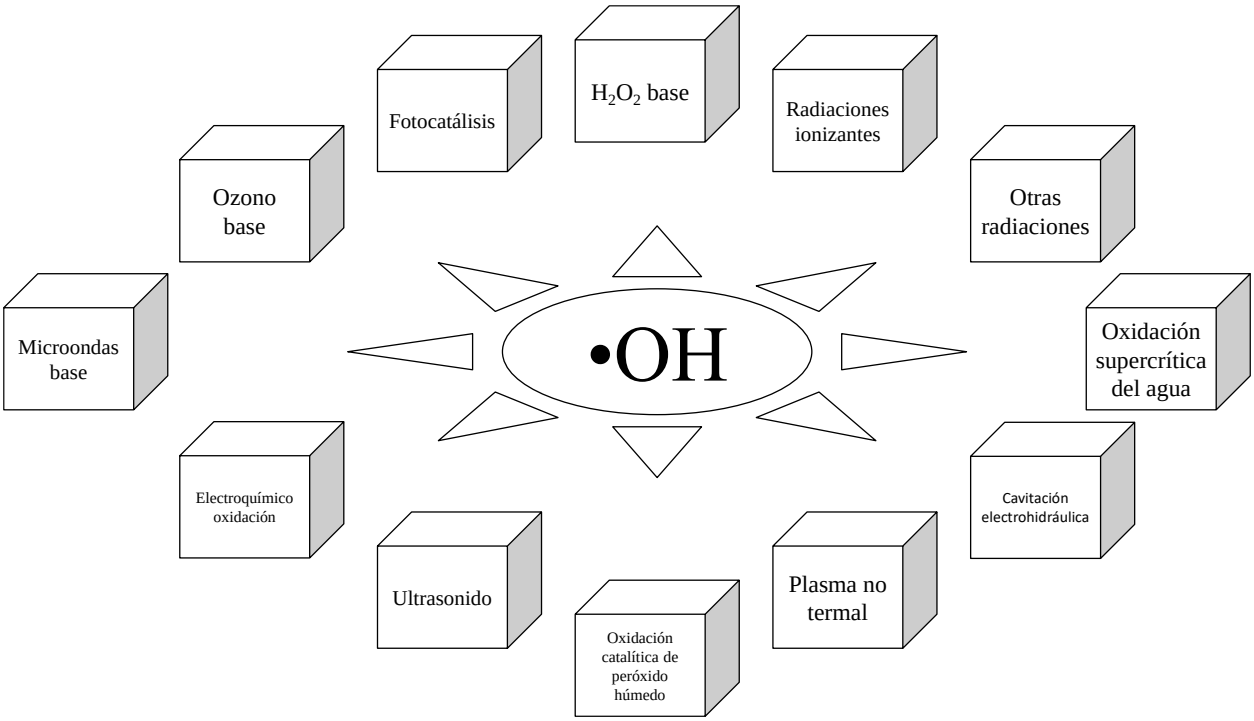

Figura 6. Proceso de oxidación avanzada (Ameta, 2018)

Recientemente, los POAs basados en SO_4^{-}• han sido notables por su potencial oxidación-reducción es similar o incluso mayor (2.5–3.1 V, E^{θ}=2.8V) que el •OH (1.9-2.7V) (Chen, Wu and Hong, 2020) y la vida útil (30-40 μs) al del •OH (20 ns), lo que garantiza que el SO_4^{-}• radical sulfato ataca el contaminante de manera efectiva (Babu *et al.*, 2019; Li *et al.*, 2019).

Durante la mineralización que se produce con los POAs generalmente ocurre un aumento en la biodegradabilidad del agua residual y también se genera una desintoxicación de las aguas residuales (Babu *et al.*, 2019). Para llegar a la mineralización completa los procesos pueden llegar un costo elevado si se generan intermedios resistentes a la degradación química, porque consumen una cantidad sustancial de energía y productos químicos al aumentar la duración del tratamiento, por esa razón se han utilizado los POAs como procesos de pretratamiento para descomponer los compuestos orgánicos recalcitrantes en intermedios biodegradables, que podrían tratarse con procesos biológicos (Cai *et al.*, 2020).

1.4.1. Métodos electroquímicos

Los tratamientos electroquímicos son de gran interés por ser uno de los POAs con mayor potencial, su principal ventaja es que pueden operarse en condiciones de seguridad, presentan respeto al medio ambiente, versatilidad, condiciones operativas muy suaves, alta eficiencia, facilitan su automatización, sin transporte o almacenamiento de oxidantes y muy alta eliminación de varios tipos de contaminantes (Ma et al., 2018; Brillas, 2020). Entre otras ventajas destacan:

- Los procesos pueden ser catódicos y/o anódicos dependiendo como se hacen más efectivos los tratamientos electroquímicos.
- Se pueden llegar a acoplar los tratamientos electroquímicos de aguas residuales en celdas divididas
- Se pueden operar por fuentes renovables.
- Las aguas residuales reales que son tratadas con estos tratamientos provienen de las empresas textiles, farmacéuticas, químicas, plantas de aguas residuales urbanas y de lixiviados en vertederos y se aplican después de un tratamiento secundario. O bien como pretratamiento para después utilizar un proceso biológico en la degradación de compuestos orgánicos. Estos pueden llegar a mineralizar eficientemente diferentes contaminantes como plaguicidas, colorantes azoicos y algunos ácidos orgánicos de menor tamaño (Li et al., 2019).

1.4.1.1. Electroflotación

La electroflotación (EF) surge por la necesidad de tecnologías capaces de separar pequeñas partículas de la solución, que no se eliminan con los métodos habituales. Este tratamiento fue propuesto por Elmore en 1904 donde lo utilizarían para la flotación de minerales valiosos. Pero hasta 1965 fue cuando se utilizó por primera vez en el campo del tratamiento de aguas residuales, presentando una alta eficiencia para la separación de fases sólidas de líquidas.

Con la EF se pueden separar de un líquido incluso las partículas más pequeñas, porque en las superficies del electrodo, lo que mejora la flotación de partículas pequeñas, durante la electrólisis de una solución acuosa.

La EF está acompañada por otros procesos electroquímicos como electrodiálisis, electroforesis, electrocoagulación, etc., que se dan simultáneamente (Kyzas and Matis, 2016; Santiago *et al.*, 2018).

La EF se ha utilizado para separar aceite de agua o emulsiones de aceite, remueve tintes y metales pesados de cuerpos de agua y aguas residuales. También se aplica como tratamiento preliminar para el agua proveniente de sistemas de enfriamiento y de lavado en procesos industriales, en emulsiones de sustancias orgánicas, además en la recuperación y separación de minerales, extracción de compuestos suspendidos de metales pesados y no ferrosos. De igual manera se aplica como tratamiento para aguas residuales de biodiesel y restaurantes, entre otros (Santiago *et al.*, 2018).

1.4.1.2. Electrooxidación

La electrooxidación (EO) es una técnica electroquímica, la cual utiliza electrodos específicos, por ejemplo: DDB, Pt, IrO_2, SnO_2, etc., los DDB han demostrado un mayor poder de oxidación en comparación con los otros, debido a su amplia ventana de potencial eléctrico. El material del ánodo es importante para la creación de oxidantes en las aguas residuales.

La EO con DDB produce una reacción de transferencia directa en la superficie del ánodo de especies oxidantes hacia los compuestos contenidos en los desechos, debido a la electrólisis del agua que genera principalmente radicales hidroxilos •OH (ecuación 1), ellos son altamente inestables, reactivos y no selectivos. Los •OH producen la oxidación de contaminantes (ecuación 2 en esta los contaminantes orgánicos se reflejan con un R) a la par se generan intermedios y subproductos (Radha and Sirisha, 2018; González, Dominguez and Correia, 2020).

$$H_2O + DDB \rightarrow DDB(\bullet OH) + H^+ + e^- \quad (1)$$

$$R + DDB(\bullet OH) \rightarrow CO_2 + H_2O \quad (2)$$

Los radicales DDB (•OH) fisisorbidos pueden reaccionar entre sí para producir H_2O_2, ecuación 3.

$$2DDB(\bullet OH) \rightarrow DDB + H_2O_2 \quad (3)$$

Una buena dispersión de fluidos promueve el transporte de masa y a una buena distribución (corriente y potencial óptimas), esto maximizan la eficiencia de mineralización y minimizan el consumo de energía (Cornejo *et al.*, 2020).

1.4.1.3. Electrocoagulación

La electrocoagulación (EC) es un tratamiento utilizado para agua y agua residual, donde se usa una celda electroquímica en la cual se introducen un ánodo (electrodo de sacrifico) y un cátodo, a ellos se les aplica corriente directa para llevarse a cabo el tratamiento, produciendo reacciones electroquímicas en el ánodo y el cátodo. Se ha utilizado aluminio, cobre, hierro, acero inoxidable, platino y zinc como electrodos (Prajapati *et al.*, 2016; Elnenay *et al.*, 2017; Hu *et al.*, 2017; Elnakar and Buchanan, 2020; Safwat, 2020; Sun *et al.*, 2020).

La ecuación 4 involucra la reacción que ocurre en el ánodo donde se introduce corriente continua para generar un ion metálico ($M^{n+}_{(aq)}$), en la ecuación 5 la reducción de agua ocurre en el cátodo, para generar OH^- y H_2 que promueven la formación de complejos hidroxi ($M(OH)_{n(s)}$), estos dependen del pH y el metal involucrado (ecuación 6). Posteriormente, se lleva a cabo la adsorción de contaminantes coloidales en la superficie por flotación o sedimentación (Dia *et al.*, 2017; Fayad *et al.*, 2017; Qi, You and Ren, 2017; Sandhwar and Prasad, 2017; Barrera, Balderas and Bilyeu, 2018; AlJaberi, 2019).

Reacción anódica

$$M_{(s)} \rightarrow M^{n+}_{(aq)} + ne^- \quad (4)$$

Reacción catódica

$$2H_2O + 2e^- \rightarrow 2OH^- + H_2 \quad (5)$$

Reacción de la solución

$$M^{n+}_{(aq)} + nOH^- \rightarrow M(OH)_{n(s)} \quad (6)$$

La Figura 7 ilustra el tratamiento de EC con las reacciones electroquímicas que se producen en los electrodos y las que ocurren en solución acuosa.

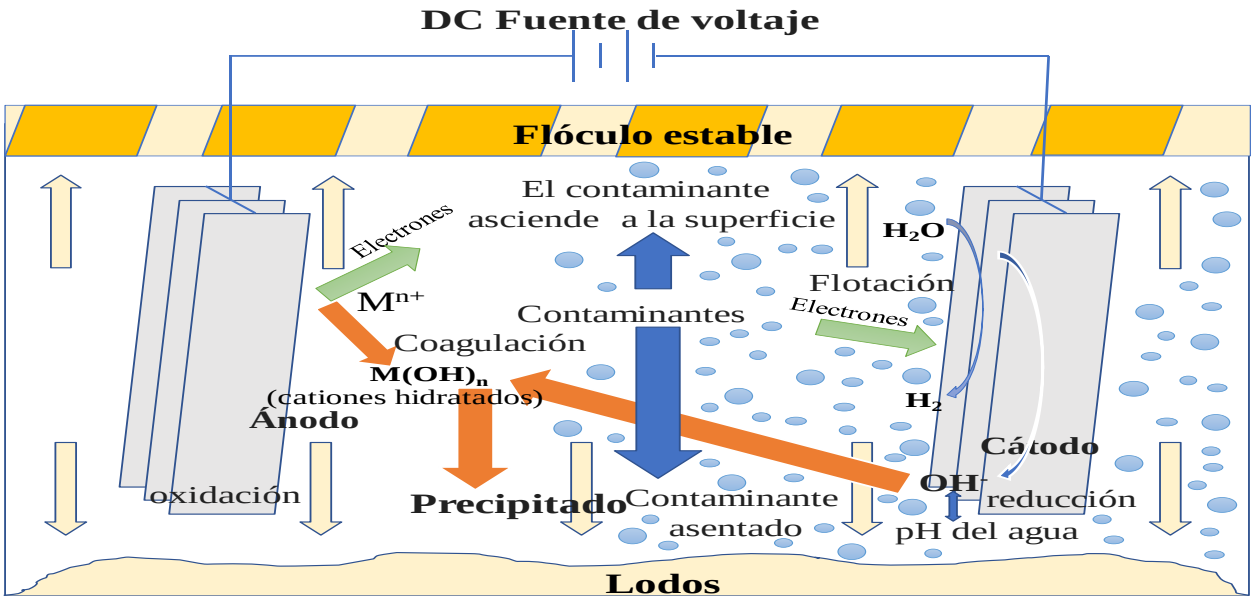

Figura 7. Tratamiento de la EC (Hakizimana et al., 2017)

1.5. Reactores electroquímicos en flujo continúo

Los estudios acerca de la tecnología de electrocoagulación se basan en sistemas por lotes, y sólo en los últimos años los investigadores están centrando su atención en el sistema continúo. El sistema continúo se vuelve más económico que el lote y más adecuado en los sistemas productivos con alta tasa de generación de residuos (Mores *et al.*, 2016). En la Tabla 1 se muestran las características de los reactores en continúo y el batch. En comparación con los métodos

convencionales, los reactores de flujo continúo tienen una serie de ventajas de procesamiento. Por ejemplo, el espacio de las reacciones químicas realizadas en el flujo se extiende de manera significativa, lo que permite que los parámetros de temperaturas y presiones sean más altos (hasta 350 ° C y 200 bar). La transferencia masa/calor, la velocidad de reacción se incrementa significativamente con reacciones heterogéneas (Mohamed *et al.*, 2016). La transferencia de masa se encuentran bajo una condición hidrodinámica especial, frecuentemente llamada flujo helicoidal o de remolino (Contigiani, González and Bisang, 2018).

Tabla 1. Comparación entre sistemas en lote y en continúo (Barrera, 2014).

Lote	**Continúo**
Sin alimentación de flujo-volumen constante	Flujo constante
Las concentraciones en el sistema cambian con el tiempo	Las concentraciones en el sistema son constantes
El desempeño del sistema está relacionado con el tiempo reacción	El desempeño del sistema está relacionado con el tiempo de residencia en el reactor
El contenido en el reactor se encuentra bien mezclado	Variación en el mezclado

Las variables de operación que deben considerarse para los reactores en flujo continúo son el tiempo de retención hidráulica, densidad de corriente (*J*), la pérdida de masa de los electrodos de sacrificio (se determina comparando los pesos iniciales con los finales), velocidad del flujo de entrada, etc. Los rectores en continúo se han aplicado para procesos de electrocoagulación para retirar; sílice hidratada, fluoruro y arsénico del agua subterránea (Contigiani *et al.*, 2018), fósforo y la turbidez de las aguas residuales (Mores *et al.*, 2016), para aguas grises (Bani and Smith, 2012; Chen, Su and Hsu, 2012), eliminación de nitratos (Kumar and Goel, 2010), tratamiento de efluentes industriales (Tejocote-Pérez *et al.*, 2010), etc.

Como se mencionó anteriormente, la energía aplicada es mediante corriente directa para la electrólisis, lo cual algunos autores han analizado los costos asociados al consumo energético (Rosales *et al.*, 2018), sin embargo, una alternativa es utilizar energía renovable, en este caso la energía solar la cual es proporcionada por paneles solares como se mencionará a continuación.

1.6. Energía solar

La creciente escasez y el costo de los combustibles fósiles, e incentivos para reducir las emisiones de gases de efecto invernadero, han conducido a un creciente interés en las formas de reducir el consumo de energía, en particular en el sector residencial. El uso de las energías renovables (como la solar, la geotérmica, la energía hidroeléctrica, la energía eólica y la biomasa) (Iluz and Abu-Ghosh, 2016; Michel *et al.*, 2016; Urban *et al.*, 2016), las cuales generalmente se perciben como tecnologías limpias y favorables para el medio ambiente (Yenneti *et al.*, 2016).

La energía solar es una fuente de energía renovable libre sin emisiones de gases. Por esta razón el número de plantas de energía operadas parcial o totalmente por energía solar ha ido en aumento de manera significativa. A pesar de que el uso actual de la energía solar para la generación de electricidad en el mundo es de aproximadamente 1% del consumo mundial de energía. Se tiene que tomar en cuenta que la energía solar se puede obtener directamente a través de paneles solares fotovoltaicos o indirectamente a través de un sistema térmico solar. Cuando se utilizan los paneles solares, la energía producida se puede almacenar o inyectar directamente a la red pública (Ozlu and Dincer, 2016).

La demanda mundial de energía fotovoltaica aumentó de 1 GW (GW) en 2004 a 57 GW en 2015: una tasa de crecimiento anual de más del 20%, más rápida que cualquier otra industria, incluidas otras industrias emergentes de energía renovable. Se ha sugerido que la energía fotovoltaica será el tipo principal de desarrollo de energía en el futuro (Xu *et al.*, 2018).

Las principales desventajas de los sistemas fotovoltaicos son que la temperatura del panel aumenta debido a las radiaciones y la pérdida de reflejos que ocurre cuando el ángulo de incidencia difiere de cero (Rahmatmand *et al.*, 2018).

1.6.1. Fundamentos de la tecnología fotovoltaica

Los dispositivos fotovoltaicos utilizan comúnmente material semiconductor para inducir la electricidad, en el que se utiliza comúnmente silicio. El principio de este dispositivo es activar

electrones dando energía adicional. Este dispositivo funciona en el principio de que los electrones se activan de un estado de energía más bajo a estado de energía más alto a partir de la adición de energía de la luz solar. Esta activación a su vez crea un número de huecos y electrones libres en el semiconductor dando así origen a la electricidad. El silicio monocristalino, silicio policristalino, silicio microcristalino, etc. se utilizan comúnmente como semiconductores en los sistemas fotovoltaicos. Los sistemas fotovoltaicos se componen de celdas, módulos y matrices para la generación de energía. Además, diversos medios de regulación, control de estructuras, dispositivos electrónicos, conexiones eléctricas y dispositivos mecánicos se utilizan para mejorar la eficiencia operativa. Los sistemas fotovoltaicos se han valorado en kilovatios pico (kWp), que es una cantidad de potencia eléctrica suministrada por un sistema fotovoltaico cuando el sol está directamente en el senil. Su durabilidad varía de acuerdo con el estado de mantenimiento y de carga. Un panel fotovoltaico bien desarrollado puede funcionar satisfactoriamente hasta 10 años con un 90% de eficiencia y a sus 25 años con un 80% de eficiencia. Su eficiencia no es consistente ya que está influenciado por muchos factores ambientales, en particular por la intensidad de la luz solar (Kannan and Vakeesan, 2016).

Los sistemas fotovoltaicos usan las propiedades fotofísicas de los semiconductores materiales para crear electricidad directamente a partir de los fotones de la luz solar (Khemila *et al.*, 2018). Los cuales al tener mayor cantidad de paneles solares conectados en paralelo incrementa el voltaje (*U*) y al conectarlos en serie aumentan la corriente (Valero *et al.*, 2008; Pavón-silva *et al.*, 2018).

La velocidad de reacción es mayor si existe una mayor irradiación solar aunque esto contribuya a que la temperatura sea más alta, mientras más elevada sea la cantidad de paneles, existe más generación de energía (Zhang *et al.*, 2013). A mayor conductividad eléctrica (*CE*) en el medio se produce mayor corriente haciendo que disminuya el voltaje. Por esa razón en los días más soleados se genera más energía eléctrica que en los días nublados (Dermentzis *et al.*, 2016).

Los datos de irradiación promedio que se generan durante el tiempo del tratamiento se grafican, después se realiza una regresión polinomial, esta ecuación se integra para calcular el área bajo la curva (García-García *et al.*, 2015; Hussin *et al.*, 2017). En la gráficas que se realizaron en el 2018

por Millan se muestran curvas donde se ve el punto máximo conocido como medio día solar, en ese momento el panel absorbe la mayor cantidad de irradiación solar (Millán *et al.*, 2018).

Existen importantes trabajos realizados desde el 2008 al 2018 (Tabla 2), donde se han utilizado energía solar como fuente de alimentación para generar corriente eléctrica. Diferentes materiales se han utilizado como ánodos de sacrificio: aluminio, cobre, zinc y acero inoxidable para remover diferentes contaminantes.

Tabla 2. Trabajos realizados con electrocoagulación y energizados con energía fotovoltaica

Tipo de aguas residuales o contaminante	**Modo de operación del reactor**	**Material de electrodo**	**Condiciones de operación**	**Porcentaje de remoción**	**Referencia**
Efluente textil (efluente sintético Remazol RB 133)	Continúo	Aluminio y Acero inoxidable	τ= 23 min, *U*=12.8 V, *Q*= 0.6 L/h, *J* = 10 mA/cm^2, *CE*= 500 mS/cm y pH= 6	99.3 % de decoración	(Valero *et al.*, 2008)
Remoción de fosfato	Continúo	Aluminio	Los electrodos con una distancia= 35 mm, *CE*= 1135 µS/cm, día soleado, Se utilizaron tres paneles fotovoltaicos suministrados con 400 W/m^2	97.77% de fosfato total	(Zhang *et al.*, 2013)
Remoción de Cromo	Continúo	Hierro	*Q* = 0.5 L/h, *J* =10 mA/cm^2, *U*= 6.7 V y τ= 24 min	99.7% de cromo	(Dermentzis *et al.*, 2015)
Agua industrial	Batch	Cobre	*I*= 3 A y pH 4	97% de DQO 91% del color y la turbidez, 48% de COT	(García-García *et al.*, 2015)
Remoción de cobre	Continúo	Aluminio	*J* = 30 mA/cm^2 y pH 4.5	99% de concentración de cobre, 62.2 de DQO	(Dermentzis *et al.*, 2016)
Efluente textil (Tinte azul brillante Remazol)	Continúo y Batch	Aluminio	*J* = 4mA/cm^2, Tiempo de Operación= 10 min y Agitación=150 rpm	Batch 91% de DQO, 95% de color Continúo 91.5% de	(Naje *et al.*, 2016)

				DQO, 95.5% de color	
Remoción de plomo	Batch	Zinc	J= 1.13mA/cm^2 y Tiempo de tratamiento=10min	99.9% de concentración plomo	(Hussin *et al.*, 2017)
Efluente textil sintético (eliminar un tinte azo)	Batch	Aluminio	I= 3 A y 4 A	70% del colorante y 70% de color	(Pavón-Silva *et al.*, 2018)
Eliminación de un tinte textil	Continúo	Aluminio	J de 100 a 400 A/m^2, Q de entrada=15 L/h y Distancia de electrodos=1cm	99% de turbidez y 95% de color	(Khemila *et al.*, 2018)
Agua residual	Continúo	Hierro y Aluminio	pH=7.75 y CE=11 mS/cm^2 y la energía no es constante se aplicó durante 4 días, el punto más alto es de 425mA que se encuentra en el primer día	25 % de remoción oxifluorfeno	(Millán *et al.*, 2018)

CAPÍTULO 2. JUSTIFICACIÓN, HIPÓTESIS Y OBJETIVOS

2.1. JUSTIFICACIÓN

La población mundial está en constante crecimiento y esto implica un mayor consumo de servicios, medicamentos, productos químicos, ropa, alimentos y productos básicos. El impacto de estas industrias en el medio ambiente es innegable y la industria del chocolate no es la excepción. Para satisfacer la demanda mundial, el chocolate se produce en grandes cantidades cada año. Sin embargo, la industria del chocolate genera diferentes tipos de desechos, como compuestos volátiles (di y tri terpenos), flavonoides, polifenoles, pirrol, metilxantinas, aldehídos, mezclas de fosfolípidos, cetonas, cacao líquido, triglicéridos de mantequilla, alcoholes alifáticos, glicolípidos, furanos, esteroles y grasas saturadas (Jin *et al.*, 2017; Kindlein *et al.*, 2018; Magalhães *et al.*, 2018; Toker *et al.*, 2018). Esto ha motivado la búsqueda de tratamientos efectivos para reducir la cantidad de estos contaminantes antes de hacer una descarga. En este contexto, se han preferido los tratamientos biológicos. Sin embargo, este tipo de tratamientos son largos y requieren un control fino de las variables operativas para que los microorganismos sobrevivan (Esparza-Soto *et al.*, 2019).

De acuerdo con lo anteriormente expuesto la justificación científica del trabajo se enfoca en proponer un tratamiento que utilice la EC en flujo continuo para tratar agua residual de una industria chocolatera, lo cual permitió la evaluación del comportamiento de un reactor en flujo continúo ante diferentes cargas orgánicas. Otra contribución importante es que se utilizaron diferentes materiales electródicos, tradicionalmente se han venido aplicando electrodos de aluminio, hierro y cobre, una propuesta innovadora de este proyecto es la aplicación de electrodos de zinc. Adicionalmente el sistema de EC se energizó mediante energía fotovoltaica, utilizando celdas solares, un controlador, batería, interruptores termomagnéticos, con la finalidad de disminuir los costos de energía asociados y hacer un proceso más sustentable y amigable con el ambiente.

En consecuencia, esta investigación contribuyó a la remoción de más del 50 por ciento de DQO, Color y turbidez en un agua residual de la industria chocolatera.

2.2. HIPÓTESIS

El tratamiento de EC en flujo continúo debe ser activado por energía fotovoltaica para proporcionar un ahorro de energía y operar en condiciones óptimas de pH, material electródico (Al, Zn y Cu) y de densidad de corriente; con lo cual presente una remoción eficientemente de los contaminantes de un agua residual que provenga de una industria chocolatera.

2.3. OBJETIVOS

2.3.1. Objetivo general

Evaluar el comportamiento de un reactor de electrocoagulación en batch, utilizando electrodos activos de Zn, Al y Cu. Los electrodos más eficientes se aplicarán en un proceso batch con recirculación y en flujo continúo, y el sistema se energizarán con energía fotovoltaica, para el tratamiento de agua residual de una industria chocolatera.

2.3.2. Objetivos específicos

1. Estudiar el comportamiento de un reactor electroquímico en batch con diferentes electrodos activos de Cu, Al y Zn, para determinar el efecto del material anódico respecto a la eficiencia de remoción.
2. Determinar para cada sistema las condiciones óptimas de operación: densidad de corriente y pH, para el tratamiento de agua residual de una industria chocolatera. Las condiciones óptimas se determinarán por medio del estudio cinético en función de la DQO.
3. Cuantificar y caracterizar los lodos residuales de los diferentes sistemas mediante SEM-EDS e IR.
4. Determinar las condiciones óptimas de operación de un sistema de EC mediante una columna de flujo descendente en modo batch con recirculación y en flujo continúo.
5. Implementar un panel fotovoltaico para el tratamiento electroquímico acoplando un controlador de corriente y una batería de flujo profundo.
6. Realizar la caracterización del agua residual cruda y tratada mediante los parámetros

fisicoquímicos indicados en métodos estándar y las normas oficiales mexicanas.

7. Determinar los costos asociados al consumo y ahorro energético de un sistema de EC convencional vs. EC acoplado a un panel solar.

CAPÍTULO 3. METODOLOGÍA

3.1. Materiales, reactivos y equipo

En la Tabla 3 se indican los materiales, reactivos y equipos necesarios para llevar a cabo esta investigación.

Tabla 3. Materiales, equipos y reactivos

Materiales	Equipos	Reactivos
Buretas	Potenciómetro	Agua desionizada
Electrodos de Zinc	Fuente de poder	Sulfato de sodio
Electrodos de Cobre	Digestor para DQO	Hidróxido de sodio
Electrodos de Aluminio	Balanza	Agua destilada
Embudos de filtración	Parrilla	Viales DQO rango 20-1500 mg/l
Gradillas	Shimadzu Total Organic Carbon Analyzer (model L_{CPH}) equipada con un inyector automático.	
Matraces volumétricos	HACH $_{DR5000\ y\ 6000}$	
Matraces Erlenmeyer	Computadora	
Vidrio de reloj	Perkin Elmer Model Lambda 25 UV/Vis	
Embudo de filtración con placa porosa	Espectroscopía de Infrarrojo Bruker, modelo TENSOR 27	
Matraces Kitasato	Microscopio Confocal de barrido láser (CLSM), modelo TCS SPE / CTR 4000, marca LEICA	
Vasos de precipitado	Microscopía electrónica de barrido y análisis del detector EDS modelo JEOL JSM-6400 (SEM) (con electrones retrodispersados (BSE) (10-20 kv), acoplado a un FlexSEM, modelo SU 1000 (Hitachi) Electronic Data Systems (EDS)) (hasta 20 kv) con detector Bruker Quantax 75/80 de bajo vacío	
Termómetro		

Encendedor
Espátulas
Escobillas
Pinzas
Portaobjetos
Bureta
Pipetas
Probetas
Placas de Petri
Tubos de ensayo
Matraces volumétricos
Reactor tipo Batch
Micropipetas
Reactor de EC para flujo batch con recirculación y continúo
Agitador/mezclador

3.2. Metodología general

La Figura 8 muestra la metodología general llevada a cabo en este proyecto de investigación, a continuación, se describe cada una de las etapas.

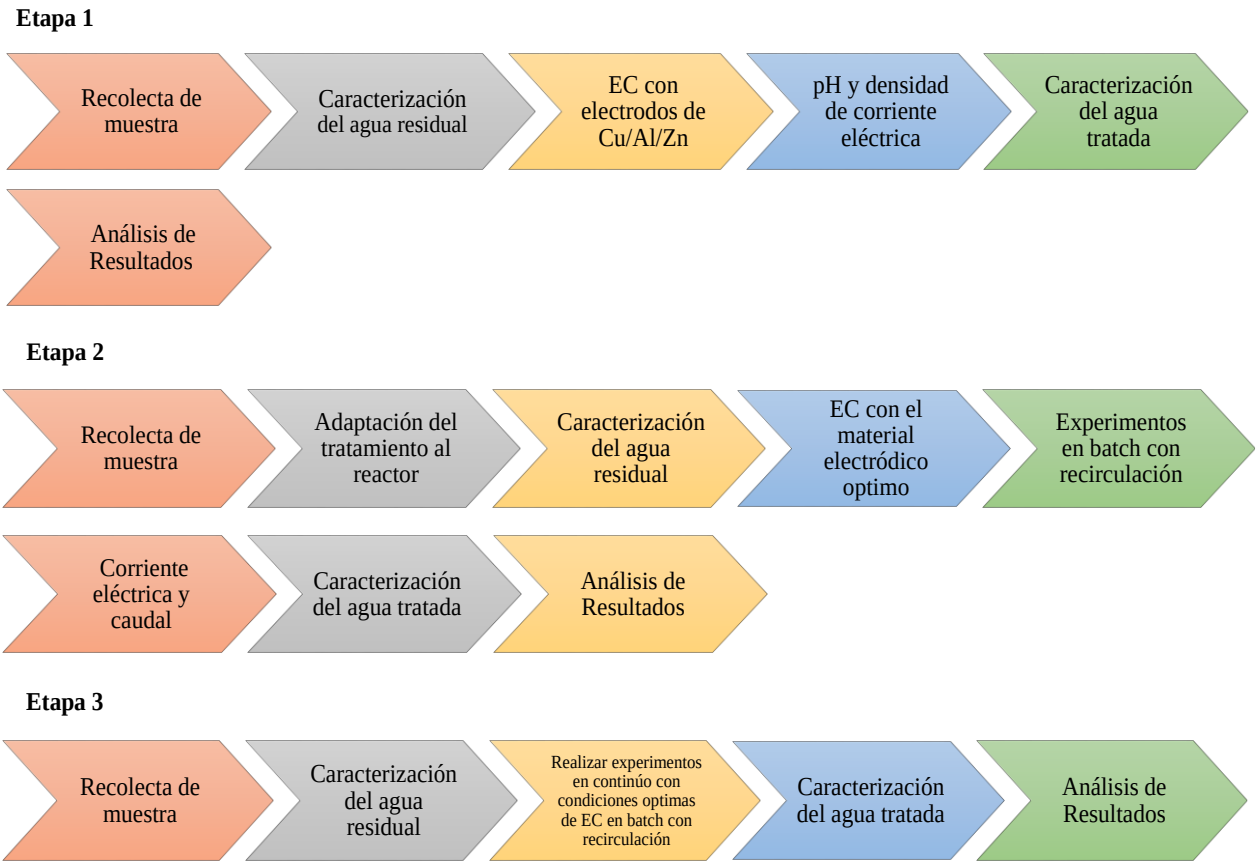

Figura 8. Diagrama de la metodología para desarrolló de la EC en continúo con energía solar para aguas residuales

3.2.1. Tratamiento en sistema batch sin recirculación

El tratamiento EC de un agua residual de una industria chocolatera se estudió utilizando un reactor cilíndrico que funciona en modo discontinúo (batch). Las características se muestran en la Tabla 4; el reactor tiene dimensiones de 22.4 cm de altura y 7.5 cm de diámetro, con una capacidad volumétrica máxima de 2 L. Se utilizó un volumen de 1.220 L utilizado para todas las pruebas, agitado magnéticamente durante el tratamiento. Se diseñó una configuración de electrodos rectangulares de cobre, zinc y aluminio, como placas de ánodo / cátodo, de dimensiones: 19.5 cm

× 2.4 cm, un área anódica de 280.8 cm^2. La corriente suministrada era 0.1 y 0.5A (*j* 1.781 mA/cm^2 y 0.356 mA/cm^2), alimentada por un panel solar, conectado a un controlador de carga. Se añadió sulfato de sodio (1 M) como electrolito de soporte para lograr 1.781 mA/cm^2 y aumentar la *CE* (de 624.7 µS / cm a 1658 µS / cm). Durante el proceso se tomaron diferentes alícuotas cada 10 minutos por hora de tiempo de tratamiento. Los pH de trabajo fueron 4.38 (pH natural de la muestra) y 7, el último se ajustó con NaOH 7.5 M. La configuración experimental se muestra en la Figura 9.

Al encontrar las condiciones óptimas de EC en batch de cada material electródico se realizó la caracterización fisicoquímica y por último se analizan los resultados.

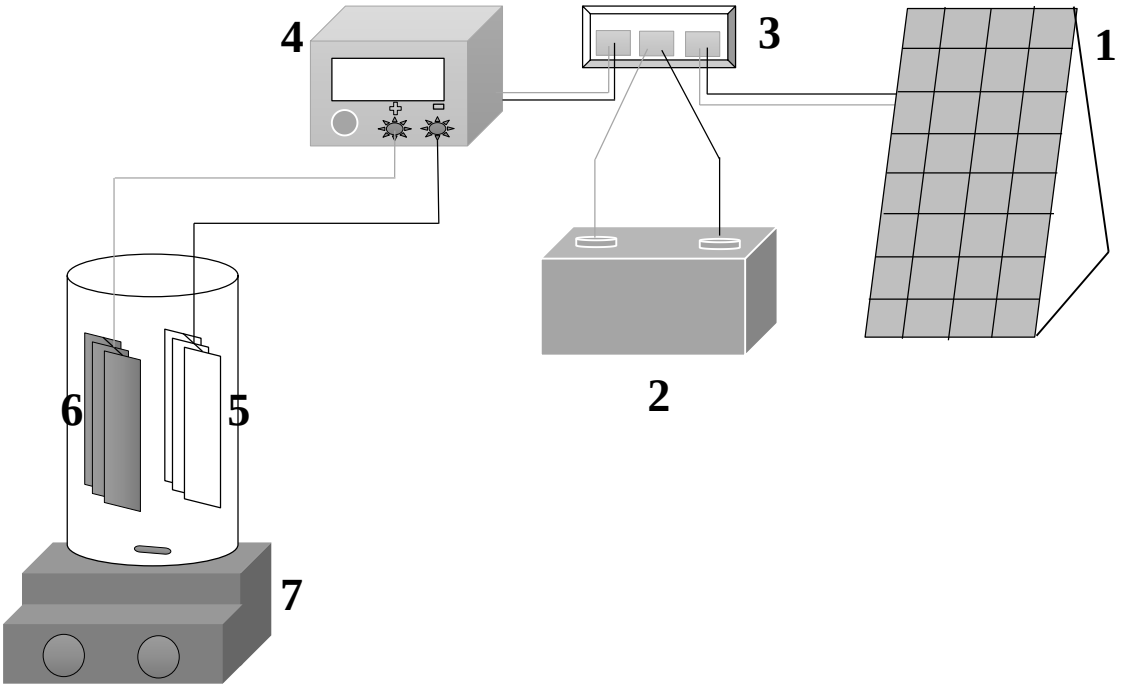

Figura 9. Tratamiento de EC en batch:1) Panel solar, 2) Batería de ciclo profundo, 3) Controlador de carga solar, 4) Controlador de corriente, 5) Cátodo, 6) Ánodo, 7) Agitador magnético

Tabla 4. Características de la metodología de la Etapa 1

Parámetro	**Sistema**		
	Al-Al	**Cu-Cu**	**Zn-Zn**
Cantidad de electrodos (ánodo /cátodo)	3:3 ánodo-cátodo		
Dimensiones de los electrodos	19.5 cm de largo por 2.4 cm de ancho		
Dimensión del reactor	7.5 cm diámetro y 22.4 cm altura		
Área anódica	280.8 cm^2		
pH	4 y 7		
Densidad de Corriente	0.356 y 1.7806 mA/cm^2		
Volumen	1.220 L		
Tiempo	60 minutos		

Se realizo un diseño factorial 2^2 para cada material, en total son 4 combinaciones de cada material como se observa en la Tabla 5.

Tabla 5. Diseño factorial 2^2

No. de experimentos	**Material del electrodo**	**pH**	***J* (mA/cm²)**
1	Al/Zn/Cu	4	0.356
2	Al/Zn/Cu	4	1.7806
3	Al/Zn/Cu	7	0.356
4	Al/Zn/Cu	7	1.7806

3.2.2. Tratamiento en sistema en batch con recirculación

Para el tratamiento de EC en un reactor tipo batch con recirculación, se utilizaron las características mencionadas en la Tabla 6.

El reactor EC consiste en una columna de flujo descendente paralelo, con forma de cilindro (100 cm de altura y 5 cm de diámetro) con una capacidad de 1.964 L. El sistema se muestra en la figura

10. Se puede observar que la solución se alimenta en la parte superior de la columna y se recircula a través de todo el sistema. Esta tecnología explota un orificio en la parte superior de la columna para producir un efecto venturi que promueve la transferencia de masa. Los electrodos de aluminio se colocaron dentro de la columna, como electrodos se utilizaron dos placas de aluminio, como ánodo/cátodo, las dimensiones de los electrodos es de 92.5 cm de longitud, 0.318 cm de espesor y un ancho de 2.4 cm. Los electrodos tienen un volumen total dentro de la columna de 0.282 L, por lo tanto, el volumen libre total dentro de la columna fue de 1.682 L. Sin embargo, en todos los experimentos se utilizó un volumen total de 6. La energía se suministró por una batería de flujo profundo la cual fue cargada por un panel solar, conectado a un controlador de carga. La densidad de corriente suministrada a los electrodos fue de 1.779 y 3.559 mA/cm^2. A las muestras se les agregaron sulfato de sodio (1 M) para aumentar la *CE* de 785.8 a 1680 μS/cm.

Al encontrar las condiciones óptimas de EC en batch con recirculación de cada material electródico se realizó la caracterización fisicoquímica y por último se analizaron los resultados.

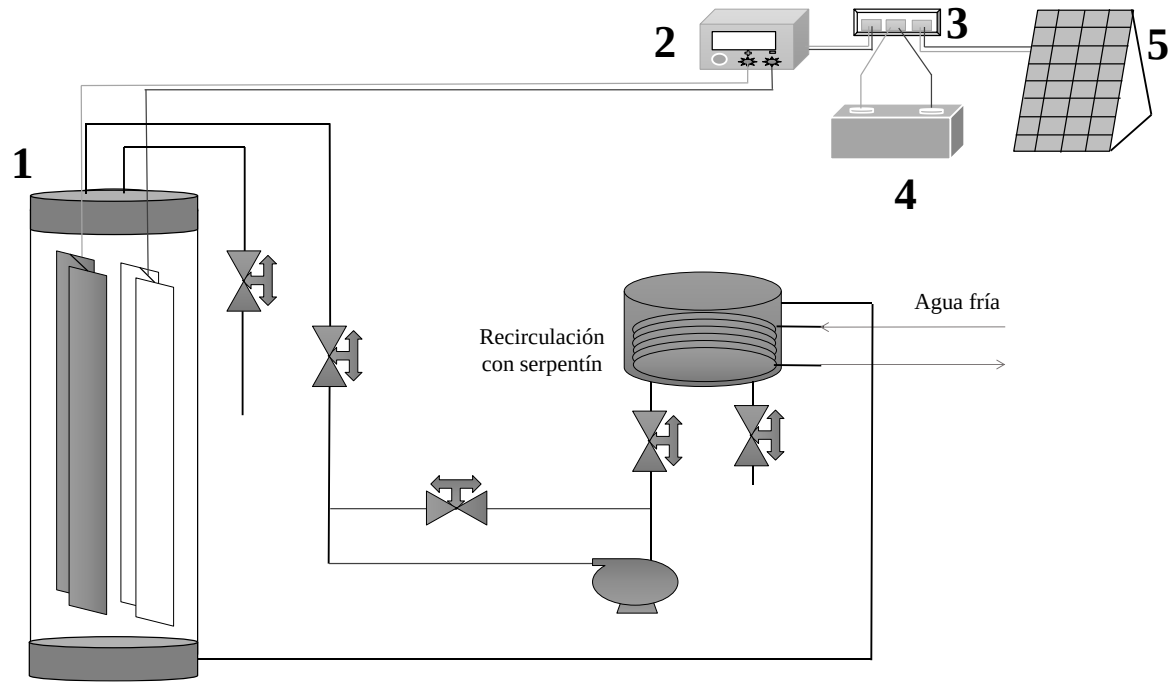

Figura 10. Reactor de EC para flujo batch con recirculación y continúo; 1) Reactor electroquímico de columna de flujo descendente (DCER), 2) Control de corriente, 3) Controlador de carga solar, 4) Batería, 5) Panel solar.

Tabla 6. Características de la metodología de la Etapa 2

Parámetro	**Sistema**
Material del electrodo (ánodo /cátodo)	2:2 ánodo-cátodo
Material de los electrodos	Aluminio
Tiempo de tratamiento	60 min
Dimensiones de los electrodos	92.5 cm de largo por 2.4 cm de ancho
Área anódica	888 cm^2
pH	6.379
Densidad de corriente	1.781 y 3.562 mA/cm^2
Volumen	6 L
Tipo de convección	Recirculación
Temperatura	26 °C
Volumen en la columna	1.682 L
Caudal	0.06 y 0.32L/s
Tiempo de residencia	28.033 y 52.562 s

Se realizo un diseño factorial 2^2 para cada material en total, son 4 combinaciones de cada material como se observa en la Tabla 7.

Tabla 7. Diseño factorial 2^2

No. de experimentos	***J*** **(mA/cm²)**	**Caudal (L/s)**
1	3.562	0.32
2	3.562	0.06
3	1.781	0.32
4	1.781	0.06

3.2.3. Metodología para reactor en continúo

Se realizo la EC en continúo con la misma muestra de EC en batch con recirculación y con las condiciones óptimas obtenidas de estos experimentos como se muestran en la Tabla 8, las variables consideradas fueron la cantidad de electrodos, tipo de material electródico, área anódica, densidad de corriente, volumen, tiempo de tratamiento, tipo de convección, volumen en la columna, caudal, tiempo de residencia, temperatura dimensiones de los electrodos y pH.

Tabla 8. Características de la metodología de la Etapa 3

Parámetro	Sistema
Material del electrodo (ánodo /cátodo)	2:2 ánodo-cátodo
Material de los electrodos	Aluminio
Tiempo de tratamiento	10 min
Dimensiones de los electrodos	92.5 cm de largo por 2.4 cm de ancho
Área anódica	888 cm^2
pH	6.379
Densidad de corriente	3.562 mA/cm^2
Volumen	6 L
Tiempo de residencia	28.033 s
Caudal	0.06 L/s
Volumen en la columna	1.682 L
Tipo de convección	Recirculación
Temperatura	26 °C

El proceso de EC en flujo continúo se realizó en el mismo reactor que el tratamiento de EC en batch con recirculación con energía fotovoltaica, considerando las condiciones óptimas en función del porcentaje de remoción de DQO, color y turbiedad del proceso en batch con recirculación.

3.3. Técnicas de caracterización fisicoquímica

3.3.1 Toma de muestra

Se obtuvieron muestras de aguas residuales industriales de los efluentes de una industria del chocolate ubicada en el Estado de México, sin tratamiento previo; fueron recolectados en recipientes de plástico y almacenados a 4 ° C para caracterización y tratamientos electroquímicos. Los parámetros fisicoquímicos se caracterizaron de acuerdo con los procedimientos de los métodos estándar (APHA/AWWA/WEF, 2012).

3.3.2. Caracterización inicial y final del agua residual

Se caracterizó el agua residual industrial antes y después del tratamiento de la EC, la eficiencia de los sistemas se evaluó en términos de la DQO, color y turbidez. Para evaluar las condiciones óptimas se realizó una caracterización completa de acuerdo con las normas oficiales mexicanas como se muestra en la Tabla 9.

Tabla 9. Parámetros y métodos para la caracterización del agua residual

Parámetro	**Método**
DBO_5	NMX-AA-028-SCFI-2001
Color	Método HACH DR_{5000}
Cloruros	NMX-AA-073-SCFI-2001
Nitritos	Método HACH DR_{6000}
Nitratos	Método HACH DR_{6000}
Nitrógeno amoniacal	Método HACH DR_{6000}
Nitrógeno total	Método HACH DR_{6000}
pH	Método de HANNA HI $_{98191}$
Sulfatos	NMX-AA-074-SCFI-2014
Floruros	Electrodo selectivo
Turbidez	HF Scientific® Micro100 Laboratory Turbidimeter

3.3.3. Caracterización espectrofotométrica

Mediante la técnica de UV-Vis, se realizó un barrido de las muestras de agua residual y tratada en un rango de 200-900 nm. Mediante esta técnica se determina las absorbancias máximas de la muestra, permitiendo identificar cualitativamente algunas sustancias presentes en la muestra.

El fundamento de la espectrometría se debe a la capacidad de las moléculas para absorber radiaciones, el espectro UV-visible está dividido en dos partes el UV cercano (195-400 nm) y visible (400-780 nm). Las transiciones electrónicas entre los orbitales atómicos y moleculares son producidas por la radiación electromagnética que incide sobre la materia, esto hace que sólo uno o un conjunto de átomos sean capaces de absorber la radiación (denominados cromóforos a estos grupos). El UV-Vis absorbe una especie química y el sistema adquiere energía que produce la transición de un electrón de un estado basal a uno excitado. La radiación electromagnética se produce por E que es la energía trasportada en radiación o fotón (J fotón^{-1}), calculado con la ecuación (8) la que necesita de e que es la velocidad de la luz (2.9979 x 10^8 m s^{-1}) por h que es la constante de Planck (6.6256 x 10^{-34} J s fotón^{-1}) entre λ que es la longitud de onda (m) o de igual manera h que es la constante de Planck (6.6256 x 10^{-34} J s fotón^{-1}) por υ que es una frecuencia de la radiación (s^{-1}). La ecuación de Planck está relacionada con la energía de la transición (Wayne, 1991; Skoog, West and Holler, 2005).

$$E = h\upsilon = he/\lambda \tag{8}$$

3.3.4. Determinación de DQO

Mediante esta técnica se mide la materia orgánica e inorgánica que es susceptible a oxidarse con un oxidante fuerte, el oxidante consumido se refleja en términos de su equivalencia en oxígeno (mg/L O_2).

Esta técnica es muy empleada utilizando el método de American Publish Health Association, pero en este caso se utilizó la norma (NMX-AA-030/2-SCFI-2011) donde utilizan como agente oxidante el dicromato de potasio ($K_2Cr_2O_7$), el sulfato de plata (Ag_2SO_4) es el catalizador que

oxida los compuestos y el mercurio ($HgSO_4$) es el inhibidor de haluros, sulfuros, sulfitos, etc. Lo anterior se encuentra en un medio ácido (H_2SO_4), al estar el tubo preparado se le agrega la muestra en solución y se lleva a digestión a una temperatura de 150 °C en 120 min. Después el tubo se deja enfriar (temperatura ambiente) y se mide el valor en un espectrofotómetro (Hach DR 5000) (APHA/AWWA/WEF, 2012). Esta técnica se usa en aguas naturales y residuales (aguas residuales municipales e industriales).

3.3.5. Carbono orgánico total (COT)

El seguimiento se realizó mediante un analizador TOC-L Shimadzu Total Organic Carbon analyzer. Para realizar la medición se lleva a cabo una combustión completa de la muestra a 680 °C introduciendo una corriente de oxígeno puro, en un horno el cual tiene un catalizador de platino soportado en alúmina. Al formase dióxido de carbono y agua, con respecto al agua, esta se evapora y el CO_2 es arrastrado por una corriente de aire de ultra pureza (Infra 32020), hacia un analizador de infrarrojo no dispersivo, el cual se relaciona directamente con el carbono presente en la muestra. Con ello se obtienen el Carbón total (CT) y Carbón inorgánico (CI), el COT se obtiene por diferencia de estos (Santana Martínez, 2019; Shimadzu, 2020).

3.3.6. Fluorescencia

Esta técnica se llevó acabo en un Microscopio invertido con lámpara de Hg, modelo CTR 4000, marca Leica, con tres lentes objetivas de 10, 40 y 63X y filtros fluorescentes 13, N2.1 y A y Microscopio con focal de barrido láser modelo TCS SPE, Leica con láseres para longitudes de onda de 405, 488, 532 y 635 nm.

Se realizó en las siguientes condiciones; Su montaje es directo en cubreobjetos. Se emplearon los aumentos de 10X y 40X los bloques de filtros 13, N2.1 y A, los cuales presentan una luz de emisión verde, rojo y azul respectivamente. Las muestras presentan auto-fluorescencia y presentan emisión para los 3 bloques de filtros, por lo anterior no se empleó ningún tipo de marcador ni filtros. Las imágenes empleadas para el análisis de resultados se encuentran en verde ya que aquí se observó la máxima emisión de señal (515 nm), revelando más detalles de la superficie de los electrodos.

3.3.7. Análisis de los lodos

La microscopía electrónica de barrido y los análisis de detectores EDS se realizaron con la ayuda de JEOL JSM-6400 (SEM) (con electrones retrodispersados (EEB) (10-20 kv), acoplados a un sistema de datos electrónicos (EDS) FlexSEM, modelo SU 1000 (Hitachi) (hasta 20 kv) con el detector Quantax 75/80 Bruker bajo vacío, MAG: 500x, HV: 20kV, WD: 11.3-11.6mm, Px: 0.32µm y 80µm. Esto se utiliza para conocer la composición elemental, textural y propiedades morfológicas

La espectroscopía infrarroja por transformada de Fourier se realizó mediante la afinidad IR Shimadzu-1S. Se utilizó en un espectrofotómetro infrarrojo por transformada de Fourier para identificar los principales grupos funcionales de compuestos orgánicos en un rango de 3999-399 cm^{-1}.

El análisis previo se llevó a cabo para caracterizar el lodo obtenido del tratamiento EC, después de secar a 105ºC, durante 24 h, con el objetivo de establecer la composición del lodo a partir de estos análisis.

CAPÍTULO 4. RESULTADOS Y DISCUSIÓN

En este apartado están los resultados y las discusiones que se generaron en este trabajo, las cuales se encuentran dentro de un artículo publicado y dos artículos enviados, estos se presentan en las secciones 4.1, 4.2 y 4.3 respectivamente, además en la sección 4.4. se presentan resultados no publicados.

4.1. Artículo científico 1. Solar-photovoltaic electrocoagulation of a chocolate industry wastewater: Anodic material effect (aluminium, copper and zinc)

El artículo fue enviado a la revista Journal of Environmental Chemical Engineering, de la editorial ScienceDirect.

4.1.1. Acuse de envío de artículo

Gmail

VIOLETA garcia <violetamaricruz@gmail.com>

Track your recent Co-Authored submission to JECE
1 mensaje

Journal of Environmental Chemical Engineering <eesserver@eesmail.elsevier.com> 21 de junio de 2020, 10:45
Responder a: Journal of Environmental Chemical Engineering <jece@elsevier.com>
Para: violetamaricruz@gmail.com

*** Automated email sent by the system ***

Dear Dr. Violeta García Orozco,

You have been listed as a Co-Author of the following submission:

Journal: Journal of Environmental Chemical Engineering
Title: Solar-photovoltaic electrocoagulation of a chocolate industry wastewater: Anodic material effect (aluminium, copper and zinc)
Corresponding Author: Gabriela Roa
Co-Authors: Violeta M García Orozco, Master; Ivonne Linares-Hernández, PhD; Reyna Natividad- Rangel, Ph.D; Patricia Balderas-Hernández, Ph.D; Carlos E Barrera Díaz, Ph.D;

To be kept informed of the status of your submission, register or log in (if you already have an Elsevier profile).

Register here: https://ees.elsevier.com/jece/default.asp?acw=&pg=preRegistration.asp&user=coauthor&fname=Violeta&lname=García Orozco&email=violetamaricruz@gmail.com

Or log in: https://ees.elsevier.com/jece/default.asp?acw=&pg=login.asp&email=violetamaricruz@gmail.com

If you did not co-author this submission, please do not follow the above link but instead contact the Corresponding Author of this submission at groam@uaemex.mx;gabyroam@gmail.com.

Thank you,

Journal of Environmental Chemical Engineering

4.1.2. Artículo Científico enviado

Solar-photovoltaic electrocoagulation of a chocolate industry wastewater: Anodic material effect (aluminium, copper and zinc)

Violeta Maricruz García-Orozco[a], Ivonne Linares-Hernández[b], Reyna Natividad[c], Patricia Balderas-Hernández[c], Carlos E. Barrera-Díaz[c], Gabriela Roa-Morales[c*]

[a]*Facultad de Química, Universidad Autónoma del Estado de México, Paseo Colón, Intersección Paseo Tollocan S/N, 50120 Toluca, MEX, México*

[b] *Instituto Interamericano de Tecnología y Ciencias de Agua (IITCA), Universidad Autónoma del Estado de México, Km.14.5, carretera Toluca-Atlacomulco, C.P 50200 Toluca, Estado de México, México*

[c]*Centro Conjunto de Investigación en Química Sustentable UAEM-UNAM, Universidad Autónoma del Estado de México, Carretera Toluca-Atlacomulco, Km 14.5, Campus San Cayetano, 50200 Toluca, MEX, México*

**Corresponding author* E-mail: groam@uaemex.mx (G. Roa-Morales)

Highlights

EC process using Zn, Al, and Cu electrodes was supplied and energized by solar energy.

Aluminum electrodes showed the best removal of COD, Color and Turbidity

A current regulator and a deep cycle battery guarantees the same energy in the process

The biodegradability index was increased from 0.49 to 0.59

ABSTRACT

An industrial wastewater from a chocolate factory with an acid pH (4.38), with a high content of organic matter of (COD = 9566 mg/L), Biochemical oxygen demand (BOD_5) of 4666.97 mg/L, biodegradability index (BI) of 0.49 and Total organic carbon (TOC) of 1318.7 mg/L, was treated by electrocoagulation. The wastewater sample presented important nitrogen and phosphorous contents that could cause eutrophication if discharged without previous treatment. A solar-photovoltaic electrocoagulation was proposed to treat the wastewater using aluminium, copper and zinc as anodic materials. The effect of pH (4.38 and 7), current density (1.781 mA/cm^2 and 0.356 mA/cm^2) at 60 min treatment time was studied. The Aluminium system exhibited the best results for organic parameters: COD achieving 50% removal efficiency, reducing BOD to 39%. The BI was increased considerably from 0.49 to 0.59 and TOC was diminished only 26.65%. Copper system also showed an acceptable behaviour in the organic removal to 43% COD, 53% BOD, 30.7% TOC and the BI was 0.4. And the Zinc system was slightly less efficient than copper and aluminium, where the removal achieved was 39% COD, 30% BOD_5, and 19% TOC. The BI shows an increase to 0.56, improving the biodegradability of wastewater. The quantification and characterization of sludge was carried out using Scanning electron microscopy (SEM) and Energy Dispersive Spectroscopy (EDS). Energy savings were reduced using a solar panel, however, costs associated with the use of energy were calculated. Infrared spectroscopy (IR) and fluorescence spectroscopy proved the removal of organic and nitrogenous matter.

Keywords: Chocolate industry wastewater; electrocoagulation; Zinc anode; aluminium anode; copper anode; solar-photovoltaic

Introduction

Chocolate products are the most widespread desserts and snacks around the globe [1]. In 2014, the global chocolate market was an 87.5 billion USD industry and the global chocolate consumption was 7.25 million metric tons. European consumers were the largest purchasers of chocolate products (about 11 kg annual per capita) amounting to nearly 50% of all chocolate consumption worldwide. The most popular variety was milk chocolate, a confectionary product with higher milk, sugar, emulsifier and added fat content than cacao, suspended in a continuous fat phase (cocoa butter 30-40%)[2–4].The production of milk chocolate involves mixing of ingredients, refining, conching, tempering and moulding[5]. Afterwards, the chocolate bars are cooled and packaged. The water consumption in the chocolate process is around 11,372 L/kg for moulded chocolates, followed by bagged chocolates (10,484 L/kg). However, the majority of the consumed volume is green water which is entirely due to the raw materials [1]. The chocolate manufacturing industry wastewater can be characterized as nontoxic because it is devoid of hazardous compounds, but has high contents of total solids (TS), oils, sulfates, chlorides, fluorides, phosphorous, total nitrogen, biochemical oxygen demand (BOD), chemical oxygen demand (COD) and surfactants [6]. Coming from saturated fats, polyphenols, methylxanthines aldehydes, pyrroles, mixtures of phospholipids, ketones, aliphatic alcohols, liquid cocoa butter triglycerides, glycolipids, volatile compounds di- and tri-terpenes, sterols, furans and flavonoids coming from the manufacture of chocolate [7–12].

The environmental impact of the chocolate industry is mainly due to freshwater eutrophication 0.87-0.64 g phosphorous eq./kg [1]. Problems associated with eutrophication include profuse algal blooms, excessive nuisance aquatic plants growth, negative aesthetic aspects and deoxygenation [13]. The majority of impact (57%–72%) is associated with the production of key ingredients, such as milk powder, sugar, flour and cocoa butter. Freshwater ecotoxicity (FET) is high for milk chocolate (133 g 1,4–DCB eq./kg), the main cause of this impact are the raw materials (91%–96%), with more than half associated with cocoa cultivation. Milk powder (19%–21%) and sugar (11%) also have noteworthy contributions. FET can be traced back to copper, zinc and phosphorus releases as well as to pesticides used in agriculture [1]. For example Kruszewski, Wiesław and Kowalska [14]report heavy metals contamination (cadmium Cd, lead Pb, nickel Ni) in raw cocoa and the masses resulting from the various steps of the chocolate manufacturing process.

Efficient wastewater treatment technologies include electrochemical methods, for example, electro-oxidation (EO), electroflotation (EF), and electrocoagulation (EC) [15–17].These technologies are environmentally friendly because they have a small footprint, are reliable, economic, consume less treatment time, display big volume handling capacity, do not need chemical additives and generate minimal sludge quantities. In wastewater treatment plants, EC may function as a conventional coagulation substitute [18,19].

EC is an effective technique to remove heavy metals, nonmetals, anions, and organic compounds from drinking water and wastewater [20–22].

During the EC process, an applied electrical current makes sacrificial anodes dissolve, generating active coagulant compounds and electrolytic reactions happen at the electrode surfaces. Different metals have been tested as electrodes: aluminum, copper, iron, stainless steel, platinum and zinc [17,21,23–26].

Through the anode (sacrificial electrode), a direct current is introduced to generate a metallic ion ($M^{n+}_{(aq)}$) (Equation 1). Water reduction occurs at the cathode to produce OH^- and H_2, as Equation 2 [27] shows. This promotes the formation of polyhydroxides and polyhydroxy-metallic ($M(OH)_{n(s)}$), depending on the pH and metal involved, as seen in Equation 3 [28]. After that, adsorption of colloidal pollutants on the surface by flotation or sedimentation is carried out [29].

Equations 1-3 show the reactions occurring during EC [30,31].

At the anode,

$$M_{(s)} \rightarrow M^{n+}_{(aq)} + ne^- \quad (1)$$

At the cathode,

$$2H_2O + 2e^- \rightarrow 2OH^- + H_2 \quad (2)$$

142

143 In the bulk solution,

144

145 $$M_{(aq)}^{n+} + nOH^{-} \rightarrow M(OH)_{n(s)} \quad (3)$$

146

147 EC has attracted sizeable attention because of its growing enforcement to treat wastewater for
148 different industries, like gelatine, the collagen of animal hide, bone, potato chips, carbohydrates,
149 starches, proteins, vitamins, pectins, sugars, carbohydrates, fermented products, pasta, cookies,
150 molasses, phenols, melanin, caramel and almonds [32–38].

151

152 On the other hand, electrochemical treatments need energizing direct current to be carried out,
153 although it is a limitation for this kind of treatment; solar energy can be a friendly and green option,
154 because of evergrowing fossil fuel resource limitations that give off also ill-contributing
155 greenhouse gas emissions [39,40].

156

157 The key objective of this research is to study the performance of the EC process using zinc,
158 aluminium, and copper electrodes supplied and energized by solar energy. Batch experiments were
159 performed for the treatment of real chocolate wastewater under various experimental conditions.
160 The studied variables were current densities (CDs), pH, electrolysis time, and electrode materials.
161 The response parameters were COD and colour mainly. Nevertheless, a complete characterization
162 was carried out before and after the EC process to understand the physicochemistry of water,
163 evaluating also the energy consumption and produced sludge.

164

165 **2. Materials and methods**

166

167 **2.1. Wastewater sample and characterization**

168

169 Industrial wastewater samples were obtained from the effluent of a chocolate industry located in
170 the State of Mexico. Samples were taken without previous treatment; they were collected in plastic
171 containers and stored at 4 °C for characterization and electrochemical treatments.

The physicochemical parameters were characterized according to Standard Methods Procedures [41]: chemical oxygen demand COD, BOD_5, total organic carbon (TOC), turbidity, colour, sulfates, pH, nitrites, nitrates, total nitrogen, total phosphorus, conductivity, total coliforms and fecal coliforms.

2.2. Electrocoagulation treatment

The EC treatment of a chocolate wastewater was studied using a cylindrical reactor in bench scale experimentation setup working in batch mode, with dimensions of 22.4 cm height and 7.5 cm diameter, with a maximum volumetric capacity of 2 L. A volume of 1.220 L was used for all tests, continuously stirred during treatment. A rectangular electrodes configuration was devised of copper, zinc and aluminium, as anode/cathode plates, of dimensions: 19.5 cm × 2.4 cm, an anodic area of 280.8 cm^2. The electrical current supplied was 0.1 and 0.5 A (j 1.781mA/cm^2 and 0.356 mA/cm^2), powered by a solar panel, connected to a charge controller. Sodium sulfate (1 M) was added as support electrolyte to achieve 1.781 mA/cm^2 and to increase a conductivity (from 624.7 µS / cm to 1658 µS / cm). Different aliquots were taken every 10 minutes per hour of treatment time. The working pHs were 4.38 (natural pH of the sample) and 7, this last one adjusted with NaOH 7.5 M. The experimental setup is shown in Figure 1.

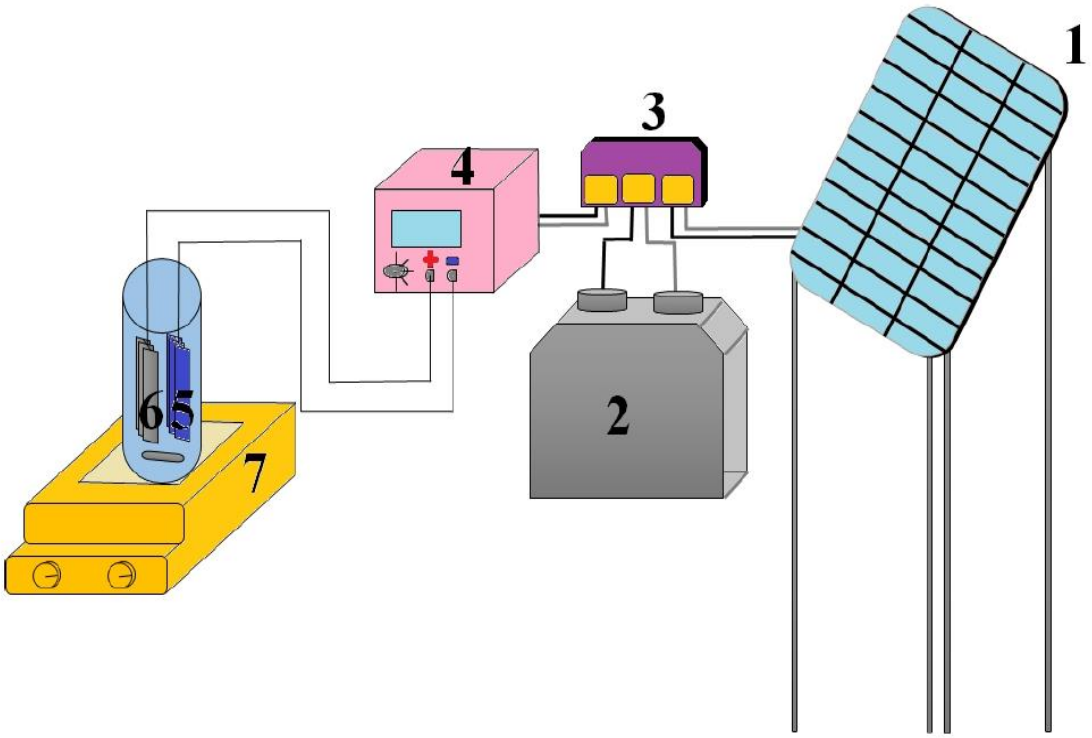

Figure 1. Experimental set up used for EC experiments: 1) Solar panel, 2) Deep cycle battery, 3) Solar charge controller, 4) Current controller, 5) Cathode, 6) Anode, 7) Magnetic stirrer

2.3.Methods of analysis

Scanning Electron Microscopy and EDS detector analysis were performed aided by a JEOL JSM-6400 (SEM) (with a backscattered electrons (BSE) (10-20 kv), coupled to a FlexSEM, model SU 1000 (Hitachi) *Electronic Data Systems (*EDS) (to 20 kv) with Quantax 75/80 Bruker detector at low vacuum, at MAG: 500x, HV:20kV, WD:11.3-11.6mm, Px:0.32µm and 80µm. This was used to know the elemental composition, textural and morphological properties.

Fourier transform infrared spectroscopy (FTIR) was performed. A Shimadzu IR affinity-1S Fourier Transform Infrared Spectrophotometer was used to identify the main functional groups of organic compounds in a range of 3999-399 cm^{-1}.

The previous analysis was carried out to characterize the sludge obtained from EC treatment, after drying at 105ºC, during 24 h, aiming to establish the composition of the sludge from these analyses.

Chemical species distribution diagrams were analysed by MEDUSA program [42]. The concentration of electrically charged species in solution is the ionic strength (*I*); this was calculated with Equation 4 [43],

$$I(mol/L) = \frac{1}{2}\sum(C_i Z_i^2) \quad (4)$$

where Z_i is the charge of each ion and C_i is the concentration of each individual ion (mol/L).

2.4. Electrical cost and consumption

Cost and energy consumption of the EC was estimated considering the theoretical dissolution of the electrode material (*W*) calculated by the Faraday's law [44] as follows,

$$W(g/L) = itM/nFv \quad (5)$$

The electrical energy consumption *E* is defined by the Equation 6 [45,46] ,

$$E\ (kWh/L) = Uit/v \quad (6)$$

where *i*, is current (A), *t* is time (s for Equation 5 and h for Equation 6), *M* is molecular weight of the electrode material (Al, Cu or Zn) (g/mol), *v* is the volume of the sample (L), *n* is the number of electrons, *F* is Faraday's constant (96485 C/mol) and *U* is voltage (V).

The electricity cost in Mexico is US$ 0.040 per kWh [47]. The cost per liter of wastewater treated can be calculated with Equation 7 [48].

$$Cost(US\$/\ L) = EC(kWh/L)(0.040) \quad (7)$$

3. Results and discussion

3.1. Physicochemical characterization of industrial wastewater

241

242 Table 1 summarizes the results of the physicochemical characterization of the industrial wastewater
243 prior treatment. The initial chocolate wastewater sample has a pH acid of 4.38, the content of
244 organic matter was characterized by COD of 9566 mg/L, BOD_5 4666.97 mg/L. The
245 biodegradability index (BI) was 0.49, according to Metcalf and Eddy [49], a wastewater with
246 BI<0.5 is not easily biodegradable. The chocolate wastewater sample presents a BI slightly under
247 this value. TOC was 1318.7 mg/L. This kind of wastewater sample from chocolate industry is
248 characterized for the presence of high nitrogen and phosphorous contents. The sample contains 95
249 mg/L as total nitrogen, 11.7 mg/L N- NH_3 mg/L, 1.3 mg/L N-NO_3^- mg/L and 0.95 mg/L N-NO_2^-
250 mg/L. On the same sample, 36.82 mg/L of PO_4^{3-} was detected**.** This N and P content is enough to
251 cause problems associated with eutrophication including profuse algal blooms, excessive growth
252 of nuisance aquatic plants, negative aesthetic aspects and deoxygenation [13]. The sample contains
253 high colour and turbidity (891 Pt-Co units and 1082.67 NTU), the presence of chloride ions was
254 detected (294.92 mg/L), so that, it is possible that during electrochemical processes chlorine gas is
255 formed, although this may help wastewater disinfection, because of $1.6x10^6$ MPN/100mL of total
256 and fecal coliforms were detected in the sample. Also, the metals, Al (0.48 mg/L), Cu (0.19 mg/L)
257 and Zn (0.35 mg/L) were characterized. Additionally, monovalent and bivalent cations were
258 determined in the sample.

259

260 **Table 1.** Chocolate wastewater characterization before and after EC treatments

Parameter	Units	Initial	Final characterization		
			Cu	Al	Zn
pH	-	4.38	5.03	4.98	4.87
Colour	Pt-Co U	891	110	81	93
COD	mg/L	9566	5431	4808	5814
BOD_5	mg/L	4666.97	2173.04	2852.84	3245.31
BOD_5/COD		0.49	0.4	0.59	0.56
TOC	mg/L	1318.7	913.62	967.21	1069.37
Nitrites	N-NO_2^- mg/L	0.95	0.31	0	0.7

Nitrates	$N\text{-}NO_3^-$ mg/L	1.3	1.3	0.6	0.7
Ammoniacal nitrogen	N- NH_3 mg/L	11.7	13.9	12.7	17.9
Total nitrogen	N mg/L	95	31	33	48
Phosphate	PO_4^{3-} mg/L	36.82	15.82	3.59	30.02
Turbidity	NTU	1082.67	88.9	19.2	283
Total coliforms	MPN/100mL	$1.6x10^6$	<200	<200	<200
Fecal coliforms	MPN/100mL	$1.6x10^6$	<200	<200	<200
Chlorides	Cl^- mg/L	294.92	225.89	158.96	192.42
Fe	mg/L	3.22	1.89	1.93	1.52
Ca	mg/L	167.39	24.55	18.22	18.73
K	mg/L	24.41	21.41	20.05	20.26
Mg	mg/L	12.35	11.37	4.13	9.93
Al	mg/L	0.48	0.19	106.4 3.14 (at pH 9)	0.24
Cu	mg/L	0.19	265.66 17.3 (at pH 9)	0.15	0.08
Zn	mg/L	0.35	0.25	0.29	198.6 2.66 (at pH 9)

3.2.Electrocoagulation treatment

3.1.1 pH effect

The initial pH is a significant parameter for EC [50]. It is worth noticing that pH increases during EC by the electrochemical reaction. This is generated by water reduction at the cathode [51,52] to produce H_2 gas and OH^- ions [53].

Figures 2, 3 and 4 show the pH effect on the COD removal at a current density of 0.356 mA/cm^2, 1 hour of treatment time and initial COD 9566 mg/L, colour 891 Pt-Co U, using Cu, Al and Zn as anodes in the electrolytic cell, pH of 4.38 (natural pH of the wastewater) and 7 (neutral pH) adjusted with sodium hydroxide.

Figure 2a shows the aluminium electrocoagulation performance and the pH influence on the COD and colour removal. 31% of COD removal was achieved at initial pH 7 and 39% at pH of 4.38. At the same time, 80-90% of colour was removed in this treatment. During EC the pH increased to 4.98 and 7.30, respectively. According to aluminium species distribution diagram (Fig. 2b), $Al(OH)_3$ was produced in this pH range (Equation 8) [54].

$$Al^{3+} + 3OH^- \rightarrow Al(OH)_3 \quad (8)$$

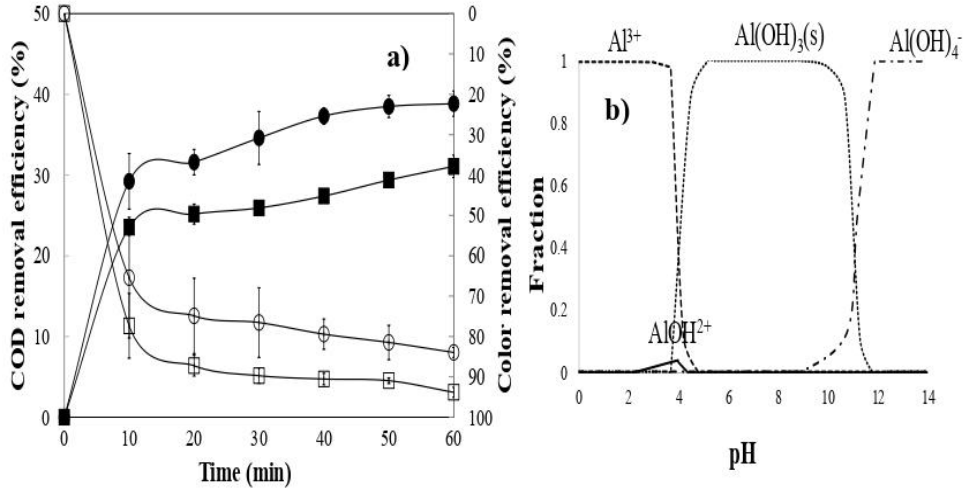

Figure 2. Aluminium electrocoagulation performance: Effect of pH on the COD and Colour removal efficiency after 60 min of treatment and 0.356 mA/cm^2, **a)** pH 4.38 (●COD and ○ Colour) and pH 7 (■COD and □Colour) and **b)** Aluminium species distribution diagram in wastewater as a function of pH (I=0.02 and Al^{3+}=1.02 mM, NO_3^- = 20.97μM, PO_4^{3-}= 0.39 mM, Cl^-= 8.32 mM, NH_3 =0.69 mM, NO_2^- =20.65 μM).

The pH evolution with time, exhibited by the copper EC system, is shown in Figure 3. It can be observed that the natural pH sample increased from 4.38 to 5.03. One of the main species formed was Cu^{2+} [55] which favours the precipitation of phosphate ions in the chocolate wastewater as

$Cu_3(PO_4)_{2(s)}$ [56] and $CuCl_2 \bullet 3Cu(OH)_2$ [57](Equations 11-12). Equations 9-10 show the chemical reactions that occurred in the aqueous media. At neutral pH, the samples pH increased to 8.02 and $Cu(OH)_2$ (s) was formed at this pH [58]. The best removal of 37% COD and 80% of colour were achieved after 60 min of treatment time at an initial pH of 4.38.

In the EC process, different species contributed to destabilization of the organic and inorganic macromolecules by charge neutralization [59], these produce the agglomeration of neutral colloidal entities, promoting the flotation by hydrogen gas or precipitation by sedimentation [60].

$$Cu_{(s)} \rightarrow Cu^{2+}_{(aq)} + 2e^- \quad (9)$$

$$Cu_{(s)} + 2H_2O_{(l)} \rightarrow Cu(OH)_{2(s)} + H_{2(g)} \quad (10)$$

$$3Cu^{2+} + 2H_2PO_4^- \rightarrow Cu_3(PO_4)_2 + 4H^+ \quad (11)$$

$$2Cu_2O + 2HCl + 2H_2O + O_2 \rightarrow CuCl_2.3Cu(OH)_2 \quad (12)$$

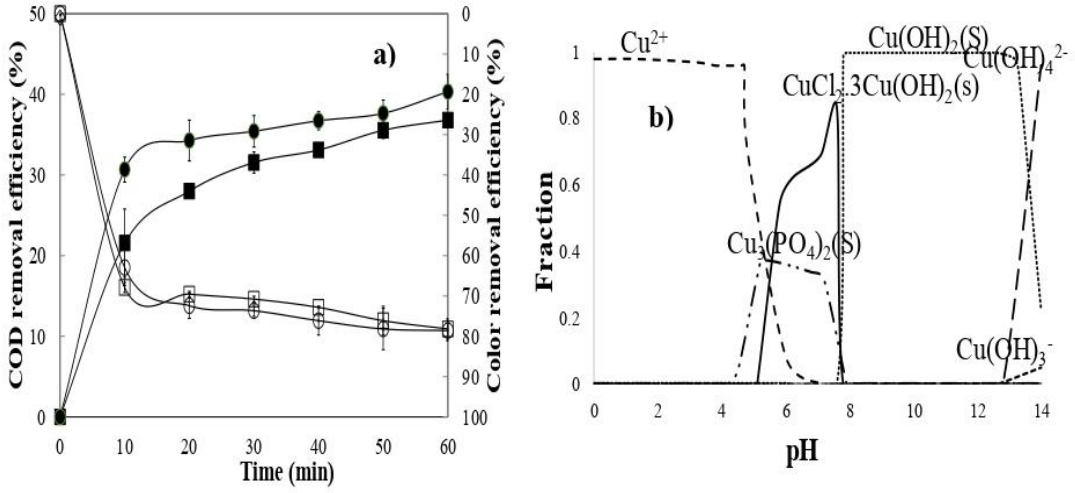

Figure 3. Copper electrocoagulation performance: Effect of pH on the COD and Colour removal at 60 min treatment and 0.356 mA/cm^2, **a)** pH 4.38 (●COD and ○ Colour) and pH 7 (■COD and □Colour) and **b)** Copper species distribution diagram in wastewater as a function of pH (I=0.02 and Cu^{2+}=1.53mM, NO_3^- = 20.97µM, PO_4^{3-}= 0.39 mM, Cl^-= 8.32 mM, NH_3 =0.69 mM, NO_2^- =20.65 µM).

316

317 Further, the Zn system showed a pH increase from 4.38 to 4.87, while the neutral pH sample
318 increased to 7.74. Figure 4 shows the behaviour of COD and colour removal efficiency observed
319 at these pHs in the Zn system. In both treatments, 39% of COD and 90% of colour were eliminated.
320 Equation 13 shows the anodic oxidation in the electrochemical cell, and Equations 14-16 show the
321 chemical reactions occurring in solution [61–66]. This electrode material produced a smaller
322 coagulant amount than Al or Cu, however a good removal of COD and phosphates were observed
323 in this system.

324

325 $$Zn \rightarrow Zn^{2+} + 2e^{-} \quad (13)$$

326 $$Zn^{2+} + 2H_2O \rightarrow Zn(OH)_{2(s)} + 2H^{+} \quad (14)$$

327 $$ZnO_{(s)} + H^{+} \rightarrow ZnOH^{+} \quad (15)$$

328 $$3Zn^{2+} + 2H_2PO_4^{-} + 4H_2O \rightarrow Zn_3(PO_4)_2.4H_2O + 4H^{+} \quad (16)$$

329

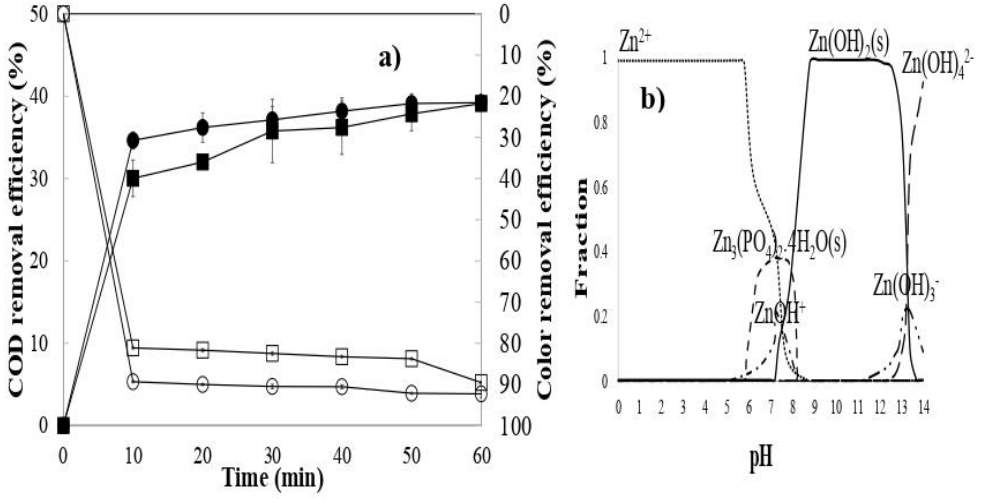

330

331

332

333 **Figure 4.** Zinc electrocoagulation performance: Effect of pH on the COD and Colour removal at
334 60 min treatment and 0.356 mA/cm^2, **a)** pH 4.38 (●COD and ○ Colour) and pH 7 (■COD and
335 □Colour) and **b)** Zinc species distribution diagram in wastewater as a function of pH (I=0.02 and
336 Zn^{2+}=1.53mM, NO_3^- = 20.97µM, PO_4^{3-}= 0.39 mM, Cl^-= 8.32 mM, NH_3 =0.69 mM, NO_2^- =20.65
337 µM).

338

339 **3.3.Effect of current density**

340

341 Current density (*j*) is one of the most significant parameters in the EC [67], this controls the anodic
342 dissolution, bubble generation, flocs growth, the shift in pH, the consumption of energy in the
343 treatment, conductivity and the quantity of solids generated [68].

344

345 Figure 5 shows the behaviour and effect produced by the *j* at 1.781mA/cm^2 and 0.356 mA/cm^2,
346 using Al, Cu and Zn anodes, at natural pH of 4.38. It is well known that increasing *j,* improves the
347 removal efficiency of organic and inorganic pollutants [69] because the anodic dissolution is
348 increased. As we can see, Figures 5a and 5b show that the best results were observed at *j* 1.781
349 mA/cm^2 with Al and Cu electrodes [70–72]. Al system presented the best performance with a
350 removal of 50% COD and 91% colour, Cu system shows a lower removal than Aluminium, 44%
351 COD and 88% colour were achieved.

352

353 Figure 5c shows the best removal efficiencies for the zinc system, 39% COD and 92% colour
354 removal were obtained at the smallest *j* (0.356 mA/cm^2).

355

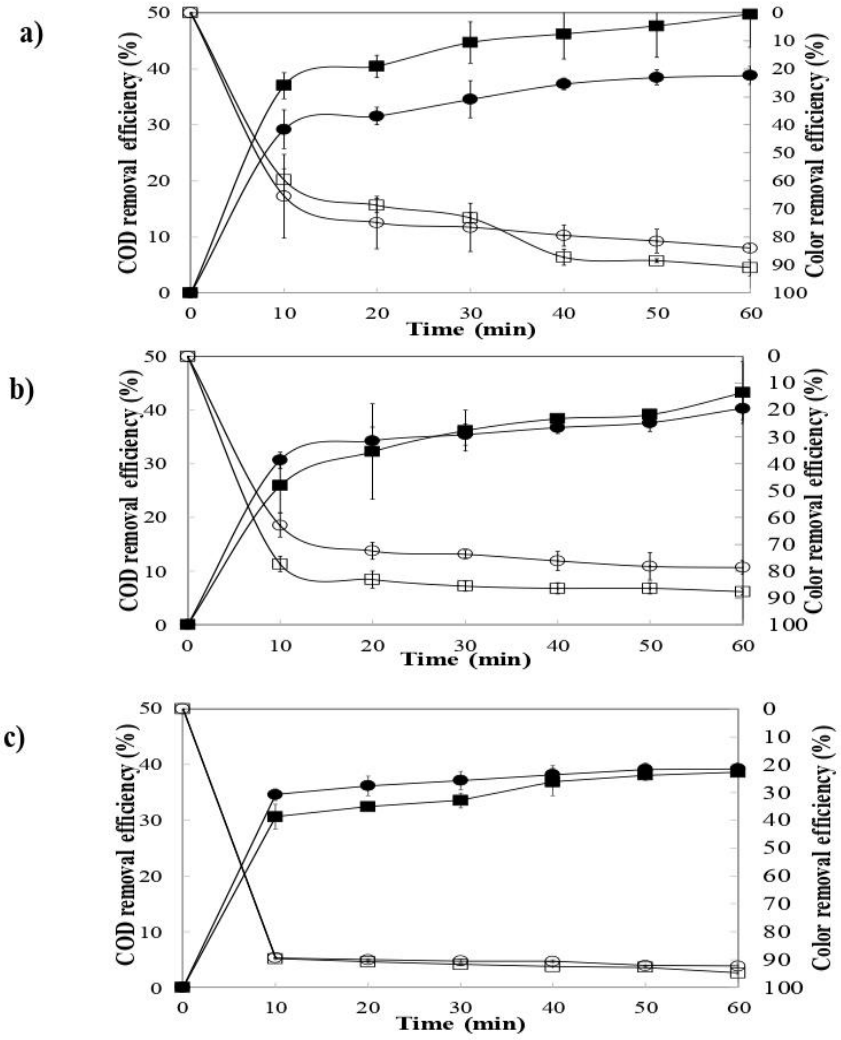

Figure 5. Electrocoagulation performance: Effect of current density, *j,* on the COD and Colour removal at 60 min of treatment time and pH 4.38 a) Aluminium system, b) Copper system; c) Zinc system. DQO (■1.781mA/cm^2 and ●0.356 mA/cm^2) and Colour (□1.781mA/cm^2 and ○0.356 mA/cm^2).

3.4.Kinetics

The kinetic data of the assessed treatments were analysed using basic power law models, however, a low correlation coefficient was obtained. Hence, the Behnajady-Modirshahla–Ghanbery model (BMG) was used. This is also called two step model [73].

BMG has been intensively employed for connecting multiple operational parameters in reactions involving AOPs (Advanced Oxidation Processes) [74]. The kinetic BMG is shown in the Equation 17 [75],

$$C_t = (1 - [t/(m + bt)]) * C_0 \quad (17)$$

where C_t is the COD and Colour concentration at time t, the initial concentration of COD and Colour at time t=0 min is C_0, t is the reaction time in min [76]. 1/m is the COD or colour removal rate at the beginning of the process and 1/b is the maximum theoretical fraction of removal [77].

Figure 6 shows a) the COD removal and b) the colour removal. The m and b constants are given in Table 2, these constants were calculated with the software Statistica 10 StatSoft®. The high correlation coefficients showed that the applied kinetic model displayed good correspondence with the data [78]. BMG model represents well the experimental data because the EC occurred in two stages: coagulation occurred very fast during the first 10 minutes and then sedimentation occurred during the last 50 min. Figure 6a shows that COD removal is faster with Al Electrodes and Figure 6b shows that after 40 min of treatment, the Colour removal is the same with the three different materials but at different reaction rates.

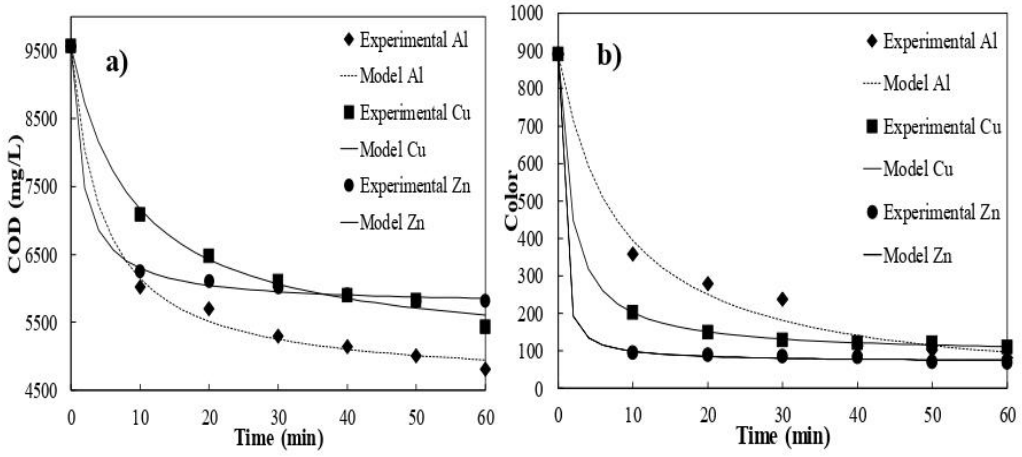

Figure 6. Kinetic BGM modeling of the a) COD and b) colour removal; Al electrodes (♦), Cu electrodes (■) and Zn electrodes (●)

In can be observed in Table 2 that the smallest *m* corresponds to the Zn system. This means that Zn is the material that produces a faster initial removal rate of both, COD and colour. Even so, constant *b* revealed that Al was the material producing a greater Colour and COD removal % at the end of the process.

Table 2. The coefficients of determination and characteristic constants of BMG

Electrode material	Colour Removal			COD Removal		
	m (min)	b	r^2	m (min)	b	r^2
Al	8.070848	0.986366	0.98661708	8.700301	1.926605	0.9957448
Cu	1.781608	1.113641	0.999911	18.787766	2.105534	0.99517004
Zn	0.380186	1.085942	0.9996909	4.171368	2.507814	0.99879533

3.5. Physicochemical characterization of industrial wastewater after EC treatments

Table 1 shows the physicochemical characterization of the chocolate industry wastewater before and after EC for Cu, Al and Zn systems.

Aluminium system rendered the best results for organic and inorganic parameters: COD was reduced from 9566 mg/L to 4808 mg/L which represents a 50% removal and BOD was reduced from 4666.97 to 2852.84 mg/L, achieving 39% removal. The BI was increased considerably from 0.49 to 0.59. TOC diminished only 26.65% because EC does not mineralize the organic matter. Colour and turbidity were considerably improved: 90 and 98% were achieved, respectively. Regarding total nitrogen, it was reduced from 95 to 33 mg/L and ammoniacal nitrogen was slightly increased from 11.7 to 12.7 mg/L, final nitrates concentration (0.6 mg/L) and nitrites were not detected. Also, phosphate ions were reduced to 90%. The electrochemical reduction of NO_3^- is reported by some authors to occur according to Equation 18 and 19 [79],

$$8e^- + NO_{3(aq)}^- + 10H_{(aq)}^+ \rightarrow NH_{4(aq)}^+ + 3H_2O_{(l)} \quad (18)$$

$$NH_4^+ + OH^- \leftrightarrow NH_3.H_2O \leftrightarrow NH_3 + H_2O \quad (19)$$

Total and fecal coliforms show a 99% reduction. This can be ascribed to the Cl^- ions present in the solution. Equations 20-22 describe the chlorine production at the anode and the hypochlorite formation in solution [80].

$$2Cl^- \rightarrow Cl_2 + 2e \quad (20)$$

$$Cl_2 + H_2O \rightarrow HClO + H^+ + Cl^- \quad (21)$$

$$HClO \rightarrow H^+ + ClO^- \quad (22)$$

For the Aluminium system, the final pH was 4.98 then the formation of $Al(OH)_3$(s) in the Figure 7a) is observed.

The copper system was the second best in the organics removal. The obtained removal results with copper electrodes were: 43% COD, 53% BOD, 30.7% TOC and the BI was 0.4. Nitrogenous matter exhibits a similar behaviour than Al system. TN was reduced 67%, ammoniacal nitrogen was also increased from 11.7 to 13.9 mg/L, nitrates did not present any change and nitrites were reduced from 0.95 to 0.31 mg/L. According to Equation 11 and Figure 7, the phosphate precipitation was carried out in the Cu system as $Cu_3(PO_4)_2$, 57% of removal was obtained. 87% of colour and 91.7% of turbidity were achieved. In addition, 99% of total and fecal coliforms were removed using Cu EC system due to Equations 20-22 were performed.

On the other hand, Na_2SO_4 was added as support electrolyte, then Figure 7 shows the species that are produced by adding SO_4^{2-} (6.59 mM). In the Cu system, the increase of pH was 5.03, then Cu^{2+}, $Cu_3(SO_4)(OH)_4$(s), $Cu_4SO_4(OH)_{6(s)}$[81], $CuSO_4$ [82] and $Cu_3(PO_4)_2$(s) in Figure 7b) could be formed, according to Equations 9,11 and 23-25.

$$Cu^{2+} + SO_4^{2-} \rightarrow CuSO_4 \quad (23)$$

$$4Cu^{2+} + SO_4^{2-} + 6(OH)^- \rightarrow Cu_4SO_4(OH)_6 \quad (24)$$

$$3Cu^{2+} + 4OH^- + SO_4^{2-} \leftrightarrow Cu_3(SO_4)(OH)_4 \quad (25)$$

The Zinc system was slightly less efficient than Cu and Al since the removal achieved was 39% COD (from 9566 to 5814 mg/L), 30% BOD_5 (from 4666 to 3245.31 mg/L), 19% TOC (1318.7 to

1069.37 mg/L). The BI shows an increase from 0.49 to 0.56, improving the biodegradability of wastewater, colour and turbidity presented a reduction of 89.5 mg/L and 73.86% respectively. Total and fecal coliforms were reduced to 99%. The reduction of TN was only 49% and this system achieved a higher formation of ammoniacal nitrogen (from 11.7 to 17.9 mg/L), nitrates and nitrites achieved a concentration of 0.7 mg/L (46% and 26% respectively). Phosphates were slightly diminished (18.46%). In general, PO_4^{3-} can be also adsorbed in the form of a complex with the hydroxides and this depends on the sacrificial anodic material. This is reflected in the production of sludge that can be removed by sedimentation and flocculation.

The increase of pH to 6.88 in the Zn system, promotes the formation of Zn^{2+}, $Zn_3(PO_4)_2.4H_2O(s)$, $ZnOH^+$, $ZnSO_4$ [83], and $Zn_4(OH)_6SO_4$[84], as it is shown in the Figure 7c). The reactions occurring in this system are 13,15-16 and 26-27,

$$Zn^{2+} + SO_4^{2-} \leftrightarrow ZnSO_4 \quad (26)$$

$$Zn(OH)_2 + 3Zn^{2+} + 4OH^- + SO_4^{2-} \rightarrow Zn_4(OH)_6SO_4 \quad (27)$$

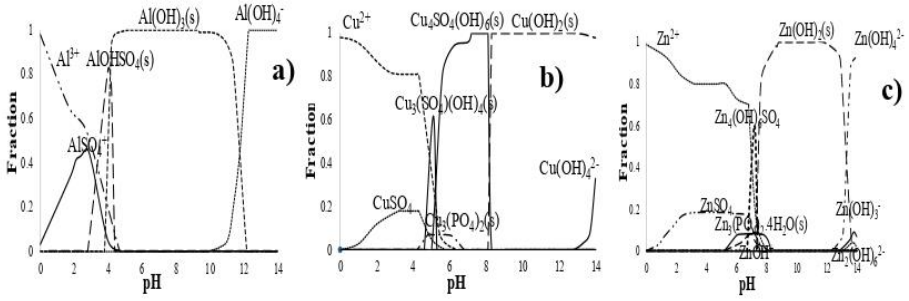

Figure 7. Species distribution diagrams in wastewater as a function of pH at j= 1.781mA/cm^2 with electrodes a) Al (Al^{3+}= 5.11mM and I=0.058), b) Cu (Cu^{2+}= 7.65mM and I=0.050) and c) Zn (Zn^{2+}= 7.65 mM and I=0.050)

The sludge content was determined for each system Al, Cu and Zn that produced 1.31, 1.15 and 0.41 g/L of sludge, per treatment [85].

3.6. UV-Vis spectroscopy

Figure 8 shows the Uv-Vis spectra of the best conditions for each treatment, the samples were diluted 1/20 for the analyses; turbidity, organic and inorganic matter were reduced considerably after treatments.

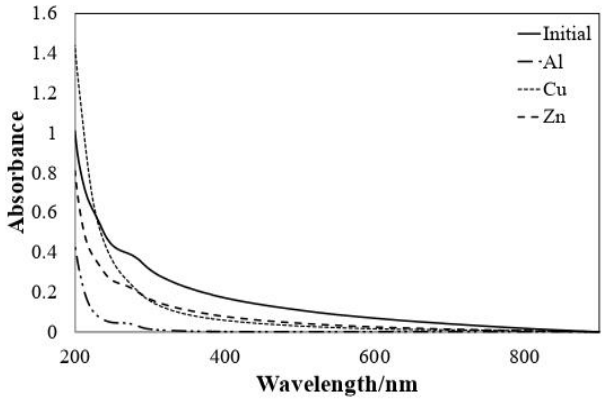

Figure 8. Uv-Vis Spectra of Al 1.781mA/cm^2, Cu 1.781mA/cm^2 and Zn 0.356 mA/cm^2

Aluminum is the material with the lowest absorbance in a range of 200-900 nm, after EC. This material removed all turbidity from the sample, but there is still organic matter seen at the 200-325 nm wavelength; the same spectrum is shown in this range as in the sample treated with Zinc electrodes. It is not known to which species this absorbance is related, but it is completely removed with the Copper electrodes. Thus, the increase in absorbance is due to the link of Copper with the organic matter of the medium.

Zinc and copper have the same absorbances of 325-900 nm, but Zinc has a turbidity three times greater than copper. This was reflected on the COD concentration.

3.7. Sludge Characterization

After EC treatment, the sludge was characterized by SEM and EDS. Figure 9, shows the heterogeneous and irregular morphology of the a)Al, b) Cu and c) Zn sludge, [86].

The analysed samples section showed the following elements in common C, O, Si, S, P, Fe, Mg and Al. The quantitative analysis indicate that average mass % of chemical constituents of the sludge sample are: **a)** C 21.01%, O 56.97%, Na 0.39%, Mg 0.76%, Al 18.00%, Si 1.00%, S 1.02%, Ca 0.38% and P 0.13%, **b)** C 55.28%, O 37.08%, Si 0.44%, S 0.53%, Cu 5.23%, P 0.60%, Fe 0.51%, Mg 0.18% and Al 0.15%, and **c)** C 30.16%, O 28.83%, Mg 0.45%, Al 0.19%, Si 1.10%, P 0.67%, S 0.58%, Ca 0.81%, Fe 0.54%, Zn 31.34%, K 0.29% and Na 5.06%.

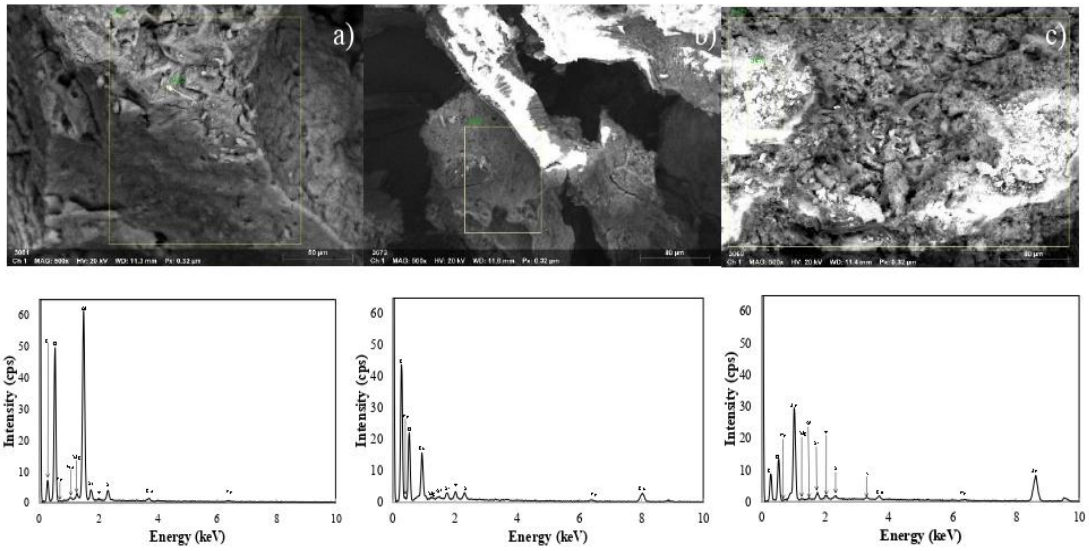

Figure 9. SEM and EDS images of sludge generated during EC process with electrodes of a) Al, b) Cu and c) Zn

These elements are associated to the organic matter (carbon) and inorganic ions from chocolate wastewater, as well as the anodic metals that were removed after the EC process [87].

The Figure 10 depicts the FTIR spectrum which exhibits different bands in the 3000–3700 cm^{-1} range, assigned to the stretching vibration of O-H bonds of the different polymorphs of $Al(OH)_3$, $Cu(OH)_2$ and $Zn(OH)_2$ [88].

The peak at 1637-1647 cm^{-1} represents hydroxyl bending and γ′(OH) water bending vibration or overtones of hydroxyl bending [89].

Peaks at 2919-2921 and 2851-2855 cm^{-1}, correspond to the C-H stretching mode of saturated C-C bonds, showing the presence of hydrocarbons in the sludge [90], while the peak around 1051-1075 was assigned to carbonate mode. A stretching vibration of the Al-O bond at 554 cm^{-1} was also observed in the Al [91]. In addition, the presence of conjugated carbon–carbon bond is indicated by the presence of a medium intensity band at 1464-1469 [92]. Peaks at 1745 in the Al, Cu systems and 1744 cm^{-1} in the Zn can be associated to stretching vibration of C=O [93].

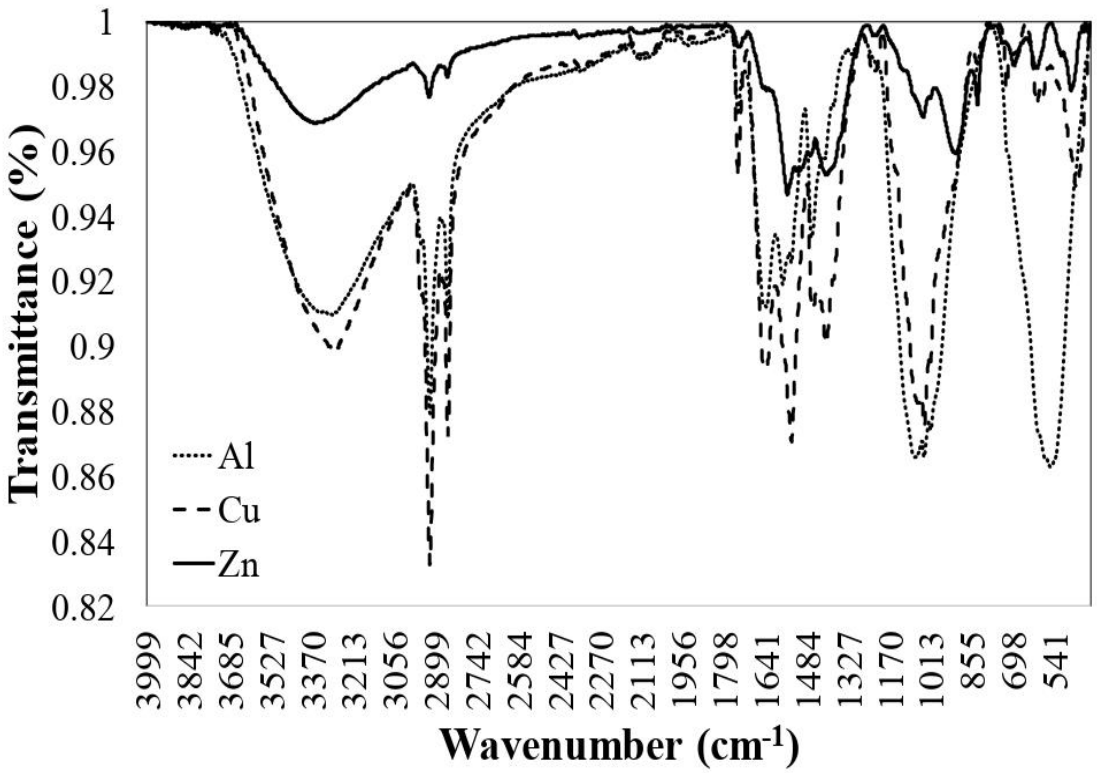

Figure 10.FTIR spectra of sludge generated during EC process with electrodes of a) Al, b) Zn and c) Cu.

3.8. Operating cost of the EC process

The operating costs in this work were calculated by Equation 6, for each electrical material at its best conditions. The calculations were made based on the quantity of electricity that has passed through the electrochemical cell [94] and the results are summarized in Table 3. Actually, these costs can be taken as savings since the energy was supplied by a deep cycle battery of which the CD was controlled by a current regulator.

The deep cycle battery was charged by a solar panel. Thus, the supplied solar irradiation was a function of the site where the experiment was conducted, while the instantaneous solar irradiation was observed to vary with the meteorological conditions: roughly, sunny or cloudy [95]. Average solar radiation was obtained from the values of NASA [96]. This work was carried out with the following coordinates: 19.399, -99.714. The program estimated the value of 5.46 kWh/m^2/day.

Faradaic efficiency (FE) was calculated with Equation 28 [97] where C(measured) is equal to the metal measured concentration in the bulk solution divided by C(faraday) that is the theoretical concentration calculated by Faraday's law. The FE close to 1 means optimum system performance and the production of Cu(II), Al(III) and Zn(II). Through this Equation, it is shown that the Zinc electrode gives off almost twice the theoretical, because the solid phase is always in equilibrium with the liquid phase with fast external mass transport [98], this happened by the Zn oxidation with the simultaneous water reduction to form hydrogen, applied current (i), and solution pH [99,100]. With the electrodes of Al and Cu, there was a FE> 100 because the applied current was diverted to secondary electrochemical reactions to proceed [101].

$$FE\% = [C(measured)/C(faraday)](100) \quad (28)$$

Table 3. Operating costs and Faradaic efficiency

Electrode material	**Costs**		**Theoretical concentration of the sacrificial anode**	**Faradaic efficiency (%)**
	Units			
	kwh/L	Cent (US)/L	mg/L	
Aluminum	0.0044	0.0176	138	77.1
Zinc	0.0003	0.0012	100	198.6
Copper	0.0037	0.0148	486	54.7

561 According to the results observed in table 3, FE is higher when the Zn electrodes are used at a
562 current density of 0.356 mA/cm^2. This is because zinc hydroxides generate ZnO(s) (Equation 29)
563 [102]. This produces a layer on the anode, which may generate electro-oxidation as shown in
564 Equation 30, because of ZnO has the capacity to function as a photoanode [103]. Due to this the
565 sludge production is very small.

566 $$Zn(OH)_2 \rightarrow ZnO + H_2O \quad (29)$$

567 $$H_2O + ZnO \rightarrow ZnO(^{\circ}OH) + H^+ + e^- \quad (30)$$

568

569 As current density increases, however, the FE decreases to 27.68% with a C(faraday) equal to 500
570 mg/L and a C(measured) equal to 138.4 mg/L.

571

572 **4. Conclusions**

573

574 An industrial wastewater sample from chocolate industry was characterized according to standard
575 methods. High nitrogen and phosphorous contents were identified and this could cause
576 eutrophication if such wastewater is discharged without a previous treatment.

577 A solar-photovoltaic electrocoagulation system was proposed to treat the chocolate wastewater
578 using Al, Cu and Zn as anodic materials. The effect of pH (4.38 and 7), current density (1.781
579 mA/cm^2 and 0.356 mA/cm^2) at 60 min treatment were studied.

580 The Aluminium system exhibited the best results for organic parameters. The achieved COD
581 removal was 50% and BOD was reduced 39%. The BI was increased considerably from 0.49 to
582 0.59. TOC was diminished only 26.65%

583 The Copper system also showed a promising behaviour in the organics removal: 43% COD, 53%
584 BOD, 30.7% TOC and the BI was 0.4.

585

586 The Zinc system was found to be slightly less efficient than the Cu and Al systems. The removal
587 achieved were 39% COD, 30% BOD_5,19% TOC. The BI shows an increase from 0.49 to 0.56,
588 improving the biodegradability of wastewater. Colour and turbidity presented a reduction of 89.5
589 % and 73.86%, respectively.

590

591 The energy cost of the three treatments is low, if the electricity grid was to be used. In this case,
592 the real cost regarding electricity consumption is nil because solar energy was used.
593
594
595 **Acknowledgment**
596
597 We are grateful for financial support provided by the CONACYT, scholarship CVU 626446. We
598 thank Universidad Autómoma Del Estado de México Projects number 4986/2020CIB and
599 4967/2020 CIB for the support and the infrastructure provided to carry out the research project and
600 to the Autonomous University of Campeche for the analysis of FRX and SEM-EDS. Finally, to the
601 technicians; Dr. Ildefonso Esteban Pech Pech, Mtra. Yolanda Espinosa Morales, Mtra. Lizbeth
602 Triana Cruz and Mtra. Melina Tapia Tapia for the analysis of SEM-EDS, XRF and IR. The
603 technical support of Citlalit Martínez is also acknowledged.
604
605 **References**
606
607 [1] A. Konstantas, H.K. Jeswani, L. Stamford, A. Azapagic, Environmental impacts of
608 chocolate production and consumption in the UK, Food Res. Int. 106 (2018) 1012–1025.
609 https://doi.org/10.1016/j.foodres.2018.02.042.
610 [2] F.P. Francis, C. Ramalingam, Hybrid hydrogel dispersed low fat and heat resistant
611 chocolate, J. Food Eng. (2019). https://doi.org/10.1016/j.jfoodeng.2019.03.012.
612 [3] P.J. Gallo, R. Antolin Lopez, I. Montiel, Associative Sustainable Business Models: Cases
613 in the bean-to-bar chocolate industry, J. Clean. Prod. 174 (2018) 905–916.
614 https://doi.org/10.1016/j.jclepro.2017.11.021.
615 [4] M. Kiumarsi, D. Majchrzak, S. Yeganehzad, H. Jäger, M. Shahbazi, Comparative study of
616 instrumental properties and sensory profiling of low-calorie chocolate containing
617 hydrophobically modified inulin. Part 1: Rheological, thermal, structural and external
618 preference mapping, Food Hydrocoll. 104 (2020) 105698.
619 https://doi.org/10.1016/j.foodhyd.2020.105698.
620 [5] S.T. Beckett, Industrial Chocolate Manufacture and Use, 4 th, Singapore: Blackwell.,
621 2009.

[6] F. Recanati, D. Marveggio, G. Dotelli, From beans to bar: A life cycle assessment towards sustainable chocolate supply chain, Sci. Total Environ. 613–614 (2018) 1013–1023. https://doi.org/10.1016/j.scitotenv.2017.09.187.

[7] Y. Jin, S. Kang, D. Hee, Y. Jin, W. Ri, Y. Min, S. Park, Calorie reduction of chocolate ganache through substitution of whipped cream, J. Ethn. Foods. 4 (2017) 51–57. https://doi.org/10.1016/j.jef.2017.02.002.

[8] H.K. Khuntia, N. Janardhana, H.N. Chanakya, Fractionation of FOG (fat, oil, grease), wastewater and particulate solids based on low-temperature solidification and stirring, J. Water Process Eng. 34 (2020) 101167. https://doi.org/10.1016/j.jwpe.2020.101167.

[9] M. Kindlein, E. Elts, H. Briesen, Phospholipids in chocolate: Structural insights and mechanistic explanations of rheological behavior by coarse-grained molecular dynamics simulations, J. Food Eng. (2018). https://doi.org/10.1016/j.jfoodeng.2018.02.014.

[10] I. Magalhães, L.D.F. Vilela, C. Santos, N. Lima, R.F. Schwan, Volatile compounds and protein profiles analyses of fermented cocoa beans and chocolates from different hybrids cultivated in Brazil, Food Res. Int. (2018) #pagerange#. https://doi.org/10.1016/j.foodres.2018.04.012.

[11] S.A. Patil, V.P. Surakasi, S. Koul, S. Ijmulwar, A. Vivek, Y.S. Shouche, B.P. Kapadnis, Electricity generation using chocolate industry wastewater and its treatment in activated sludge based microbial fuel cell and analysis of developed microbial community in the anode chamber, Bioresour. Technol. 100 (2009) 5132–5139. https://doi.org/10.1016/j.biortech.2009.05.041.

[12] O.S. Toker, N. Konar, I. Palabiyik, H.R. Pirouzian, S. Oba, D.G. Polat, E.S. Poyrazoglu, O. Sagdic, Formulation of Dark Chocolate as a Carrier to Deliver Eicosapentaenoic and Docosahexaenoic acids: Effects on Product Quality, Food Chem. (2018). https://doi.org/10.1016/j.foodchem.2018.02.019.

[13] P.I. Omwene, M. Kobya, O.T. Can, Phosphorus removal from domestic wastewater in electrocoagulation reactor using aluminium and iron plate hybrid anodes, Ecol. Eng. 123 (2018) 65–73. https://doi.org/10.1016/j.ecoleng.2018.08.025.

[14] B. Kruszewski, M.W. Obiedziński, J. Kowalska, PT SC Faculty of Food Sciences , Department of Food Technology , Warsaw University of Life, J. Food Compos. Anal. (2017). https://doi.org/10.1016/j.jfca.2017.12.012.

653 [15] G.Z. Kyzas, K.A. Matis, Electroflotation process: A review, J. Mol. Liq. 220 (2016) 657–
654 664. https://doi.org/10.1016/j.molliq.2016.04.128.
655 [16] E. GilPavas, I. Dobrosz-Gómez, M.Á. Gómez-García, Optimization of sequential chemical
656 coagulation - electro-oxidation process for the treatment of an industrial textile
657 wastewater, J. Water Process Eng. 22 (2018) 73–79.
658 https://doi.org/10.1016/j.jwpe.2018.01.005.
659 [17] S.M. Safwat, Treatment of real printing wastewater using electrocoagulation process with
660 titanium and zinc electrodes, J. Water Process Eng. 34 (2020) 101137.
661 https://doi.org/10.1016/j.jwpe.2020.101137.
662 [18] B.K. Nandi, S. Patel, Effects of operational parameters on the removal of brilliant green
663 dye from aqueous solutions by electrocoagulation, Arab. J. Chem. 10 (2013) S2961–
664 S2968. https://doi.org/10.1016/j.arabjc.2013.11.032.
665 [19] U. Tezcan Un, S.E. Onpeker, E. Ozel, The treatment of chromium containing wastewater
666 using electrocoagulation and the production of ceramic pigments from the resulting sludge,
667 J. Environ. Manage. 200 (2017) 196–203. https://doi.org/10.1016/j.jenvman.2017.05.075.
668 [20] J. Lu, Z. Wang, X. Ma, Q. Tang, Y. Li, Modeling of the electrocoagulation process: A
669 study on the mass transfer of electrolysis and hydrolysis products, Chem. Eng. Sci. 165
670 (2017) 165–176. https://doi.org/10.1016/j.ces.2017.03.001.
671 [21] C. Hu, J. Sun, S. Wang, R. Liu, H. Liu, J. Qu, Enhanced efficiency in HA removal by
672 electrocoagulation through optimizing flocs properties: Role of current density and pH,
673 Sep. Purif. Technol. 175 (2017) 248–254. https://doi.org/10.1016/j.seppur.2016.11.036.
674 [22] D.T. Moussa, M.H. El-Naas, M. Nasser, M.J. Al-Marri, A comprehensive review of
675 electrocoagulation for water treatment: Potentials and challenges, J. Environ. Manage. 186
676 (2017) 24–41. https://doi.org/10.1016/j.jenvman.2016.10.032.
677 [23] A.M.H. Elnenay, E. Nassef, G.F. Malash, M.H.A. Magid, Treatment of drilling fluids
678 wastewater by electrocoagulation, Egypt. J. Pet. 26 (2017) 203–208.
679 https://doi.org/10.1016/j.ejpe.2016.03.005.
680 [24] A.K. Prajapati, P.K. Chaudhari, D. Pal, A. Chandrakar, R. Choudhary, Electrocoagulation
681 treatment of rice grain based distillery effluent using copper electrode, J. Water Process
682 Eng. 11 (2016) 1–7. https://doi.org/10.1016/j.jwpe.2016.03.008.
683 [25] D. Sun, X. Hong, K. Wu, K.S. Hui, Y. Du, K.N. Hui, Simultaneous removal of ammonia

and phosphate by electro-oxidation and electrocoagulation using RuO2–IrO2/Ti and microscale zero-valent iron composite electrode, Water Res. 169 (2020) 115239. https://doi.org/10.1016/j.watres.2019.115239.

[26] H. Elnakar, I. Buchanan, Soluble chemical oxygen demand removal from bypass wastewater using iron electrocoagulation, Sci. Total Environ. 706 (2020) 136076. https://doi.org/10.1016/j.scitotenv.2019.136076.

[27] Z. Qi, S. You, N. Ren, Wireless Electrocoagulation in Water Treatment Based on Bipolar Electrochemistry, Electrochim. Acta. 229 (2017) 96–101. https://doi.org/10.1016/j.electacta.2017.01.151.

[28] N. Fayad, T. Yehya, F. Audonnet, C. Vial, Preliminary purification of volatile fatty acids in a digestate from acidogenic fermentation by electrocoagulation, Sep. Purif. Technol. (2017). https://doi.org/10.1016/j.seppur.2017.04.041.

[29] V.K. Sandhwar, B. Prasad, Terephthalic acid removal from aqueous solution by electrocoagulation and electro-Fenton methods: Process optimization through response surface methodology, Process Saf. Environ. Prot. 107 (2017) 269–280. https://doi.org/10.1016/j.psep.2017.02.014.

[30] F.Y. AlJaberi, Operating cost analysis of a concentric aluminum tubes electrodes electrocoagulation reactor, Heliyon. 5 (2019) e02307. https://doi.org/10.1016/j.heliyon.2019.e02307.

[31] O. Dia, P. Drogui, G. Buelna, R. Dub??, B.S. Ihsen, Electrocoagulation of bio-filtrated landfill leachate: Fractionation of organic matter and influence of anode materials, Chemosphere. 168 (2017) 1136–1141. https://doi.org/10.1016/j.chemosphere.2016.10.092.

[32] M. Kobya, H. Hiz, E. Senturk, C. Aydiner, E. Demirbas, Treatment of potato chips manufacturing wastewater by electrocoagulation, Desalination. 190 (2006) 201–211. https://doi.org/10.1016/j.desal.2005.10.006.

[33] G. Roa-Morales, E. Campos-Medina, J. Aguilera-Cotero, B. Bilyeu, C. Barrera-Díaz, Aluminum electrocoagulation with peroxide applied to wastewater from pasta and cookie processing, Sep. Purif. Technol. 54 (2007) 124–129. https://doi.org/10.1016/j.seppur.2006.08.025.

[34] M. Kobya, S. Delipinar, Treatment of the baker's yeast wastewater by electrocoagulation, J. Hazard. Mater. 154 (2008) 1133–1140. https://doi.org/10.1016/j.jhazmat.2007.11.019.

715 [35] D. Valero, J.M. Ortiz, V. García, E. Expósito, V. Montiel, A. Aldaz, Electrocoagulation of
716 wastewater from almond industry, Chemosphere. 84 (2011) 1290–1295.
717 https://doi.org/10.1016/j.chemosphere.2011.05.032.
718 [36] N. Lakshmi Kruthika, S. Karthika, G. Bhaskar Raju, S. Prabhakar, Efficacy of
719 electrocoagulation and electrooxidation for the purification of wastewater generated from
720 gelatin production plant, J. Environ. Chem. Eng. 1 (2013) 183–188.
721 https://doi.org/10.1016/j.jece.2013.04.017.
722 [37] C. Tsioptsias, D. Petridis, N. Athanasakis, I. Lemonidis, A. Deligiannis, P. Samaras, Post-
723 treatment of molasses wastewater by electrocoagulation and process optimization through
724 response surface analysis, J. Environ. Manage. 164 (2015) 104–113.
725 https://doi.org/10.1016/j.jenvman.2015.09.007.
726 [38] A.S. Fajardo, R.F. Rodrigues, R.C. Martins, L.M. Castro, R.M. Quinta-Ferreira, Phenolic
727 wastewaters treatment by electrocoagulation process using Zn anode, Chem. Eng. J. 275
728 (2015) 331–341. https://doi.org/10.1016/j.cej.2015.03.116.
729 [39] B. Michel, N. Mazet, P. Neveu, Experimental investigation of an open thermochemical
730 process operating with a hydrate salt for thermal storage of solar energy: Local reactive
731 bed evolution, Appl. Energy. 180 (2016) 234–244.
732 https://doi.org/10.1016/j.apenergy.2016.07.108.
733 [40] F. Urban, S. Geall, Y. Wang, Solar PV and solar water heaters in China: Different
734 pathways to low carbon energy, Renew. Sustain. Energy Rev. 64 (2016) 531–542.
735 https://doi.org/10.1016/j.rser.2016.06.023.
736 [41] APHA/AWWA/WEF, Standard Methods for the Examination of Water and Wastewater,
737 Stand Meth, 2012.
738 [42] I. Puigdomenech, Hydrochemical Equilibrium Constants Database (MEDUSA), Royal
739 Institute of Technology, Stockholm, Sweden., (1997).
740 [43] F. Paillet, C. Barrau, R. Escudi, E. Trably, ScienceDirect Inhibition by the ionic strength of
741 hydrogen production from the organic fraction of municipal solid waste, (2019) 1–10.
742 https://doi.org/10.1016/j.ijhydene.2019.08.019.
743 [44] B.K. Nandi, S. Patel, Effects of operational parameters on the removal of brilliant green
744 dye from aqueous solutions by electrocoagulation, Arab. J. Chem. 10 (2017) S2961–
745 S2968. https://doi.org/10.1016/j.arabjc.2013.11.032.

[45] L.S. Thakur, P. Mondal, Simultaneous arsenic and fluoride removal from synthetic and real groundwater by electrocoagulation process: Parametric and cost evaluation, J. Environ. Manage. 190 (2017) 102–112. https://doi.org/10.1016/j.jenvman.2016.12.053.

[46] F. Hussin, F. Abnisa, G. Issabayeva, M.K. Aroua, Removal of lead by solar-photovoltaic electrocoagulation using novel perforated zinc electrode, J. Clean. Prod. 147 (2017) 206–216. https://doi.org/10.1016/j.jclepro.2017.01.096.

[47] (Comisión Federal de Electricidad) CFE, Consulta tu tarifa, 2019. (n.d.). https://app.cfe.mx/aplicaciones/ccfe/tarifas/tarifas/Tarifas_casa.asp?Tarifa=DACTAR1&anio=2018 (accessed May 19, 2020).

[48] V.M. Garcia Orozco, C.E. Barrera Diaz, G. Roa Morales, I. Linares Hernandez, A Comparative Electrochemical-Ozone Treatment for Removal of Phenolphthalein, J. Chem. 2016 (2016). https://doi.org/10.1155/2016/8105128.

[49] Metcalf, Eddy, Wastewater Engineering: Treatment and Reuse. McGraw-Hill, editor. 1058., 2013.

[50] P.J. Panikulam, N. Yasri, E.P.L. Roberts, Electrocoagulation using an oscillating anode for kaolin removal, J. Environ. Chem. Eng. 6 (2018) 2785–2793. https://doi.org/10.1016/j.jece.2018.04.020.

[51] N. Fayad, T. Yehya, F. Audonnet, C. Vial, Preliminary purification of volatile fatty acids in a digestate from acidogenic fermentation by electrocoagulation, Sep. Purif. Technol. 184 (2017) 220–230. https://doi.org/10.1016/j.seppur.2017.04.041.

[52] M. Elazzouzi, K. Haboubi, M.S. Elyoubi, Electrocoagulation flocculation as a low-cost process for pollutants removal from urban wastewater, Chem. Eng. Res. Des. 117 (2017) 614–626. https://doi.org/10.1016/j.cherd.2016.11.011.

[53] M. Kobya, E. Gengec, E. Demirbas, Operating parameters and costs assessments of a real dyehouse wastewater effluent treated by a continuous electrocoagulation process, Chem. Eng. Process. Process Intensif. 101 (2016) 87–100. https://doi.org/10.1016/j.cep.2015.11.012.

[54] A. Barhoumi, S. Ncib, A. Chibani, K. Brahmi, W. Bouguerra, E. Elaloui, Industrial Crops & Products High-rate humic acid removal from cellulose and paper industry wastewater by combining electrocoagulation process with adsorption onto granular activated carbon, Ind. Crop. Prod. 140 (2019) 111715. https://doi.org/10.1016/j.indcrop.2019.111715.

[55] M. Priya, J. Jeyanthi, Removal of COD, oil and grease from automobile wash water effluent using electrocoagulation technique., Microchem. J. 150 (2019) 104070. https://doi.org/10.1016/j.microc.2019.104070.

[56] S. Aksu, Electrochemical equilibria of copper in aqueous phosphoric acid solutions, J. Electrochem. Soc. 156 (2009). https://doi.org/10.1149/1.3215996.

[57] E.A. Dowman, Conservation in Field Archaeology, ilustrada, Universidad de Virginia, 1970.

[58] C. Barrera Díaz, B. Frontana Uribe, B. Bilyeu, Removal of organic pollutants in industrial wastewater with an integrated system of copper electrocoagulation and electrogenerated H2O2, Chemosphere. 105 (2014) 160–164. https://doi.org/10.1016/j.chemosphere.2014.01.026.

[59] K. Sardari, J. Askegaard, Y.H. Chiao, S. Darvishmanesh, M. Kamaz, S.R. Wickramasinghe, Electrocoagulation followed by ultrafiltration for treating poultry processing wastewater, J. Environ. Chem. Eng. 6 (2018) 4937–4944. https://doi.org/10.1016/j.jece.2018.07.022.

[60] K. Sardari, P. Fyfe, D. Lincicome, S.R. Wickramasinghe, Aluminum electrocoagulation followed by forward osmosis for treating hydraulic fracturing produced waters, Desalination. 428 (2018) 172–181. https://doi.org/10.1016/j.desal.2017.11.030.

[61] E.P. Banczek, P.R.P. Rodrigues, I. Costa, The effects of niobium and nickel on the corrosion resistance of the zinc phosphate layers, Surf. Coatings Technol. 202 (2008) 2008–2014. https://doi.org/10.1016/j.surfcoat.2007.08.039.

[62] O. Girčiene, R. Ramanauskas, L. Gudavičiute, A. Martušiene, Formation of conversion Zn-Ni-Mn phosphate coatings on steel and corrosion behaviour of phosphated specimens in a chloride-contaminated alkaline solution, Chemija. 24 (2013) 182–189.

[63] Y.D. Xu, S. Qi, L. Wang, M. Shi, N. Ding, Z.C. Pang, Q. Wang, X.D. Peng, Effects of Hydroxylamine Sulfate and Sodium Nitrite on Microstructure and Friction Behavior of Zinc Phosphating Coating on High Carbon Steel, Chinese J. Chem. Phys. 28 (2015) 197–202. https://doi.org/10.1063/1674-0068/28/cjcp1411201.

[64] S. Garcia-Segura, M.M.S.G. Eiband, J.V. de Melo, C.A. Martínez-Huitle, Electrocoagulation and advanced electrocoagulation processes: A general review about the fundamentals, emerging applications and its association with other technologies, J.

808 Electroanal. Chem. 801 (2017) 267–299. https://doi.org/10.1016/j.jelechem.2017.07.047.
809 [65] M. Doerre, L. Hibbitts, G. Patrick, N. Akafuah, Advances in Automotive Conversion
810 Coatings during Pretreatment of the Body Structure: A Review, Coatings. 8 (2018) 405.
811 https://doi.org/10.3390/coatings8110405.
812 [66] Y. Orita, M. Akizuki, Y. Oshima, Kinetic analysis of zinc oxide anisotropic growth in
813 supercritical water, J. Supercrit. Fluids. 154 (2019) 104609.
814 https://doi.org/10.1016/j.supflu.2019.104609.
815 [67] K.S. Hashim, N. Jasim, A. Shaw, D. Phipps, P. Kot, A.W. Alattabi, M. Abdulredha, R.
816 Alawsh, Separation and Puri fi cation Technology Electrocoagulation as a green
817 technology for phosphate removal from river water, 210 (2019) 135–144.
818 https://doi.org/10.1016/j.seppur.2018.07.056.
819 [68] M.A. Mamelkina, R. Tuunila, M. Sillänpää, A. Häkkinen, Systematic study on sulfate
820 removal from mining waters by electrocoagulation, Sep. Purif. Technol. 216 (2019) 43–50.
821 https://doi.org/10.1016/j.seppur.2019.01.056.
822 [69] B.M.B. Ensano, L. Borea, V. Naddeo, V. Belgiorno, M.D.G. de Luna, M. Balakrishnan,
823 F.C. Ballesteros, Applicability of the electrocoagulation process in treating real municipal
824 wastewater containing pharmaceutical active compounds, J. Hazard. Mater. (2018).
825 https://doi.org/10.1016/j.jhazmat.2018.07.093.
826 [70] N. Dizge, C. Akarsu, Y. Ozay, H.E. Gulsen, S.K. Adiguzel, M.A. Mazmanci, Sono-
827 assisted electrocoagulation and cross-flow membrane processes for brewery wastewater
828 treatment, J. Water Process Eng. 21 (2018) 52–60.
829 https://doi.org/10.1016/j.jwpe.2017.11.016.
830 [71] T. Foudhaili, T. V Rakotonimaro, C.M. Neculita, L. Coudert, O. Lefebvre, Journal of
831 Environmental Chemical Engineering Comparative e ffi ciency of microbial fuel cells and
832 electrocoagulation for the treatment of iron-rich acid mine drainage, J. Environ. Chem.
833 Eng. 7 (2019) 103149. https://doi.org/10.1016/j.jece.2019.103149.
834 [72] A. Mohammadi, A. Khadir, R.M.A. Tehrani, Journal of Environmental Chemical
835 Engineering Optimization of nitrogen removal from an anaerobic digester e ffl uent by
836 electrocoagulation process, J. Environ. Chem. Eng. 7 (2019) 103195.
837 https://doi.org/10.1016/j.jece.2019.103195.
838 [73] M.A. Behnajady, N. Modirshahla, F. Ghanbary, A kinetic model for the decolorization of

C . I . Acid Yellow 23 by Fenton process, 148 (2007) 98–102. https://doi.org/10.1016/j.jhazmat.2007.02.003.

[74] Z. Chen, X. Dou, Y. Zhang, M. Yang, D. Wei, Rapid thermal-acid hydrolysis of spiramycin by silicotungstic acid under microwave irradiation, Environ. Pollut. (2019). https://doi.org/10.1016/j.envpol.2019.02.074.

[75] E. Pinheiro, S.E.C. Bottrel, M.C.V.M. Starling, M.M.D. Leão, C.C. Amorim, Degradation of carbendazim in water via photo-Fenton in Raceway Pond Reactor : assessment of acute toxicity and transformation products, (2018).

[76] S. Tunc, O. Duman, Monitoring the Decolorization of Acid Orange 8 and Acid Red 44 from Aqueous Solution Using Fenton ' s Reagents by Online Spectrophotometric Method : E ff ect of Operation Parameters and Kinetic Study, (2013).

[77] C. Arat, E. Biçer, Electrochemical Monitoring of Decolorization of Diazo Dye Evans Blue by Fenton Process under Anaerobic Conditions : Kinetics and Optimization 1, 51 (2015) 730–742. https://doi.org/10.1134/S1023193515080029.

[78] S.S. Celalettin Ozdemir, Muhammed K Oden, and D. Guclu, The sonochemical decolorisation of textile Coloration Technology, (2011) 268–273. https://doi.org/10.1111/j.1478-4408.2011.00310.x.

[79] K. W. Whitten, R. E. Davis, L. Peck, G.G. Stanley, Student Solutions Manual, 2013.

[80] C. Comninellis, G. Chen, Electrochemistry for the Environment, 1st ed., 2010. https://doi.org/10.1007/978-0-387-68318-8.

[81] R.E. Lobnig, R.P. Frankenthal, D.J. Siconolfi, J.D. Sinclair, M. Stratmann, Mechanism of Atmospheric Corrosion of Copper in the Presence of Submicron Ammonium Sulfate Particles at 300 and 373 K, 141 (1994) 2935–2941.

[82] F. Habashi, S.A. Mikhail, Reduction of binary sulfate mixtures containing CuSO 4 by H 2 , Can. J. Chem. 54 (1976) 3651–3657. https://doi.org/10.1139/v76-525.

[83] S. Koter, M. Kultys, B. Gilewicz-Łukasik, I. Koter, Modeling the transport of sulfuric acid and its sulfates (MgSO4, ZnSO4, Na2SO4) through an anion-exchange membrane, Desalination. 342 (2014) 75–84. https://doi.org/10.1016/j.desal.2013.10.025.

[84] C. Qiao, L. Shen, L. Hao, X. Mu, J. Dong, W. Ke, J. Liu, B. Liu, Corrosion kinetics and patina evolution of galvanized steel in a simulated coastal-industrial atmosphere, J. Mater. Sci. Technol. 35 (2019) 2345–2356. https://doi.org/10.1016/j.jmst.2019.05.039.

[85] F.U. Kac, M. Kobya, E. Gengec, Removal of humic acid by fixed-bed electrocoagulation reactor: Studies on modelling, adsorption kinetics and HPSEC analyses, J. Electroanal. Chem. 804 (2017) 199–211. https://doi.org/10.1016/j.jelechem.2017.10.009.

[86] S.U. Khan, D.T. Islam, I.H. Farooqi, S. Ayub, F. Basheer, Hexavalent Chromium Removal in an Electrocoagulation Column Reactor: Process Optimization using CCD, Adsorption kinetics and pH modulated Sludge formation, Process Saf. Environ. Prot. (2018). https://doi.org/10.1016/j.psep.2018.11.024.

[87] J.E.L. Villa, C.D. Pereira, S. Cadore, A novel, rapid and simple acid extraction for multielemental determination in chocolate bars, Microchem. J. 121 (2015) 199–204. https://doi.org/10.1016/j.microc.2015.03.008.

[88] A. Oulebsir, T. Chaabane, S. Zaidi, K. Omine, V. Alonzo, A. Darchen, T.A.M. Msagati, V. Sivasankar, Preparation of mesoporous alumina electro-generated by electrocoagulation in NaCl electrolyte and application in fluoride removal with consistent regenerations, Arab. J. Chem. (2017). https://doi.org/10.1016/j.arabjc.2017.04.007.

[89] A. Hubdar, A. Maitlo, J. Lee, J.Y. Park, J. Kim, K. Kim, J.H. Kim, An energy-efficient air-breathing cathode electrocoagulation approach for the treatment of arsenite in aquatic systems, J. Ind. Eng. Chem. (2019). https://doi.org/10.1016/j.jiec.2019.01.026.

[90] M. Elazzouzi, A. El Kasmi, K. Haboubi, M.S. Elyoubi, A novel electrocoagulation process using insulated edges of Al electrodes for enhancement of urban wastewater treatment: Techno-economic study, Process Saf. Environ. Prot. 116 (2018) 506–515. https://doi.org/10.1016/j.psep.2018.03.006.

[91] M. Molano-mendoza, D. Donneys-victoria, N. Marriaga-cabrales, M. Angel, G. Li, F. Machuca-martínez, MethodsX Synthesis of Mg-Al layered double hydroxides by electrocoagulation, MethodsX. 5 (2018) 915–923. https://doi.org/10.1016/j.mex.2018.07.019.

[92] O. Sahu, D.G. Rao, R. Gopal, A. Tiwari, D. Pal, Treatment of wastewater from sugarcane process industry by electrochemical and chemical process: Aluminum (metal and salt), J. Water Process Eng. 17 (2017) 50–62. https://doi.org/10.1016/j.jwpe.2017.03.005.

[93] P. Aswathy, R. Gandhimathi, S.T. Ramesh, P. V Nidheesh, Department of Civil Engineering , National Institute of Technology , Tiruchirappalli , Department of Civil Engineering , Vimal Jyothi Engineering College , Chemperi , Kannur , Sep. Purif.

Technol. (2016). https://doi.org/10.1016/j.seppur.2016.01.001.

[94] D.G. Bassyouni, H.A. Hamad, E.-S.Z. El-Ashtoukhy, N.K. Amin, M.M.A. El-Latif, Comparative performance of anodic oxidation and electrocoagulation as clean processes for electrocatalytic degradation of diazo dye Acid Brown 14 in aqueous medium, J. Hazard. Mater. 335 (2017) 178–187. https://doi.org/10.1016/j.jhazmat.2017.04.045.

[95] C. Phalakornkule, T. Luanwuthi, P. Neragae, E.J. Moore, A continuous-flow sparged packed-bed electrocoagulator for dye decolorization, J. Taiwan Inst. Chem. Eng. 64 (2016) 124–133. https://doi.org/10.1016/j.jtice.2016.03.046.

[96] (National Aeronautics and Space) NASA, POWER Data Access Viewer, (2018). https://power.larc.nasa.gov/data-access-viewer/ (accessed May 19, 2020).

[97] A.S. Naje, S. Chelliapan, Z. Zakaria, M.A. Ajeel, K. Sopian, H.A. Hasan, Electrocoagulation by solar energy feed for textile wastewater treatment including mechanism and hydrogen production using a novel reactor design with a rotating anode, RSC Adv. 6 (2016) 10192–10204. https://doi.org/10.1039/C5RA26032A.

[98] K. (The U. of B.C. Lukas Dubrawski, A THESIS SUBMITTED IN PARTIAL FULFILMENT OF THE REQUIREMENTS FOR THE DEGREE, Columbia, 2013.

[99] C.M. Van Genuchten, K.N. Dalby, M. Ceccato, S.L.S. Stipp, K. Dideriksen, Factors affecting the Faradaic efficiency of Fe(0) electrocoagulation, J. Environ. Chem. Eng. 5 (2017) 4958–4968. https://doi.org/10.1016/j.jece.2017.09.008.

[100] T.B. Pavón-silva, H. Romero-tehuitzil, G. Munguia, J. Huacuz-villamar, Photovoltaic Energy-Assisted Electrocoagulation of a Synthetic Textile Effluent, 2018 (2018).

[101] S. Müller, T. Behrends, C.M. van Genuchten, Sustaining efficient production of aqueous iron during repeated operation of Fe(0)-electrocoagulation, Water Res. 155 (2019) 455–464. https://doi.org/10.1016/j.watres.2018.11.060.

[102] M. Kumar, C. Sasikumar, Electrodeposition of Nanostructured ZnO Thin Film: A Review, Am. J. Mater. Sci. Eng. 2 (2014) 18–23. https://doi.org/10.12691/ajmse-2-2-2.

[103] C.B. Ong, L.Y. Ng, A.W. Mohammad, A review of ZnO nanoparticles as solar photocatalysts: Synthesis, mechanisms and applications, Renew. Sustain. Energy Rev. 81 (2018) 536–551. https://doi.org/10.1016/j.rser.2017.08.020.

4.2. Artículo científico 2. Electrocoagulation of chocolate industry wastewater in a 1 downflow column electrochemical reactor

En este apartado se encuentra el acuse de recibido del artículo, con el que se demuestra, que el articulo ya fue enviado en la revista Fuel, su factor de impacto es de 5.578, su editorial es ScienceDirect.

4.2.1. Acuse de envió del artículo

Gmail **VIOLETA garcia <violetamaricruz@gmail.com>**

Submission Confirmation
1 mensaje

Fuel <eesserver@eesmail.elsevier.com> 6 de marzo de 2020, 18:31
Responder a: Fuel <fuel@elsevier.com>
Para: reynanr@gmail.com, rnatividadr@uaemex.mx
Cc: violetamaricruz@gmail.com, gabyroamo@yahoo.com.mx, ivonnelinares1978@yahoo.com.mx, sejir@gmail.com, marcsalgado.94@gmail.com

*** Automated email sent by the system ***

Fuel
Title: RESIDUAL WATER ELECTROCOAGULATION OF A CHOCOLATE INDUSTRY IN A DOWNFLOW COLUMN ELECTROCHEMICAL REACTOR
Authors: Violeta M Garcia, master; Gabriela Roa, Doctor; Ivonne Linares; Irvin J Serrano; Marco Antonio Salgado-Catarino; Reyna Natividad, Ph.D.
Article Type: VSI:IMCCRE 2020

Dear Dr. Reyna Natividad,

Your submission entitled "RESIDUAL WATER ELECTROCOAGULATION OF A CHOCOLATE INDUSTRY IN A DOWNFLOW COLUMN ELECTROCHEMICAL REACTOR" has been received by Fuel.

You may check on the progress of your paper by logging on to the Elsevier Editorial System as an author. The URL is https://ees.elsevier.com/jfue/.

Your username is: reynanr@gmail.com
If you need to retrieve password details, please go to: http://ees.elsevier.com/jfue/automail_query.asp

Your manuscript will be given a reference number once an Editor has been assigned.

Thank you for submitting your work to this journal. Please do not hesitate to contact me if you have any queries.

Kind regards,

Fuel

****
For further assistance, please visit our customer support site at http://help.elsevier.com/app/answers/list/p/7923. Here you can search for solutions on a range of topics, find answers to frequently asked questions and learn more about EES via interactive tutorials. You will also find our 24/7 support contact details should you need any further assistance from one of our customer support representatives.

4.2.2. Artículo Científico enviado

ELECTROCOAGULATION OF CHOCOLATE INDUSTRY WASTEWATER IN A DOWNFLOW COLUMN ELECTROCHEMICAL REACTOR

V. M. García-Orozco[a], G. Roa-Morales[a,*], I. Linares-Hernández[b], I. J. Serrano-Jimenes[a], M. A. Salgado-Catarino[a], R. Natividad[a*]

[a]*Centro Conjunto de Investigación en Química Sustentable UAEM-UNAM, Universidad Autónoma del Estado de México, Carretera Toluca-Atlacomulco, Km 14.5, Campus San Cayetano, 50200 Toluca, MEX, México*

[b] *Instituto Interamericano de Tecnología y Ciencias de Agua (IITCA), Universidad Autónoma del Estado de México, Km.14.5, carretera Toluca-Atlacomulco, C.P 50200 Toluca, Estado de México, México*

**Corresponding author: gabyroam@gmail.com* reynanr@gmail.com Tel: Fax: 722 2766610 Ext. 7723

Highlights

- A Downflow Column Electrochemical reactor can be used for electrocoagulation
- Electrocoagulation removes a high concentration of organic and inorganic matter
- Hydrogen is produced during the electrocoagulation process
- This reactor allows to keep the hydrogen for a later utilization

Abstract

In this work, the performance of a Downflow Column Electrochemical Reactor (DCER) was assessed in an electrocoagulation process to remove organic and inorganic matter from the wastewater of a chocolate industry. To achieve so, aluminium electrodes were used as anode and cathode. The studied variables were electrical current 1.58 A (781mA/cm^2) and 3.16 A (562 mA/cm^2) and volumetric flowrate (0.060 L/s and 0.032 L/s). The joint effect of both variables was found to be important on COD removal. The processed wastewater volume was 6 L. The direct current was provided from a solar panel. The delivered charge to the system was regulated by an energy controller. Therefore, the electrical current was constant throughout the whole treatment and this leads to save energy. It was found that after the first 5 minutes of treatment, 51 COD% and 80% color were removed at 0.06 L/s and 3.16 A. Under these conditions the suspended solids were also removed. It was also concluded that one of the advantages of the assessed reactor is that the produced hydrogen is retained in the system without pressurizing the system. The resulting data were fitted by a Behnajady-Modirshahla – Ghanbery Model (BMG).

Keywords

Hydrogen production; Aluminium electrodes; Food industry; Electrochemical reactors; Electrocoagulators

77 **Introduction**

78 World population is constantly growing and this implies an increased consumption of
79 services[1,2], medicines[3], chemical products[4], clothes[5], food[6,7] and commodities[8]. The
80 impact of these industries on the environment is undeniable and the chocolate industry is not the
81 exception. In order to satisfy the worldwide demand chocolate is produced in large quantities every
82 year[9,10]. However, the chocolate industry generates different kind of waste like, that volatile
83 compounds (di and tri terpenes), flavonoids, polyphenols, pyrroles, methylxanthines, aldehydes,
84 phospholipids mixtures, ketones, liquid cocoa, butter triglycerides, aliphatic alcohols, glycolipids,
85 furans, sterols and saturated fats [11–14]. This has motivated the search for effective treatments
86 in order to reduce the amount of these pollutants before discharge. In this context, biological
87 treatments have been preferred. This type of treatments, though, are lengthy and require a fine
88 control of operational variables for the microorganisms to survive [15]. At this point, it is worth to
89 find more viable alternatives like electrochemical treatments.
90 Among electrochemical methods, Electrocoagulation (EC) allows to treat water with organic
91 matter and suspended solids. EC combines flotation, coagulation and oxidation o reduction of
92 pollutants compounds [16]. In the EC, an anode and cathode are necessary to carry out the
93 treatment. The anode works as a sacrificial electrode and by in-situ electrodissolution provides the
94 system with the coagulating agent. This anode can be made of aluminium, copper, magnesium,
95 iron, zinc and stainless steel [17–20] and in contact with the wastewater leads to hydrolysis
96 products (hydroxo-metal species) that are effective in the destabilization of pollutants.
97 Concomitantly, the reduction of water in the cathode occurs causing hydrogen gas bubbles and
98 hydroxide ions. This increases the pH in the bulk solution and produces sludge on the water surface
99 and this facilitates its removal [21]. The following reactions (Equations 1-2) occur at the anode
100 and cathode when Al electrodes are used [22].

Anode:

$$Al_{(s)} \rightarrow Al^{3+}_{(aq)} + 3e^- \quad (1)$$

Cathode:

$$2H_2O_{(l)} + 2e^- \rightarrow H_{2(g)} + 2OH^-_{(aq)} \quad (2)$$

In aqueous medium the following reaction might proceed (equations 3-5) [23–27],

$$2Al_{(s)} + 6H_2O_{(l)} \rightarrow 2Al(OH)_{3(s)} + 3H_{2(g)} \quad (3)$$

$$Al^{3+} + 3(OH)^- \rightarrow Al(OH)_3 \quad (4)$$

$$nAl(OH)^-_3 \rightarrow Al_n(OH)_{3n} \quad (5)$$

Different pollutants that have been successfully removed with EC: dyes, suspended solids, heavy metals, fluoride, hardness, arsenic, phosphate and pesticides [28–33]. This process is typically conducted in batch electrochemical cells with continuous stirring. At industrial scale, this is an alternative, however, might lead to mass transfer limitations thus reducing pollutants removal effectiveness. Therefore, this work aimed to assesses a rather novel technology in the field of electrochemistry, a Downflow Column Electrochemical Reactor (DCER). This in an ejector type reactor that was originally conceived as gas absorber. Later on, it evolved as three-phase reactor [34]. This is the first work where such technology is applied to conduct an electrocoagulation process. Aluminium electrodes were used and an effluent from the chocolate industry was treated so the effectiveness of the process was established.

2. Materials and methods

2.1. Wastewater samples

The wastewater is transported from a chocolate industry to a treatment plant. The sampling was conducted right before entering the treatment plant. The wastewater was collected in 20 L plastic containers and kept at 4 °C until treatment. However, the characterization was conducted within 24 h of collection.

2.2. Electrocoagulation treatment

DCER, consists of a downward parallel flow column, that is shaped like a cylinder (100 cm of height and 5 cm of diameter) with a capacity of 1.964 L. The system is depicted in figure 1. It can be observed that the liquid phase is fed at the top of the column and recirculated through the whole system and the breaking vessel that promotes the separation of hydrogen gas from the liquid phase in the reactor. This technology exploits an orifice on the top of the column to produce a Venturi effect that promotes mass transfer. The breaking vessel is a 5 L stainless steel reservoir with the following dimensions ($20x10^{-2}$ m in diameter and $15.9x10^{-2}$ m in height). There is a stainless steel coil heat exchanger placed inside this reservoir. By means of this coil, the temperature is kept constant since the pump transfers thermal energy to the solution. The aluminium electrodes (one pair of plates for the anode and one pair for the cathode) were placed inside the column. Between each pair of aluminium plates there was a 0.5 cm gap and between the anode and cathode the separation distance was 1cm, the aluminium plates dimensions were 92.5 cm in length, 0.318 cm of thickness and a width of 2.4 cm. The total volume of the electrodes was 0.282 L and therefore the total free volume inside the column was 1.682 L. Nevertheless, at all experiments a total volume of 6L was used and the studied liquid volumetric flowrates were 0.032 and 0.06 L/s. The

147 samples (20 mL) were taken at the point indicated in figure 1. The energy was supplied by a deep
148 flow battery charged by a solar panel, connected to a charge controller. The electrical current
149 supplied was 1.58 and 3.16 A. The initial conductivity in the sample (785.8 µS/cm) was not enough
150 to achieve the aforementioned electrical current values. Thus, sodium sulfate (1 M) was added in
151 order to increase the conductivity up to 1680 µS/cm. The working pH was 6.4 (initial pH of the
152 wastewater sample). At all experiments, the treatment time was 1h and were carried out by
153 duplicate.

154

155 **2.3.Methods of analysis**

156

157 The wastewater sample characterization was carried out according to APHA [35]. Turbidity, pH,
158 colour, total and faecal coliforms, chemical oxygen demand (COD), biochemical oxygen demand
159 (BOD_5), electrical conductivity, sulphates, nitrites, nitrates, ammoniacal nitrogen, phosphates,
160 fluoride, chlorides, Fe, Cu, Na, K, Mg, Al and Ca were determined. The samples were not filtered
161 before colour analysis, then the reported results correspond to the apparent colour.

162

163 The speciation diagrams were generated in the MEDUSA program [36]. For such a purpose the
164 total ionic force was used, it depends on the individual concentration of ions [37].
165 The sludge was quantified by determination of settleable solids in raw and treated wastewater in
166 mL/L [38]. Once the sample was filtered, the sludge was dried for 24 h at 105 °C and then weighed.

167

168

169 **2.4. Cost analysis determination**

According to literature [39–44], the cost of the EC treatment is the sum of the energy cost and electrode wear. In this work, the energy consumption of the pump and the cost generated by the sludge management were added as shown in equation 6 [45],

$$Operation\ Cost = aEC_{Electrode\ energy} + bEC_{Pump\ energy} + cEC_{Electrode} + dEC_{sludge} \quad (6)$$

Where $EC_{\text{Electrode}}$ is expressed as kg Al lost/m^3, EC_{Sludge} in kg/m^3, $EC_{\text{Electrode energy}}$ and $EC_{\text{Pump energy}}$ as kWh/ m^3, a equal to b (0.04 USD/ kWh) [46], c (2.008 USD /kg Al lost) and d is the cost of sludge confinement in Mexico (0.035 USD/kg) [45].

The amount of material released from the anode to the solution was calculated by Faraday's law (equation 7) [47–51],

$$EC_{Electrode}\ (kg/m^3) = itM/nFv \quad (7)$$

Where F is the Faraday's constant (96485 C/mol), i electrical current (A), t is time (s), v is the volume (L), n is equal to the number of electrons and M is Al atomic mass (g/mol).

To establish the cost of the energy consumed by the pump (1.119 kW) and electrodes during the treatment, Equation 8 is used [52],

$$EC_{Electrode\ energy}\ (kWh/m^3) = EC_{Pump\ energy}\ (kWh/m^3) = (iUt_1)/v \quad (8)$$

192 Where U is the voltage, t_1 is time (h), i (electrical current) and v (volume). In Mexico, the energy
193 cost is $ 0.956 (MXN currency) per kWh [53], the exchange rate for MXN to USD was considered
194 as 1 USD= 22.68 MXN.
195
196 **3. Results and discussion**
197 **3.1. Physicochemical characterization of industrial wastewater**
198 The physicochemical characteristics of the chocolate industry wastewater before EC treatment are
199 summarized in Table 1. The initial sample pH was 6.4 and it was not adjusted, all the experiments
200 were carried out at this value. The initial conductivity in the sample was 785.8 μS/cm, so sodium
201 sulfate (1 M) was added in order to increase the conductivity to 1680 μS/cm to carry out the EC
202 experiments. The chocolate industry sample showed a high organic content, COD (1732 mg/L)
203 and BOD_5 (1399.8 mg/L), the biodegradability index (BOD_5/COD) was 0.8, so the wastewater
204 sample was easily biodegradable. In addition apparent colour (1560 Pt-Co Units) and turbidity
205 (512.4 NTU) were ascribed to a high content of colloidal matter, so this type of water is suitable
206 to be treated by EC. The sample also had microbiological matter, faecal and total coliforms (1.4
207 $x10^6$ and 1.7 $x10^6$ MPN). The inorganic matter was also quantified (711.4 mg/L SO_4^{2-}). This
208 amount is the available for precipitation with the electrogenerated coagulant, phosphates were 26.9
209 mg/L. This is a low concentration in the context of chocolate industry wastewater. Ammoniacal
210 nitrogen was detected at 10 mg/L, nitrates 1.4 mg/L and nitrites 0.9 mg/L. The removal of nutrients
211 as phosphorous and nitrogen is important to reduce excessive growth of algae and the oxygen
212 depletion of the water body at the time of being discharged. Fluorides (0.3 mg/L) and chlorides
213 (169.7 mg/L) were also detected, the latter can promote indirectly the oxidation of organic matter
214 through the anodic oxidation of chlorides to chlorine gas or hypochlorite in aqueous solution.
215

The physicochemical characterization and the determination of anions and cations were of great importance to calculate the ionic strength (0.042 M) and to generate the speciation diagrams (figure 2). The concentration of Al (3.28 mM) was calculated by Faraday's law at 30 min, with a voltage of 9.65 V and a current of 3.16 A. The species diagram was generated at 1.58 A. The species diagram at pH 6.4 showed that $Al(OH)_3$ is produced by means of equation 3-4, and this resulted in a pH increase.

Table 1. Physicochemical Characteristics of wastewater before and after EC treatment.

Parameter	**Units**	**Before EC**	**After EC**	**% removal**	**NOM-001-SEMARNAT-1996. Rivers (Urban public use/Daily average)**[54]	**NOM-002-SEMARNAT-1996. (Daily average)**[55]
pH	-	6.4	7.4	-	-	-
Turbidity	NTU	512.4	37.8	92.6	-	-
Color	Pt-Co	1560	48.5	96.9	-	-
Total coliforms	MPN/100mL	$1.7x10^6$	<200	-	-	-
Fecal coliforms	MPN/100mL	$1.4x10^6$	<200	-	-	-
COD	mg/L	1732	640.5	63	-	-
BOD_5	mg/L	1399.8	329.6	76.5	150	-
Conductivity	µS/cm	1680	1495	11	-	-
Sulfates	SO_4^{2-}mg/L	711.4	519.8	26.9	-	-
Nitrites	$N\text{-}NO_2^-$ mg/L	0.9	0.4	55.6	-	-
Nitrates	$N\text{-}NO_3^-$ mg/L	1.4	1.1	21.4	-	-
Ammoniacal nitrogen	$N\text{-}NH_3$ mg/L	10	18	-	-	-
Phosphate	PO_4^{3-} mg/L	26.9	15.9	40.9	-	-

Fluoride	F^- mg/L	0.3	0.04	86.7	-	-
Chlorides	Cl^- mg/L	169.7	117.2	30.9	-	-
Fe	mg/L	1.4	0.6	57.1	-	-
Cu	mg/L	0.6	0.5	16.7	-	15
Na	mg/L	251.2	185.4	26.2	-	-
K	mg/L	10.4	8	23.1	-	-
Mg	mg/L	14.65	5.1	65.2	-	-
Al	mg/L	1.6	99.5 to pH 9 (14.09)	-	-	-
Ca	mg/L	30.3	16.7	44.9	-	-

224 * After precipitation

225

226 **3.2. Electrical current and volumetric flowrate effect**

227 Electrical current (*I*) is an important factor influencing the treatment performance of EC process
228 since this parameter controls the amount of Al released by the sacrificial anode, it also helps the
229 production of hydrogen in the cathode and the sludge generation [56].

230 Actually, figure 3 shows there is an important effect of electrical current on both, COD and Colour
231 removal. According to figure 3, the liquid volumetric flowrate also exerts an important effect on
232 COD removal but not on Colour. This effect is more pronounced in the first minutes of treatment
233 and will be further discussed later in this section. The effect of electrical current was expected
234 because enhances anodic dissolution and therefore the amount of Al released into solution.
235 Actually, the results in figure 3 suggests this step, the released of the Al into solution as limiting
236 of the process.

237 In the first 15 minutes Faraday's law was fulfilled, this means that a higher electrical current
238 removes higher COD and colour amounts. At this point it can not be said if such removal is due to
239 the inorganic compounds removal since they were only monitored at the beginning and at the end
240 of EC.

241

242 When changing liquid volumetric flowrate what is actually changing is the contact time and the
243 space velocity within the column where the electrodes are placed. In this work, this contact time
244 (τ) refers to the time that the liquid volume where the electrodes are placed (1.68 L) spends in
245 contact with the electrodes and it can also be defined as the time per pass per the electrochemical
246 section. It is worth to remember that in this section the following steps are occurring: *i*) the
247 electrochemical generation of Al^{3+} (reaction 1), *ii*) the transport of such ions to the bulk solution,
248 *iii*) formation of coagulating species (reaction 3-5) and *iv*) bonding of certain pollutants to the
249 coagulating species. It is also worth clarifying that steps iii and iv might proceed also in the rest of
250 the system, i.e. piping, pump and breaking vessel. Thus, contact time is the available time for step
251 *i* and *ii* to proceed per pass and not per treatment. The latter, treatment time, is the total time that
252 the liquid was recirculated through the whole system until the energy source was off. This
253 treatment time was 1 h for all experiments.

254 Two liquid volumetric flowrates were tested, 0.032 L/s and 0.06 L/s. The corresponding contact
255 times were 53 and 28 s, respectively. If this time is used in the Faraday Law, the amount of Al^{3+}
256 per pass can be calculated. Table 2 summarizes these values also as a function of applied electrical
257 current.

258 **Table 2.** Theoretical amount of generated Al^{3+} as a function of contact time and electrical applied
259 current

Volumetric flowrate (L/s)	Velocity (m/s)	Contact time (s)	Electric current (A)	Theoretical amount of aluminum (mg)

0.06	0.036	28.03	1.58	4.13
0.06	0.036	28.03	3.16	8.26
0.032	0.019	52.56	1.58	7.74
0.032	0.019	52.56	3.16	15.48

There is in figure 4 the effect of liquid volumetric flowrate and electrical current on the initial COD removal rate. It can be observed that there is not an effect on initial COD removal rate of applied electrical current at low volumetric flowrates. Since the generated Al^{3+} per pass increases when the applied electrical current increases (see table 2), then the observed increase in initial COD removal rate when the volumetric flowrate and the applied current increase can be ascribed to an improvement in step *i* and in mass transport, so the other three steps are also enhanced. The mass transport would be enhanced due to the increase in velocity and therefore in turbulence. When only Q_L is increased and I is kept at its lowest value, $-r_{COD,o}$ decreases despite the higher turbulence associated to the increase in velocity. This can be ascribed to the lower amount of Al^{3+} generated per pass (see table 2).

Figure 5 shows the effect of both variables, electrical current and liquid volumetric flowrate, on pH profiles. It can be observed that at all experiments, pH increases when treatment time increases. It can be observed, that volumetric flowrate affects the increase on pH only at low electrical currents while its effect is practically negligible at the highest applied electrical current. The observed increase in pH is due to the generation of hydroxide ions in the medium [21].

The best results were obtained at a high electrical current (3.16 A) and even at a fast Q_L (0.06 L / s). For this reason a full physicochemical characterization of the treated water under these

conditions was performed and the results are summarized in table 1. The characterized sample corresponds to the treatment time of 30 minutes.

As can be seen in table 1, the pH at the end of the treatment increased to 7.4 and this was ascribed to the produced aluminum hydroxides. Organic parameters as COD decreased from 1732 to 640.5 mg/L, achieving a removal efficiency of 63%. BOD was reduced from 1399.8 to 329.6 mg/L (76.5%). Thus the biodegradability index also decreased to 0.5, which is consistent with less biodegradable matter after the applied EC treatment. Turbidity and color were removed successfully, 92.6 % and 96.9% of suspended and dissolved colloids were eliminated. Microbiological parameters were decreased considerably after EC <200 MPN /100 mL of fecal and total coliforms were detected. Inorganic anions, like sulfates, were removed 26.9 % probably as aluminum sulfate, according to speciation diagrams the optimum precipitation of sulfates is pH 2-4, so that the initial sample pH (6.4) did not favor this mechanism. Phosphates were slightly diminished (40.9%). This could be ascribed to two reasons; the first one, considering the soluble chemical form at pH 6.4, as di-hydrogen and hydrogen phosphate ($H_2PO_4^-$ and HPO_4^{2-}). According to the speciation diagram, phosphates can precipitate at pH 12. The second reason of low removal could be associated to a relative low concentration of aluminum hydroxide, that although efficiently removes COD and color, the generated amount was not enough to act as a chelating agent for phosphates and other anions.

On the other hand, an increase of ammoniacal nitrogen from 10 mg/L to 18 mg/L was observed. This could be associated to the oxidation of organic nitrogen, due to the formation of chlorine gas by the anodic oxidation of chloride ions, according to equation 9,

$$2Cl^- \rightarrow Cl_2 + 2e^- \quad (9)$$

A part of the wastewater is coming from the toilets, this is very noticeable due to the high concentrations of faecal and total coliforms (urine and faeces). This contains nitrogen in the form of nitrite and nitrate [68].

Nitrates were reduced from 1.4 to 1.1 mg/L (21.4%) and nitrites from 0.9 to 0.4 mg/L (55.4%). According to Mook et al 2012, electrochemical technology can be applied to reduce nitrate ions to nitrite and finally to nitrogen gas on the cathode surface. Nitrate and nitrite ions are very soluble in water. Nitrite ions act as intermediate products and further react with water to generate nitrogen gas, ammonia and hydroxylamine (NH_2OH). Reduction of nitrate to nitrogen gas is the desired process but ammonia is usually formed, this is the main reason why ammonia nitrogen increases.

The ammonia and nitrite are the two main end products generated and are considered as major limitations to the efficacy of electrochemical denitrification. Also chlorine is oxidized at the anode and reacts with water to form hypochlorous acid (HOCl). The hypochlorite ions then react with nitrite and ammonia to produce nitrate and nitrogen [62]. Equation 10-16 represent the general mechanism involved in the electrochemical reduction of nitrate.

$$NO_3^- + H_2O + 2e^- \rightarrow NO_2^- + 2OH^- \quad (10)$$

$$NO_3^- + 3H_2O + 5e^- \rightarrow 1/2\,N_2 + 6OH^- \quad (11)$$

$$NO_3^- + 6H_2O + 8e^- \rightarrow NH_3 + 9OH^- \quad (12)$$

$$NO_2^- + 2H_2O + 3e^- \rightarrow 1/2\,N_2 + 4OH^- \quad (13)$$

$$NO_2^- + 5H_2O + 6e^- \rightarrow NH_3 + 7OH^- \quad (14)$$

$$NO_2^- + 4H_2O + 4e^- \rightarrow NH_2OH + 5OH^- \quad (15)$$

$$NO_3^- + 2H_2O \rightarrow NH_3 + 2O_2 + OH^- \quad (16)$$

The Mexican laws (NOM-001-SEMARNAT-1996 and NOM-002-SEMARNAT-1996)[54,55] do not contemplate the Al concentration in the permissible standards. The concentration of Al calculated with Faraday's law is 88.35 mg/L. The measured concentration in the bulk solution and without pH adjustment was 99.5 mg/L. The high concentration, above the theoretical could be associated to the super faradaic efficiency[63]. This occurred because into the reactor a greater wear of the anode is produced in a shorter period of time due to the mass transfer that exists in the system and it was controlled by the electrical current, as shown the Faraday's Law. After, the pH was adjusted to 9, to precipitate Al, the final concentration was 14.09 mg/L.

In this work, the electrode consumption was $88.35x10^{-3}$ kg Al lost/m^3, the electrode energy consumption was 2.54 kwh/m^3, the pump energy consumption was 93.25 kwh/m^3 and sludge production was equal to $119.2x10^{-3}$ kg/m^3 (69mL/L). The cost of this treatment was 4.01 USD/m^3. This cost was calculated taking into account the energy consumed (the pump and the electrode), the generated sludge and the wear of the electrodes.

The EC of this work was more economical with respect to energy consumption and electrode wear for the slaughterhouse (4.19±0.12kWh/m^3 and 1.29±0.00kg/m^3) [64], sugar industry (42kWh/m^3 and 0.795kg/m^3)[65] and dairy(45kWh and 1.566 kg/m^3)[66], these works removed between a 82 to 96.36% COD.

The cost of the photovoltaic installation was USD$ 284.68. This was calculated by taking into account the cost of one solar battery of deep cycle CALE of 12V/110AH (USD $132.78), one Solar Panel IUSA of 375W (USD$ 138.77) and one Solar charge controller Anself of 20A,

12V/24V (USD$13.13). Because the life of solar panels is around 20 years, the investment cost is considered minimum.

Electrocoagulation is a technique involving the electrolytic addition of coagulating metal ions directly from sacrificial electrodes. These ions coagulate with turbidity agents in the water (colloids) and allow the easier removal of pollutants. The main purpose of this study was to assess the COD and colour removal, however, a high removal of water turbidity (92.6%) was also obtained. Similar results were obtained by Rahmani 2008 on the removal of water turbidity by electrocoagulation also. It was found that in 20 minutes the removal efficiency by Al, Fe and St electrodes was 93, 91 and 51 percent, respectively [67].

In addition, it is worth pointing out that the produced hydrogen by reaction 3-4 was accumulated on top of the column and the liquid phase was downwards displaced. This is possible due to the presence of the breaking vessel (see figure 1). We believe that the ability of the system of retaining the hydrogen without pressurizing the system is an important advantage of this technology for further applications in the electrochemical field.

3.3 Modelling

The obtained results at the best conditions were fitted to power law kinetic models. A rather low correlation coefficient was obtained though. Therefore other kinetic models were tested. With the Behnajady-Modirshahla – Ghanbery Model (BMG) [71], an r^2 equal to 0.999 was obtained for Color and COD. This model is widely used for Advanced Oxidation Processes [72], and is mathematically described by Equation 17 [73],

372 $$C_t = \left(1 - (t/(m + bt_2))\right) * C_0 \quad (17)$$

373 Where C_0 is the initial sample concentration (COD or Colour, accordingly), C_t is final
374 concentration after a lapsed time (COD or Colour, accordingly) and t_2 is the treatment time in min.
375 1/m is the velocity produced at the start of the reaction and 1/b is the maximum theoretical fraction,
376 m and b being constants [74,75] calculated using Statistica 10 StatSoft®, in this case for the
377 removal of Color and COD and are summarized in Table 3.

378

379 **Table 3.** Parameters of BMG model and Correlation Coefficients (r^2)

Color removal			COD Removal		
m (min)	**b**	**r^2**	**m (min)**	**b**	**r^2**
1.1798	0.9841	0.999	2.7275	1.4776	0.999

380

381 In Figure 6 a)-b) it is observed that in this treatment in the first minutes the coagulant was generated
382 and after 10 minutes the coagulant retains the organic and inorganic matter that is in the solution
383 in a suspended way. Thus, the resulting sample is in two phases 1) the sludge and 2) the solution,
384 for that reason the Colour and COD removal is very high in the first minutes.
385 The constants m and b are smaller in Color removal than in COD, it causes that the initial removal
386 rate of Color is faster and more percentage of Color is removed than COD at the end of the reaction.
387 In the same image it is seen that the experimental results fit in an excellent way to the BMG model.

388

389 **Conclusions**

390

391 The remediation of wastewater (6L) from a chocolate industry was carried out in a Downflow
392 Column Electrochemical Reactor by electrocoagulation with aluminium electrodes under
393 recirculation. The electricity to energize the electrodes came from solar panels. It was concluded
394 that the variables that have the greatest impact on COD and color removal are the electrical current
395 and liquid volumetric flowrate. The former dictates the aluminium dose per pass of solution while
396 the latter determines the time per pass in contact with the electrodes and the effectiveness of the
397 contact between the generated Al species and pollutants. The inorganic and organic matter was
398 removed by the produced coagulant, $Al(OH)_3$, and hydrogen was simultaneously produced and
399 accumulated on top of the column. Under the studied conditions and after a treatment time of 30
400 min, the COD removal was 63% and 96.9% of colour when recirculation volumetric flowrate (Q_L)
401 was 0.06 L/s, the electrical current was 3.16 A at pH 6.4. The cost of this treatment taking into
402 account the energy consumed (the pump and the electrode), the generated sludge and the wear of
403 the electrodes were 4.01 USD/m^3. The treated effluent fulfils the mexican standard NOM-02-
404 SEMARNAT-1996. The resulting data are well represented by a Behnajady-Modirshahla –
405 Ghanbery Model (BMG).
406
407 **Acknowledgments**
408 V. García acknowledges CONACYT for financial support to conduct postgraduate studies.
409
410 **References**
411 [1] Golmohammadi A, Mattila AS, Gauri DK. Negative online reviews and consumers'
412 service consumption. J Bus Res 2020;116:27–36.
413 https://doi.org/10.1016/j.jbusres.2020.05.004.
414 [2] Galalae C, Kipnis E, Demangeot C. Reassessing positive dispositions for the consumption

415 of products and services with different cultural meanings: A motivational perspective. J
416 Bus Res 2020;115:160–73. https://doi.org/10.1016/j.jbusres.2020.04.043.
417 [3] Quadra GR, Silva PSA, Paranaíba JR, Josué IIP, Souza H, Costa R, et al. Investigation of
418 medicines consumption and disposal in Brazil : A study case in a developing country. Sci
419 Total Environ 2019;671:505–9. https://doi.org/10.1016/j.scitotenv.2019.03.334.
420 [4] Bolinius DJ, Sobek A, Löf MF, Undeman E. Evaluating the consumption of chemical
421 products and articles as proxies for diffuse emissions to the environment. Environ Sci
422 Process Impacts 2018;20:1427–40. https://doi.org/10.1039/c8em00270c.
423 [5] Stief P, Dantan J, Etienne A, Siadat A. One Consumption of France Consumer One year
424 year of of Clothing Clothing Consumption of a Female Consumer Felix to *, the , and
425 Müller a architecture of A new methodology functional physical Germany family
426 identification existing products for an assembly . Procedia CIRP 2019;80:417–21.
427 https://doi.org/10.1016/j.procir.2019.01.055.
428 [6] Tamburino L, Bravo G, Clough Y, Nicholas KA. From population to production: 50 years
429 of scientific literature on how to feed the world. Glob Food Sec 2020;24.
430 https://doi.org/10.1016/j.gfs.2019.100346.
431 [7] Tripathi AD, Mishra R, Maurya KK, Singh RB, Wilson DW. Estimates for world
432 population and global food availability for global health. Elsevier Inc.; 2018.
433 https://doi.org/10.1016/B978-0-12-813148-0.00001-3.
434 [8] Gilles RP, Gilles RP. Commodities, Consumption and Production. vol. i. 2019.
435 https://doi.org/10.1007/978-3-030-04426-8_1.
436 [9] Maddela NR, Kakarla D, García LC, Chakraborty S, Venkateswarlu K, Megharaj M.
437 Cocoa-laden cadmium threatens human health and cacao economy: A critical view. Sci

438 Total Environ 2020:137645. https://doi.org/10.1016/j.scitotenv.2020.137645.
439 [10] Konstantas A, Jeswani HK, Stamford L, Azapagic A. Environmental impacts of chocolate
440 production and consumption in the UK. Food Res Int 2018;106:1012–25.
441 https://doi.org/10.1016/j.foodres.2018.02.042.
442 [11] Magalhães I, Vilela LDF, Santos C, Lima N, Schwan RF. Volatile compounds and protein
443 profiles analyses of fermented cocoa beans and chocolates from different hybrids
444 cultivated in Brazil. Food Res Int 2018:#pagerange#.
445 https://doi.org/10.1016/j.foodres.2018.04.012.
446 [12] Kindlein M, Elts E, Briesen H. Phospholipids in chocolate: Structural insights and
447 mechanistic explanations of rheological behavior by coarse-grained molecular dynamics
448 simulations. J Food Eng 2018. https://doi.org/10.1016/j.jfoodeng.2018.02.014.
449 [13] Jin Y, Kang S, Hee D, Jin Y, Ri W, Min Y, et al. Calorie reduction of chocolate ganache
450 through substitution of whipped cream. J Ethn Foods 2017;4:51–7.
451 https://doi.org/10.1016/j.jef.2017.02.002.
452 [14] Toker OS, Konar N, Palabiyik I, Pirouzian HR, Oba S, Polat DG, et al. Formulation of
453 Dark Chocolate as a Carrier to Deliver Eicosapentaenoic and Docosahexaenoic acids:
454 Effects on Product Quality. Food Chem 2018.
455 https://doi.org/10.1016/j.foodchem.2018.02.019.
456 [15] Esparza-Soto M, Jacobo-López A, Lucero-Chávez M, Fall C. Anaerobic treatment of
457 chocolate-processing industry wastewater at different organic loading rates and
458 temperatures. Water Sci Technol 2019;79:2251–9. https://doi.org/10.2166/wst.2019.225.
459 [16] Moussa DT, El-Naas MH, Nasser M, Al-Marri MJ. A comprehensive review of
460 electrocoagulation for water treatment: Potentials and challenges. J Environ Manage

2017;186:24–41. https://doi.org/10.1016/j.jenvman.2016.10.032.

[17] Elnenay AMH, Nassef E, Malash GF, Magid MHA. Treatment of drilling fluids wastewater by electrocoagulation. Egypt J Pet 2017;26:203–8. https://doi.org/10.1016/j.ejpe.2016.03.005.

[18] Hu C, Sun J, Wang S, Liu R, Liu H, Qu J. Enhanced efficiency in HA removal by electrocoagulation through optimizing flocs properties: Role of current density and pH. Sep Purif Technol 2017;175:248–54. https://doi.org/10.1016/j.seppur.2016.11.036.

[19] Prajapati AK, Chaudhari PK, Pal D, Chandrakar A, Choudhary R. Electrocoagulation treatment of rice grain based distillery effluent using copper electrode. J Water Process Eng 2016;11:1–7. https://doi.org/10.1016/j.jwpe.2016.03.008.

[20] Tanner A, Devlin R, Kowalski MS, Zhang X, Wei V, Oleszkiewicz JA. Electrocoagulation of raw wastewater using aluminum, iron, and magnesium electrodes. J Hazard Mater 2018. https://doi.org/10.1016/j.jhazmat.2018.10.017.

[21] Dura A, Breslin CB. The removal of phosphates using electrocoagulation with Al−Mg anodes. J Electroanal Chem 2019;846:113161. https://doi.org/10.1016/j.jelechem.2019.05.043.

[22] Durango-Usuga P, Guzmán-Duque F, Mosteo R, Vazquez M V., Peñuela G, Torres-Palma RA. Experimental design approach applied to the elimination of crystal violet in water by electrocoagulation with Fe or Al electrodes. J Hazard Mater 2010;179:120–6. https://doi.org/10.1016/j.jhazmat.2010.02.067.

[23] Dolati M, Aghapour AA, Khorsandi H, Karimzade S. Boron removal from aqueous solutions by electrocoagulation at low concentrations. J Environ Chem Eng 2017;5:5150–6. https://doi.org/10.1016/j.jece.2017.09.055.

484 [24] Abdel-Aziz MH, El-Ashtoukhy ESZ, Sh. Zoromba M, Bassyouni M, Sedahmed GH.
485 Removal of nitrates from water by electrocoagulation using a cell with horizontally
486 oriented Al serpentine tube anode. J Ind Eng Chem 2020;82:105–12.
487 https://doi.org/10.1016/j.jiec.2019.10.001.
488 [25] Kobya M, Soltani RDC, Omwene PI, Khataee A. A review on decontamination of arsenic-
489 contained water by electrocoagulation: Reactor configurations and operating cost along
490 with removal mechanisms. Environ Technol Innov 2020;17.
491 https://doi.org/10.1016/j.eti.2019.100519.
492 [26] Tian Y, He W, Liang D, Yang W, Logan BE, Ren N. Effective phosphate removal for
493 advanced water treatment using low energy, migration electric–field assisted
494 electrocoagulation. Water Res 2018;138:129–36.
495 https://doi.org/10.1016/j.watres.2018.03.037.
496 [27] Elazzouzi M, El Kasmi A, Haboubi K, Elyoubi MS. A novel electrocoagulation process
497 using insulated edges of Al electrodes for enhancement of urban wastewater treatment:
498 Techno-economic study. Process Saf Environ Prot 2018;116:506–15.
499 https://doi.org/10.1016/j.psep.2018.03.006.
500 [28] Dura A, Breslin CB. Electrocoagulation using aluminium anodes activated with Mg, In
501 and Zn alloying elements. J Hazard Mater 2019;366:39–45.
502 https://doi.org/10.1016/j.jhazmat.2018.11.094.
503 [29] Emamjomeh MM. Electrocoagulation as a green technology for phosphate removal from
504 river water. Sep Purif Technol 2019;217:85. https://doi.org/10.1016/j.seppur.2019.02.019.
505 [30] Graça NS, Ribeiro AM, Rodrigues AE. Modeling the electrocoagulation process for the
506 treatment of contaminated water. Chem Eng Sci 2019;197:379–85.

https://doi.org/10.1016/j.ces.2018.12.038.

[31] Hashim KS, Jasim N, Shaw A, Phipps D, Kot P, Alattabi AW, et al. Separation and Puri fi cation Technology Electrocoagulation as a green technology for phosphate removal from river water 2019;210:135–44. https://doi.org/10.1016/j.seppur.2018.07.056.

[32] Ensano BMB, Borea L, Naddeo V, Belgiorno V, de Luna MDG, Balakrishnan M, et al. Applicability of the electrocoagulation process in treating real municipal wastewater containing pharmaceutical active compounds. J Hazard Mater 2018. https://doi.org/10.1016/j.jhazmat.2018.07.093.

[33] An C, Huang G, Yao Y, Zhao S. Emerging usage of electrocoagulation technology for oil removal from wastewater: A review. Sci Total Environ 2017;579:537–56. https://doi.org/10.1016/j.scitotenv.2016.11.062.

[34] Fishwick RP, Natividad R, Kulkarni R, McGuire PA, Wood J, Winterbottom JM, et al. Selective hydrogenation reactions: A comparative study of monolith CDC, stirred tank and trickle bed reactors. Catal Today 2007;128:108–14. https://doi.org/10.1016/j.cattod.2007.06.030.

[35] STATGRAPHICS® Centurion XVI. Statpoint Technologies.INC. n.d.

[36] Puigdomenech I. Hydrochemical Equilibrium Constants Database (MEDUSA), Royal Institute of Technology, Stockholm, Sweden. 1997.

[37] Paillet F, Barrau C, Escudié R, Trably E. Inhibition by the ionic strength of hydrogen production from the organic fraction of municipal solid waste. Int J Hydrogen Energy 2019:1–10. https://doi.org/10.1016/j.ijhydene.2019.08.019.

[38] NMX-AA-004-SCFI-2000. ANÁLISIS DE AGUA - DETERMINACIÓN DE SÓLIDOS SEDIMENTABLES EN AGUAS NATURALES , RESIDUALES Y RESIDUALES

530 TRATADAS - MÉTODO DE PRUEBA (CANCELA A LA NMX-AA-004-1977) 2000.
531 [39] Bener S, Bulca Ö, Palas B, Tekin G, Atalay S, Ersöz G. Electrocoagulation process for the
532 treatment of real textile wastewater : Effect of operative conditions on the organic carbon
533 removal and kinetic study. Process Saf Environ Prot 2019;129:47–54.
534 https://doi.org/10.1016/j.psep.2019.06.010.
535 [40] Khan SU, Islam DT, Farooqi IH, Ayub S, Basheer F. Hexavalent chromium removal in an
536 electrocoagulation column reactor: Process optimization using CCD, adsorption kinetics
537 and pH modulated sludge formation. Process Saf Environ Prot 2019;122:118–30.
538 https://doi.org/10.1016/j.psep.2018.11.024.
539 [41] Ya V, Martin N, Choo KH, Chou YH, Lee SJ, Le NC, et al. High-pressure
540 electrocoagulation system with periodic air replenishment for efficient dye wastewater
541 treatment: Reaction dynamics and cost evaluation. J Clean Prod 2019;213:1127–34.
542 https://doi.org/10.1016/j.jclepro.2018.12.249.
543 [42] Mena VF, Betancor-Abreu A, González S, Delgado S, Souto RM, Santana JJ. Fluoride
544 removal from natural volcanic underground water by an electrocoagulation process:
545 Parametric and cost evaluations. J Environ Manage 2019;246:472–83.
546 https://doi.org/10.1016/j.jenvman.2019.05.147.
547 [43] AlJaberi FY. Operating cost analysis of a concentric aluminum tubes electrodes
548 electrocoagulation reactor. Heliyon 2019;5:e02307.
549 https://doi.org/10.1016/j.heliyon.2019.e02307.
550 [44] Hussin F, Abnisa F, Issabayeva G, Aroua MK. Removal of lead by solar-photovoltaic
551 electrocoagulation using novel perforated zinc electrode. J Clean Prod 2017;147:206–16.
552 https://doi.org/10.1016/j.jclepro.2017.01.096.

553 [45] Castañeda LF, Coreño O, Nava JL, Carreño G. Removal of fluoride and hydrated silica
554 from underground water by electrocoagulation in a flow channel reactor. Chemosphere
555 2020;244:125417. https://doi.org/10.1016/j.chemosphere.2019.125417.
556 [46] CFE (Comisión Federal de Electricidad). Consulta tu tarifa. 2019 n.d.
557 https://app.cfe.mx/aplicaciones/ccfe/tarifas/tarifas/Tarifas_casa.asp?Tarifa=DACTAR1&a
558 nio=2018 (accessed May 19, 2020).
559 [47] Chen M, Dollar O, Shafer-Peltier K, Randtke S, Waseem S, Peltier E. Boron removal by
560 electrocoagulation: Removal mechanism, adsorption models and factors influencing
561 removal. Water Res 2020;170:115362. https://doi.org/10.1016/j.watres.2019.115362.
562 [48] Ziouvelou A, Tekerlekopoulou AG, Vayenas D V. A hybrid system for groundwater
563 denitrification using electrocoagulation and adsorption. J Environ Manage
564 2019;249:109355. https://doi.org/10.1016/j.jenvman.2019.109355.
565 [49] Maitlo HA, Lee J, Park JY, Kim JC, Kim KH, Kim JH. An energy-efficient air-breathing
566 cathode electrocoagulation approach for the treatment of arsenite in aquatic systems. J Ind
567 Eng Chem 2019;73:205–13. https://doi.org/10.1016/j.jiec.2019.01.026.
568 [50] Moussa DT, El-Naas MH, Nasser M, Al-Marri MJ. A comprehensive review of
569 electrocoagulation for water treatment: Potentials and challenges. J Environ Manage
570 2017;186:24–41. https://doi.org/10.1016/j.jenvman.2016.10.032.
571 [51] Liu Y, Yang J, Jiang W, Chen Y, Yang C, Wang T, et al. Experimental studies on the
572 enhanced performance of lightweight oil recovery using a combined electrocoagulation
573 and magnetic field processes. Chemosphere 2018;205:601–9.
574 https://doi.org/10.1016/j.chemosphere.2018.04.113.
575 [52] Garcia Orozco VM, Barrera Diaz CE, Roa Morales G, Linares Hernandez I. A

576 Comparative Electrochemical-Ozone Treatment for Removal of Phenolphthalein. J Chem
577 2016;2016. https://doi.org/10.1155/2016/8105128.
578 [53] Comisión Federal de Electricidad. Consulta tu tarifa 2019.
579 https://app.cfe.mx/aplicaciones/ccfe/tarifas/tarifas/Tarifas_casa.asp?Tarifa=DACTAR1&a
580 nio=2018 (accessed May 19, 2020).
581 [54] SEMARNAT. NORMA OFICIAL MEXICANA NOM-001-SEMARNAT-1996, QUE
582 ESTABLECE LOS LÍMITES MÁXIMOS PERMISIBLES DE CONTAMINANTES EN
583 LAS DESCARGAS DE AGUAS RESIDUALES EN AGUAS Y BIENES
584 NACIONALES 1996.
585 http://www.conagua.gob.mx/CONAGUA07/Publicaciones/Publicaciones/SGAA-15-
586 13.pdf (accessed June 22, 2020).
587 [55] SEMARNAT. NORMA OFICIAL MEXICANA NOM-002-SEMARNAT-1996, QUE
588 ESTABLECE LOS LÍMITES MÁXIMOS PERMISIBLES DE CONTAMINANTES EN
589 LAS DESCARGAS DE AGUAS RESIDUALES A LOS SISTEMAS DE
590 ALCANTARILLADO URBANO O MUNICIPAL 1996.
591 http://www.conagua.gob.mx/CONAGUA07/Publicaciones/Publicaciones/SGAA-15-
592 13.pdf (accessed June 23, 2020).
593 [56] Mamelkina MA, Tuunila R, Sillänpää M, Häkkinen A. Systematic study on sulfate
594 removal from mining waters by electrocoagulation. Sep Purif Technol 2019;216:43–50.
595 https://doi.org/10.1016/j.seppur.2019.01.056.
596 [57] Eyvaz M, Kirlaroglu M, Aktas TS, Yuksel E. The effects of alternating current
597 electrocoagulation on dye removal from aqueous solutions. Chem Eng J 2009;153:16–22.
598 https://doi.org/10.1016/j.cej.2009.05.028.

599 [58] Dizge N, Akarsu C, Ozay Y, Gulsen HE, Adiguzel SK, Mazmanci MA. Sono-assisted
600 electrocoagulation and cross-flow membrane processes for brewery wastewater treatment.
601 J Water Process Eng 2018;21:52–60. https://doi.org/10.1016/j.jwpe.2017.11.016.
602 [59] Foudhaili T, Rakotonimaro T V, Neculita CM, Coudert L, Lefebvre O. Journal of
603 Environmental Chemical Engineering Comparative e ffi ciency of microbial fuel cells and
604 electrocoagulation for the treatment of iron-rich acid mine drainage. J Environ Chem Eng
605 2019;7:103149. https://doi.org/10.1016/j.jece.2019.103149.
606 [60] Mohammadi A, Khadir A, Tehrani RMA. Journal of Environmental Chemical
607 Engineering Optimization of nitrogen removal from an anaerobic digester e ffl uent by
608 electrocoagulation process. J Environ Chem Eng 2019;7:103195.
609 https://doi.org/10.1016/j.jece.2019.103195.
610 [61] Chow H, Pham AL. Effective removal of silica and sulfide from oil sands thermal in-situ
611 produced water by electrocoagulation. J Hazard Mater 2019;380:120880.
612 https://doi.org/10.1016/j.jhazmat.2019.120880.
613 [62] Mook WT, Chakrabarti MH, Aroua MK, Khan GMA, Ali BS, Islam MS, et al. Removal
614 of total ammonia nitrogen (TAN), nitrate and total organic carbon (TOC) from
615 aquaculture wastewater using electrochemical technology: A review. Desalination
616 2012;285:1–13. https://doi.org/10.1016/j.desal.2011.09.029.
617 [63] Mechelhoff M, Kelsall GH, Graham NJD. Super-faradaic charge yields for aluminium
618 dissolution in neutral aqueous solutions. Chem Eng Sci 2013;95:353–9.
619 https://doi.org/10.1016/j.ces.2013.03.016.
620 [64] Asselin M, Drogui P, Benmoussa H, Blais JF. Effectiveness of electrocoagulation process
621 in removing organic compounds from slaughterhouse wastewater using monopolar and

622 bipolar electrolytic cells. Chemosphere 2008;72:1727–33.
623 https://doi.org/10.1016/j.chemosphere.2008.04.067.
624 [65] Sahu OP, Chaudhari PK. Electrochemical treatment of sugar industry wastewater: COD
625 and color removal. J Electroanal Chem 2015;739:122–9.
626 https://doi.org/10.1016/j.jelechem.2014.11.037.
627 [66] Lopes Geraldino HC, Simionato JI, De Souza Freitas, Thábata Formicoli K, Garcia JC, De
628 Carvalho Júnior O, Januario Correr C. Eficiência e custo operacional de um sistema de
629 eletrofloculação aplicado ao tratamento de efluente da indústria de laticínio. Acta Sci -
630 Technol 2015;37:401–8. https://doi.org/10.4025/actascitechnol.v37i3.26452.
631 [67] Rahmani A. Removal of water turbidity by the electrocoagulation method. J Res Health
632 Sci 2006;8:1–12.
633 [68] Hu C-W, Chang Y-J, Yen C-C, Chen J-L, Muthukumaran RB, Chao M-R. 15N-labelled
634 nitrite/nitrate tracer analysis by LC-MS/MS: Urinary and fecal excretion of nitrite/nitrate
635 following oral administration to mice. Free Radic Biol Med 2019.
636 https://doi.org/10.1016/j.freeradbiomed.2019.08.005.
637 [69] W. Whitten K, E. Davis R, Peck L, Stanley GG. Student Solutions Manual. 2013.
638 [70] Purwono, Rezagama A, Hibbaan M, Budihardjo MA. on The Process of Removing
639 Nitrogen By Using Tubular Plastic Media 2017;2508:4915–22.
640 [71] Behnajady MA, Modirshahla N, Ghanbary F. A kinetic model for the decolorization of C .
641 I . Acid Yellow 23 by Fenton process 2007;148:98–102.
642 https://doi.org/10.1016/j.jhazmat.2007.02.003.
643 [72] Chen Z, Dou X, Zhang Y, Yang M, Wei D. Rapid thermal-acid hydrolysis of spiramycin
644 by silicotungstic acid under microwave irradiation. Environ Pollut 2019.

645 https://doi.org/10.1016/j.envpol.2019.02.074.
646 [73] Pinheiro E, Bottrel SEC, Starling MCVM, Leão MMD, Amorim CC. Degradation of
647 carbendazim in water via photo-Fenton in Raceway Pond Reactor : assessment of acute
648 toxicity and transformation products 2018.
649 [74] Tunc S, Duman O. Monitoring the Decolorization of Acid Orange 8 and Acid Red 44
650 from Aqueous Solution Using Fenton ' s Reagents by Online Spectrophotometric
651 Method : E ff ect of Operation Parameters and Kinetic Study 2013.
652 [75] Arat C, Biçer E. Electrochemical Monitoring of Decolorization of Diazo Dye Evans Blue
653 by Fenton Process under Anaerobic Conditions : Kinetics and Optimization 1
654 2015;51:730–42. https://doi.org/10.1134/S1023193515080029.
655
656

657 **Figure Captions**

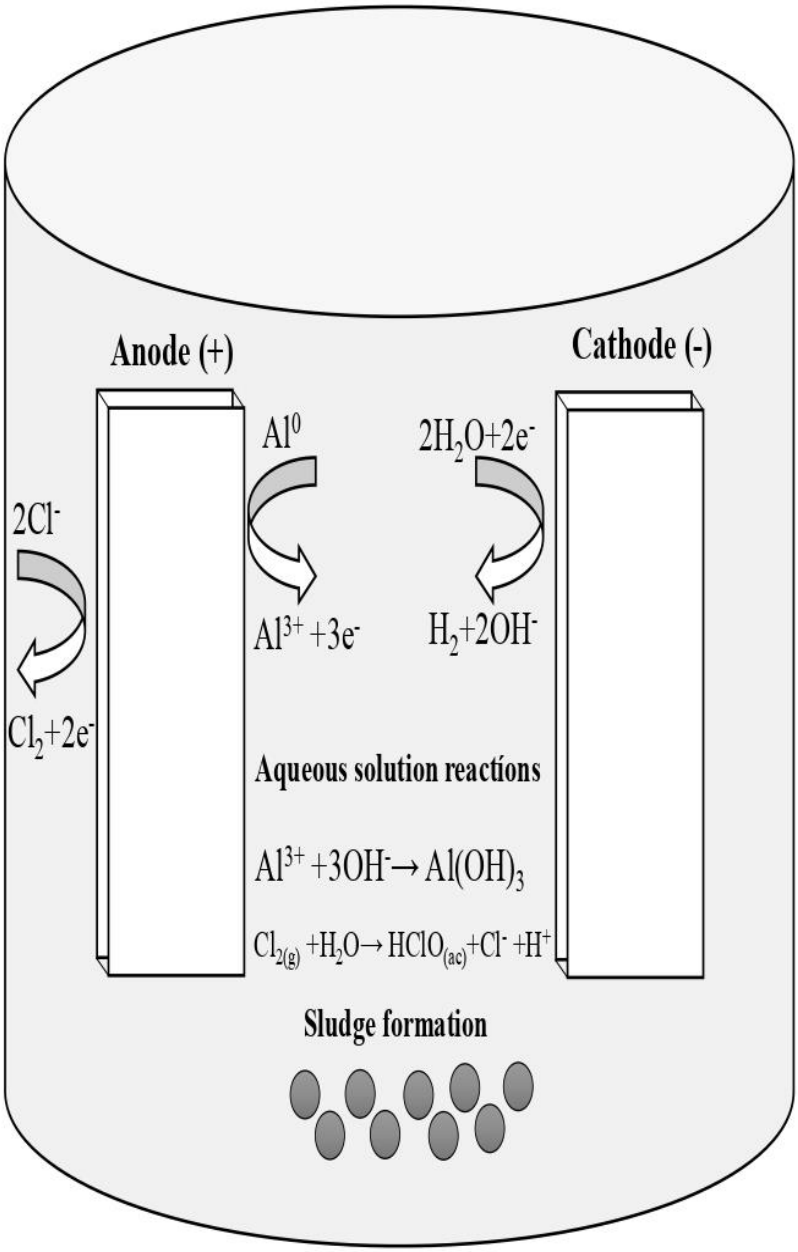

658

659 Graphical abstract

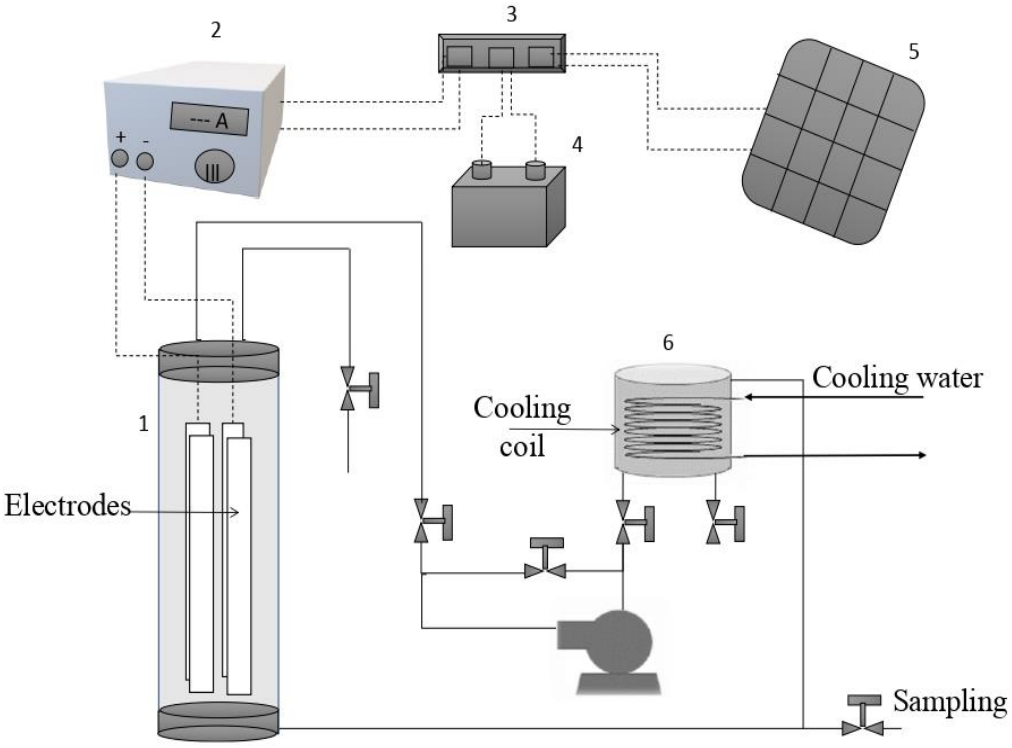

660

661 **Figure 1**. Experimental set up used for the electrocoagulation treatment. 1) Downflow Column

662 Electrochemical Reactor (DCER), 2) Current control, 3) Solar charge controller, 4) Battery, 5)

663 Solar Panel and 6) Breaking vessel

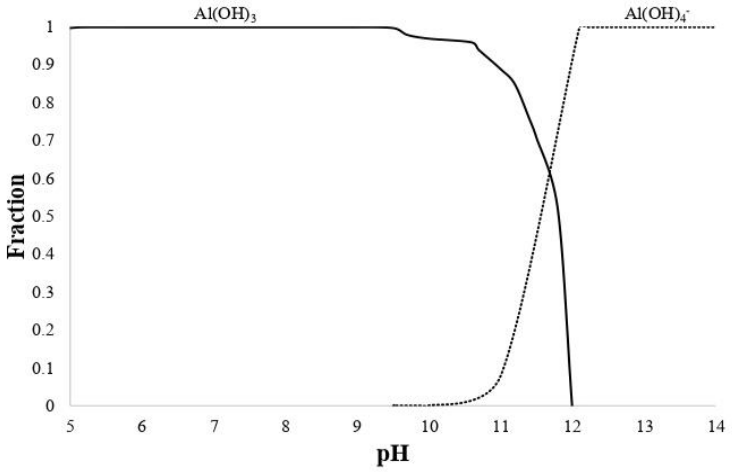

664

665 **Figure 2.** Aluminium species distribution diagram in wastewater as a function of pH.

666

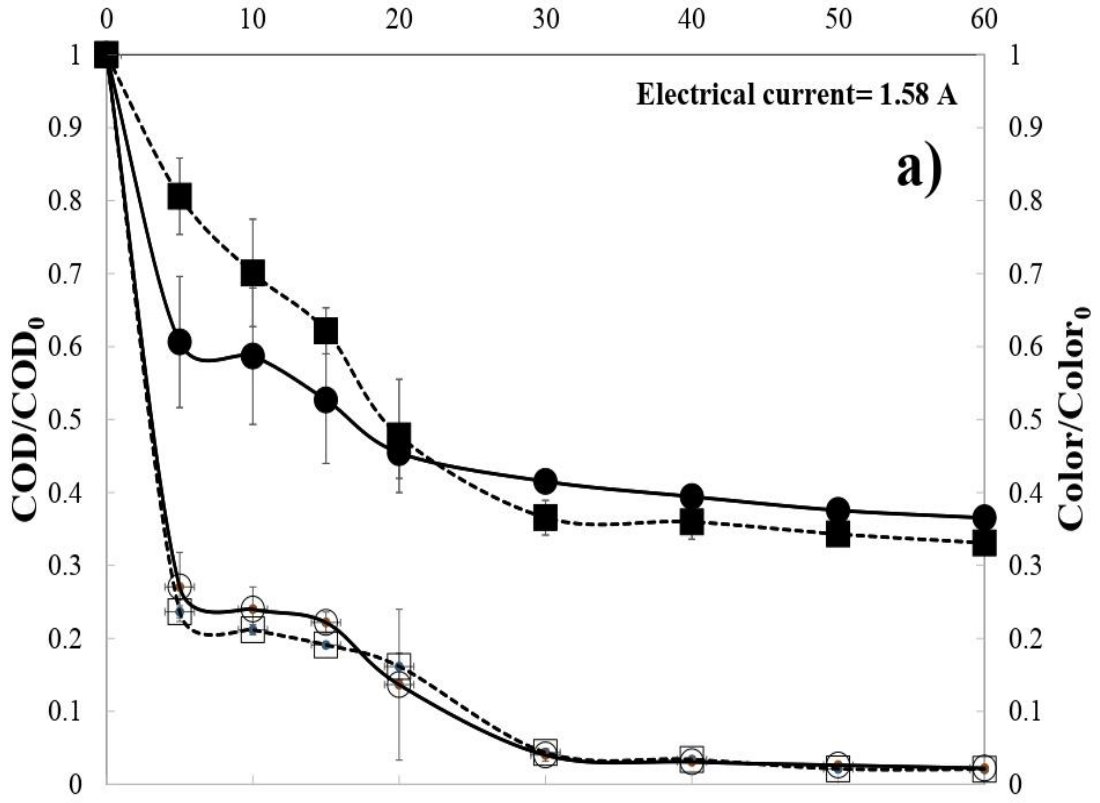
Electrical current= 1.58 A
a)
COD/COD0
Color/Color0
0
10
20
30
40
50
60
0
0.1
0.2
0.3
0.4
0.5
0.6
0.7
0.8
0.9
1

667

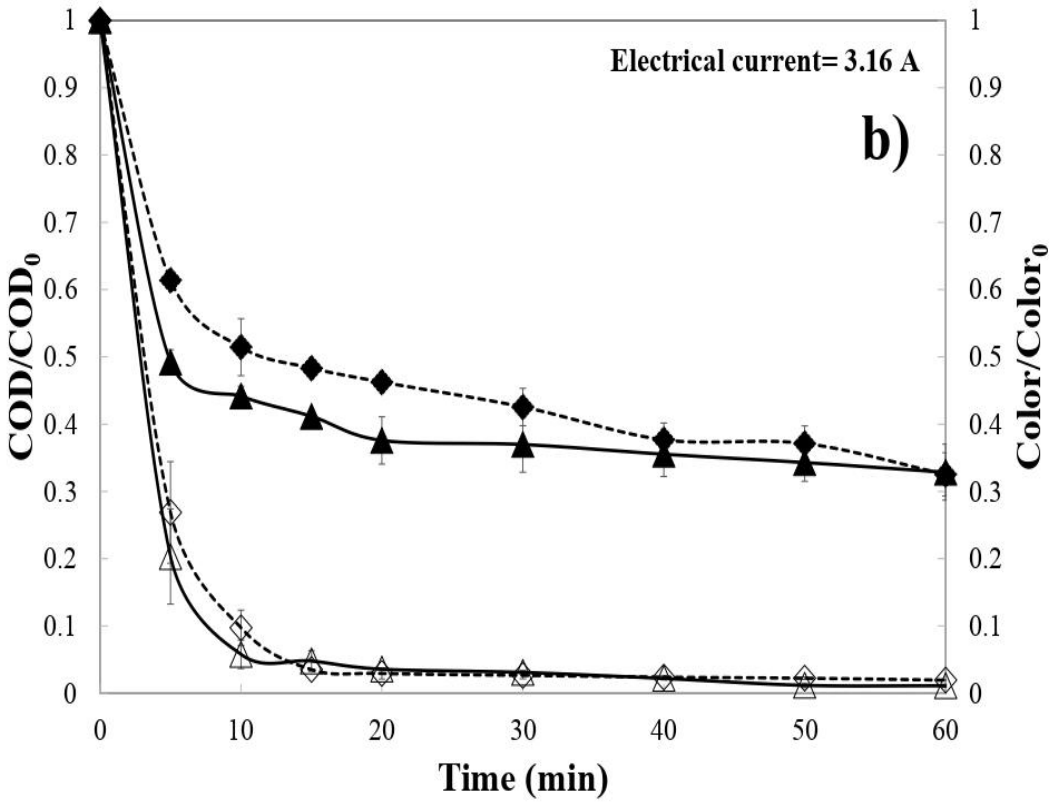

668

669 **Figure 3**. Effect of electrical current and treatment time on normalized Chemical Oxygen

670 Demand (COD) a) 1.58 A and b) 3.16 A, at Q_L 0.06 L/s and 0.032 L/s for COD (0.06 L/s ■,

671 0.032 L/s ●, 0.06 L/s ▲ and 0.032 L/s ♦) and Color (0.06 L/s □, 0.032 L/s ○, 0.06 L/s Δ and

672 0.032 L/s ◊).

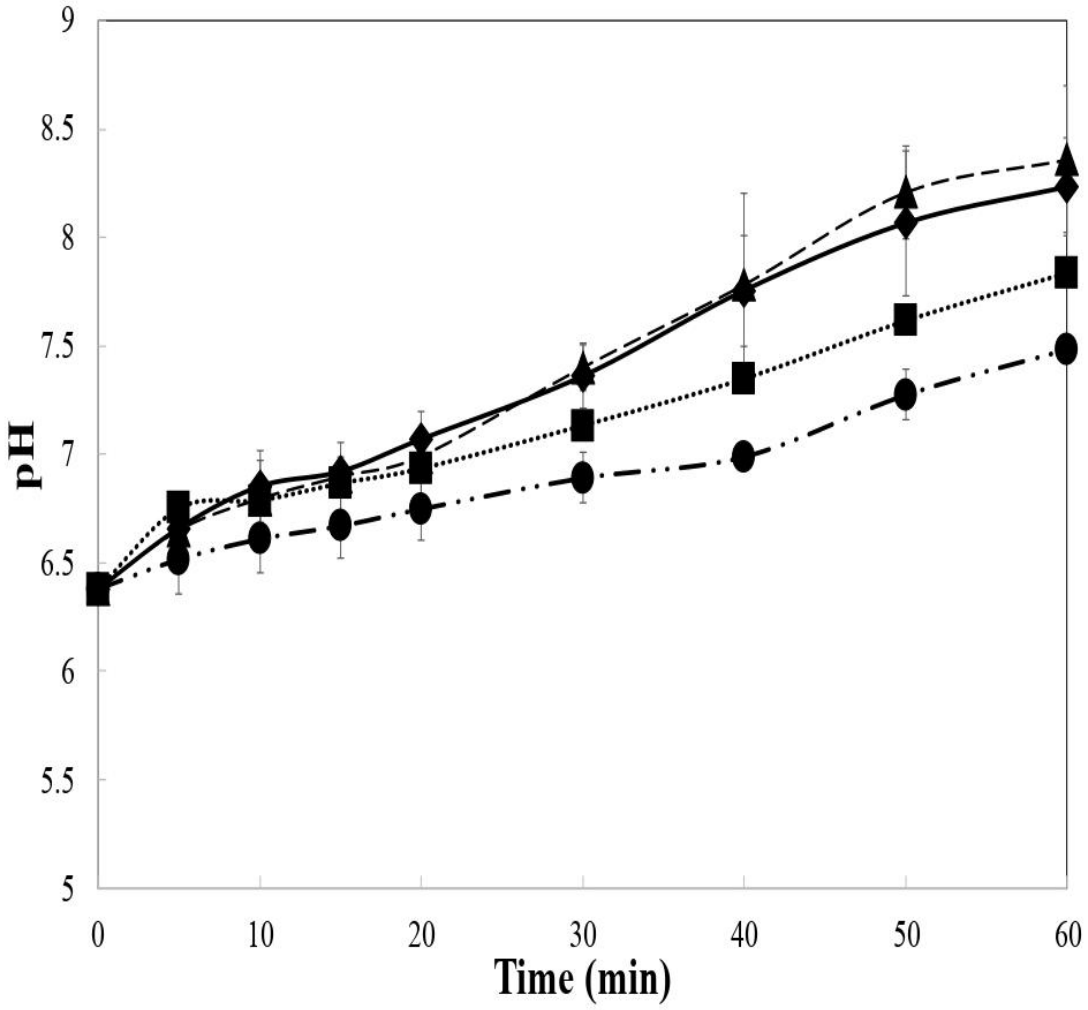

676

677 **Figure 5.** Effect of electrical current and volumetric flowrate on pH. electrical current=1.58 A

678 (0.06 L/s ■ and 0.032 L/s ●) and electrical current=3.16 A (0.06 L/s ▲ and 0.032 L/s ♦).

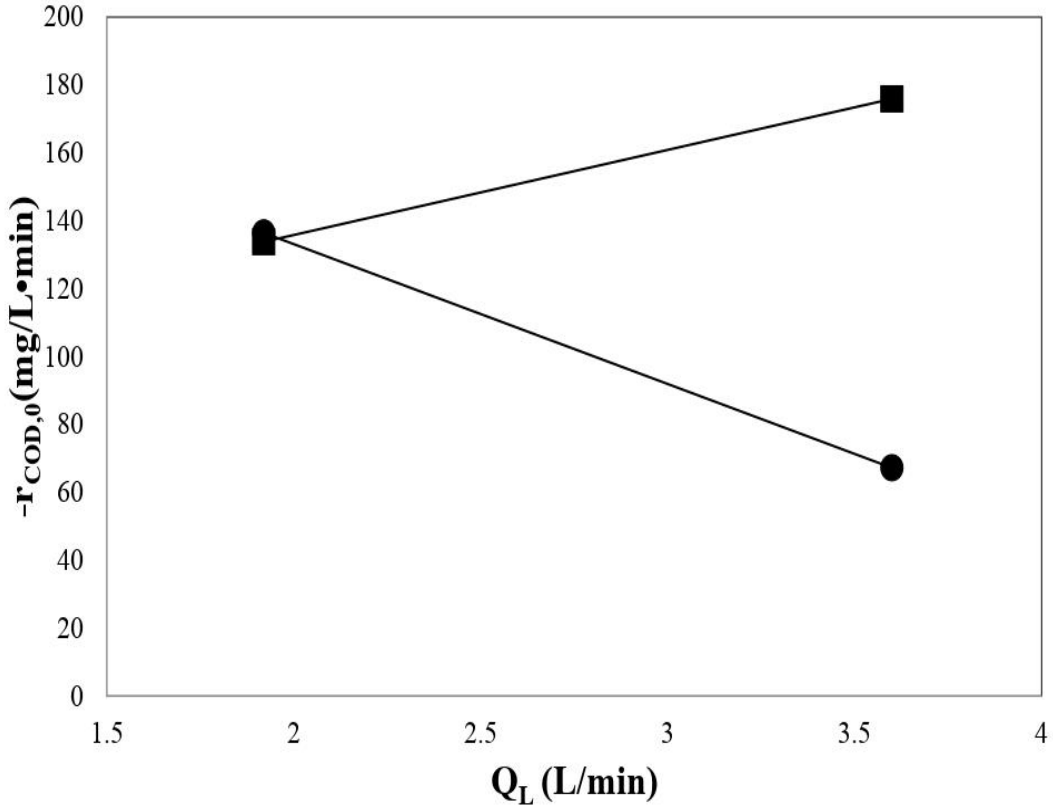

673

674 **Figure 4.** Effect of liquid volumetric flowrate (Q_L) and electrical current on initial removal rate

675 ($-r_{COD,0}$) at 1.58 A ● and 3.16 A■

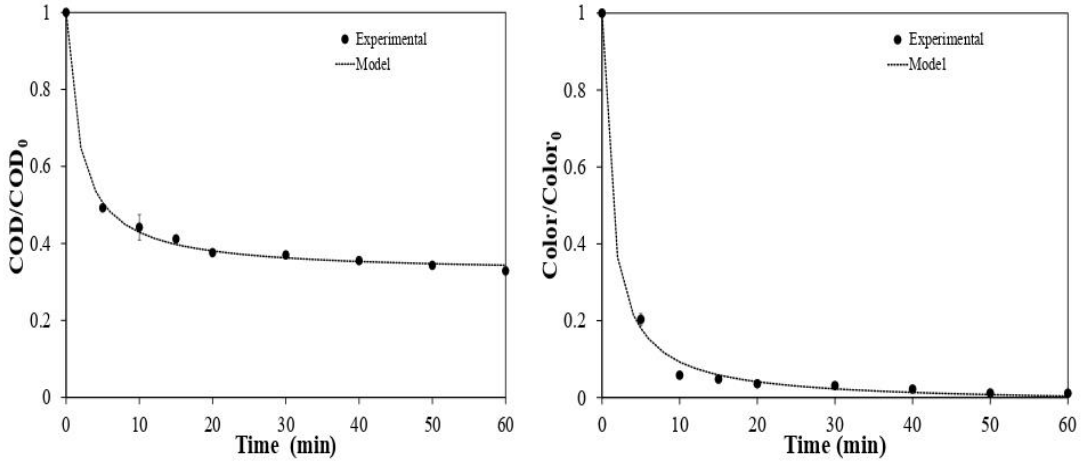

679

680 **Figure 6.** COD and Colour removal BMG modeling

4.3. Artículo científico 3. Importance of electrode tailoring in the coupling of electrolysis with renewable energy

En este apartado se encuentra el acuse de aceptado, en la revista ChemElectroChem, su factor de impacto es de 3.760.

4.3.1. Artículo aceptado

De: em.celc.0.6bf932.35deb348@editorialmanager.com <em.celc.0.6bf932.35deb348@editorialmanager.com> **En nombre de** ChemElectroChem
Enviado el: lunes, 15 de junio de 2020 15:16
Para: Manuel Andrés Rodrigo Rodrigo <Manuel.Rodrigo@uclm.es>
Asunto: Decision on your Manuscript celc.202000550 for ChemElectroChem - [EMID:5b1fb4280dcfab20]

Title: "Importance of electrode tailoring in the coupling of electrolysis with renewable energy"

DOI: 10.1002/celc.202000550
for citing the article before publication in an issue, please use this DOI number.

Dear Prof. Rodrigo,

Thank you for your submission of 15 Apr 2020. We sent the paper back to the referees and they were satisfied with the changes made, as are we - thank you for revising your manuscript according to the suggestions of the referees. Accordingly, we are pleased to inform you that the revised version of the above-mentioned manuscript has now been accepted for publication in ChemElectroChem.

4.3.2. Artículo Científico aceptado

ChemElectroChem | Articles
doi.org/10.1002/celc.202000550
Chemistry Europe
European Chemical Societies Publishing

Importance of Electrode Tailoring in the Coupling of Electrolysis with Renewable Energy

Violeta M. García-Orozco+,[b] Maria Millán+,[a] Justo Lobato,[a]
Carmen M. Fernández-Marchante,[a] Gabriela Roa-Morales,[b] Ivonne Linares-Hernández,[c]
Reyna Natividad,[b] and Manuel A. Rodrigo*[a]

In this work, the performance of an electrolyzer, used to treat a clopyralid waste and powered directly without regulation with a battery, has been evaluated and is shown to be influenced by the electrodes resistance Electrolyzers were equipped with electrodes consisting of the same boron-doped diamond (BDD) coating deposited on different substrate (Si, Ta and Nb). The results expose great differences despite using the same coating. Faster removal rates were attained with Ta- and Nb-BDD electrodes. The amount of energy required to attain the same removal efficiency showed great differences. Up to 1.95 mg/Wh of pesticide were removed when using Si, compared to 2.14 mg/Wh removed with Ta. Furthermore, the quantity and strength of the generated oxidants were also quite different. 86.78 mmol of oxidants were needed to remove a gram of pesticide with Ta-BDD and 30.57 mmol with Si-BDD. Therefore, the electrode resistance is an important aspect that must be considered in order to get a suitable design of energy storage systems that allow the green photovoltaic powering of electrochemical technologies using conventional batteries as a booster to ensure continuous operation.

1. Introduction

The United Nations Framework Convention on Climate Change has exposed the importance of the awareness about the climate change and highlighted the efforts that should be done in order to stop it. In the Conference of the Parties celebrated at the end of 2019, 121 countries and 786 companies have committed to reach net zero emission in 2050[1] and to fight for the fulfilment of the Sustainable Development Goals focused on promoting prosperity while taking care of the environment.[2] In this context, besides stopping the global warming, remediating environmental disasters caused by the improper and uncontrolled production and use of many hazardous chemicals must be a key issue to solve. Nowadays, high concentrations of persistent pollutants can be found in water bodies and soils. The high chemical stability and low biodegradability of many of these pollutants makes even possible their presence in the supply water, where they are known to affect the immune system of human beings.[3] Consequently, their removal from the natural environment is essential to reduce and get rid of their negative impact.

Electrochemical advanced oxidation processes (EAOPs) have been widely studied for the treatment of wastewater and polluted soils.[4] Among them, the conductive diamond electrochemical oxidation (CDEO) has been widely used for the oxidation of hazardous organic compounds.[5] Diamond anodes are classified as "*non-active*" electrodes. This means that they exhibit a weak interaction with the hydroxyl radical (·OH) generated on their surface which, in turn, are responsible of the organic matter oxidation. Thus, the weaker is the electrode-(·OH) interaction, the higher is the oxidation efficiency.[6] Because of the outstanding results, many researchers have focused their studies on the degradation of a huge variety of persistent organic pollutants (POPs) using boron-doped-diamond (BDD) anodes.[4a,7] In addition, BDD electrodes show a high chemical and electrochemical stability and a high electrooxidation efficiency working in a wide range of current densities and initial concentrations.[6c,8] Furthermore, this EAOP does not need the addition of reactant, using the electric energy as unique reagent.

Looking for a further environmentally friendly treatment, the use of renewable energy to power these electrochemical technologies may become a key alternative.[9] By contrast to the continuous working mode of treatment plants, the renewable power sources have an intermittent production, making necessary the development of novel powering strategies to achieve more sustainable electrochemical treatments.[10] One of them consists of the use of energy storage systems.[11] Thus, during the period in which the production of renewable energy is low, the energy storage system is expected to power the electrochemical treatment. One possibility to meet this goal is to directly couple the charged storage system with the electrolyzer, without fixing a cell potential with the assistance of

[a] M. Millán,+ Prof. J. Lobato, Dr. C. M. Fernández-Marchante, Dr. M. A. Rodrigo
Department of Chemical Engineering, Faculty of Chemical Sciences & Technologies
University of Castilla-La Mancha
Av. Camilo Jose Cela n 12, 13071 Ciudad Real, Spain
E-mail: Manuel.Rodrigo@uclm.es
[b] V. M. García-Orozco,+ Dr. G. Roa-Morales, Dr. R. Natividad
Joint Center for Research in Sustainable Chemistry (CCIQS UAEM-UNAM)
Autonomous University of the State of Mexico
Carretera Toluca-Atlacomulco km 14.5, Campus UAEMéx "El Rosedal", Toluca, State of Mexico, 50200, Mexico
[c] Dr. I. Linares-Hernández
Instituto Interamericano de Tecnología y Ciencias del Agua (IITCA)
Autonomous University of the State of Mexico
Km.14.5, carretera Toluca-Atlacomulco, C.P 50200 Toluca, Estado de México, México
[+] These authors contributed equally to this work

ChemElectroChem
Articles
doi.org/10.1002/celc.202000550
Chemistry Europe
European Chemical Societies Publishing

electronics but simply letting the storage system to provide electricity until attaining its discharge down to a reasonable level. In this case, the applied current density to the electrochemical treatment will mainly depends on the resistance of the electrochemical cell which, in turn, is mainly influenced by the electrode material resistance. Thus, the lower is the cell resistance, the lower is the energy consumption of the treatment. In order to reduce the energy demand of these electrochemical technologies, novel electrode materials should be researched, aiming to reduce the ohmic losses while maintaining the oxidation efficiency.

The development of more conductive supports for the coating of BDD electrodes could be a key alternative to reduce operative costs. A previous work has reported the use of different support for the coating of BDD electrodes, evaluating their influence on the generation of oxidant species.[12] It was found that the substrate of BDD electrodes has low influence on the production of oxidants when the characteristics of the diamond coating are similar (even that, some differences were found). Nevertheless, the oxidation efficiency and the energy consumption of these systems were not assessed, as in that case it was considered not relevant, because the energy was supplied by a conventional power supply and the system was operated in galvanostatic mode. Nonetheless, important differences were found in the cell potential needed to reach the desired current densities, being these potentials lower when using metallic supports. These important differences in the cell resistance due to the diverse nature of the electrode substrates bring up us the idea that, perhaps, this input can influence on a system in which the power comes from an energy storage device such as a conventional battery or a redox flow battery, because of the different use of the energy stored. These systems are typically used to accumulate the surplus of energy coming from wind turbines or photovoltaic (PV) panels and, hence, this has a direct application in the powering of electrolyzers with renewable energy.

In view the previous statements, the main aim of this work is to study the performance of electrolyzers equipped with electrodes consisting of the same coating on different supports (and hence with different electric resistances) when they are powered with the same charged battery. To do this, three BDD anodes with the same diamond coating and different substrate materials were tested (silicon, niobium and tantalum) to electrolyze a synthetic waste polluted with a model pollutant, comparing the degree of treatment achieved in each case and the way in which the battery was discharged. As far as the authors know, this is the first time that this type of study has been made and results can be very relevant for the design of novel treatment systems integrated with renewable energies, as these systems typically needs for an energy storage stage which helps to fit the production and demand of energy.

2. Results and Discussion

As aforementioned, the main aim of this work is to evaluate the different behavior of electrolyzers equipped with the same diamond coating on different substates when they are powered with the same fully charged battery.

In order to evaluate the performance of these electrodes, a first electrochemical characterization was developed using 1.0 g L^{-1} of Na_2SO_4 as supporting electrolyte. Figure 1 shows the lineal sweep voltammograms and the Nyquist plots of each BDD electrode. In addition, Table 1 collects the theoretical electric conductivity of the substrate materials and the ohmic

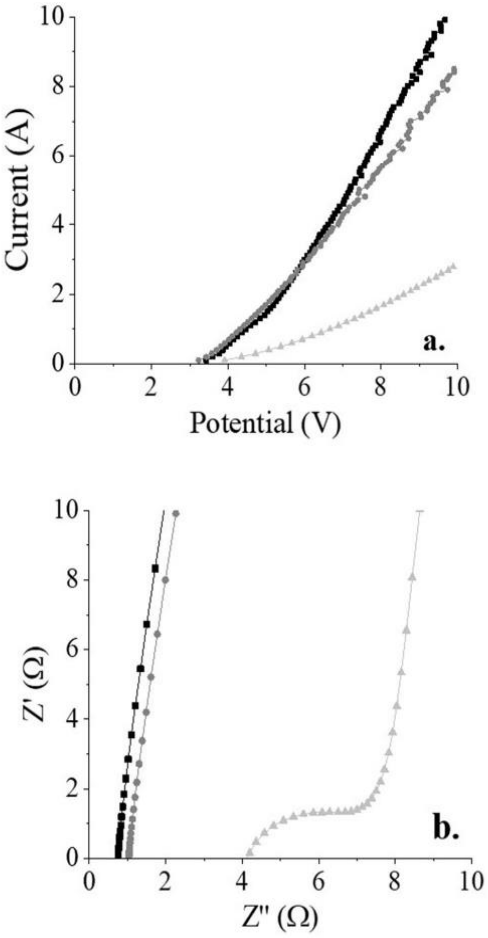

Figure 1. Linear sweep voltammograms (a) and Nyquist plots (b) for different BDD electrooxidation cells. Nb-BDD (■), Ta-BDD (●) and Si-BDD (▲). [Na_2SO_4] = 1 g L^{-1}.

Table 1. Theoretical electric conductivity of substrate materials and ohmic resistance of the BDD electrodes.

Material	Electrical conductivity of the substrate material [S m−1]	Ohmic resistance of the BDD electrodes [Ω]
Nb	$6.93 \cdot 10^6$	0.78
Ta	$7.61 \cdot 10^6$	1.03
Si	$4.35 \cdot 10^{-4}$	4.27

ChemElectroChem
Articles
doi.org/10.1002/celc.202000550
Chemistry Europe
European Chemical Societies Publishing

resistance of the different BDD electrodes. As seen in the voltammograms, there is a higher slope for the BDD electrode supported on Si, as compared to Nb- and Ta-BDD electrodes. Regarding oxygen evolution potentials (OEVs), the higher overpotential exposed by Si substrate could turn into a higher oxidation efficiency.[4c,13] Nb and Ta substrates show almost the same tendency at lower potentials. Nevertheless, the electrode supported on niobium exposes a lower slope at potential over 6 V, despite of the lower electric conductivity of this material as compared with Ta. Those results could be explained in terms of the coating film and its contact with the supporting material. The three electrodes were doped with the same concentration of boron (2500 ppm) which provides the electrode of a semi-metallic conductivity.[14] Despite the same amount of boron was deposited in the three cases, the coating films reached different thicknesses which can affect the conductivity of the electrodes. Results noticed that thinner coating films led to higher resistance. According to LSV data, over 38.2 mA cm^{-2}, Ta-BDD electrode could attain higher removal efficiencies than Nb due to the higher overpotential reached by this electrode at higher current densities.

As the coating is the same, the slope of LSV analyses curves should be directly related to the ohmic resistance that the support materials offer. Thus, the lower is the slope, the lower is the ohmic resistance of the BDD electrode, as Figure 1b shows. The Si-BDD electrode shows an ohmic resistance four times higher than that of Nb- and Ta-BDD electrodes. Considering that the lower is the ohmic resistance, the lower is the energy consumption, the energy cost of an electro-oxidation treatment using Si-BDD electrodes would be much higher, taking into account the same removal efficiency for the three BDD electrodes, especially if there is not a significant influence on the oxidation progress attained.[12]

In view of the electrochemical characterization results exposed previously, the electrochemical oxidation treatment working under the same operational conditions (galvanostatic mode) and using Si-BDD electrodes should reach the best remediation efficiency. Nevertheless, keeping in mind the different ohmic resistances showed by each electrode, the powering of the electrochemical treatment under a constant power supplied by an energy storage system, should supply different current and potential values to each electrode, which can turn into different removal efficiencies that expected under a traditional powering mode. Consequently, it is important to confirm this point and hence, to evaluate the electro-oxidation performance of each electrode in order to determine the best substrate for BDD electrodes in terms of pollutant removal and energy consumption.

Thus, with this objective, the electro-oxidation of 100 ppm of clopyralid using BDD electrodes supported on three different conductive materials and powered by a fully-charged lead-acid battery was carried out. The potential and current applied to the electrochemical treatment varied depending on the cell resistance and charge accumulated in the battery (fully charged in all cases). Figure 2 shows the potential recorded, the current applied to the cell and the total charge passed throughout the electrolyzer over 12 h of electro-oxidation treatment carried out

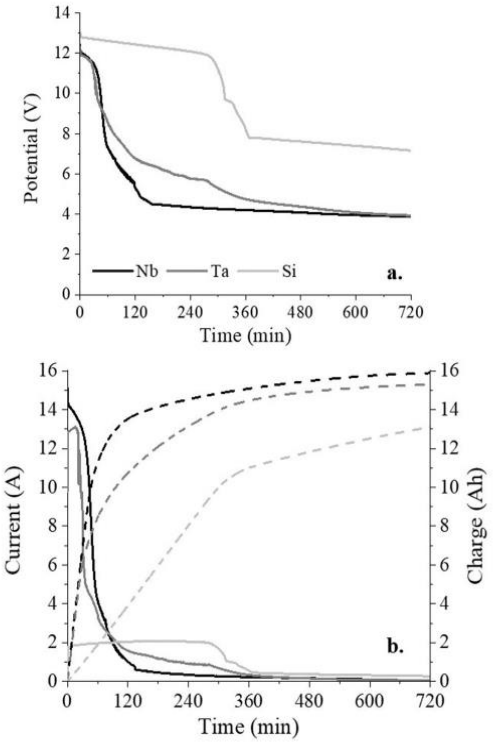

Figure 2. a) Potential recorded and b) current (solid line) and electric charge applied (dished line) to the electrooxidation treatment powered by a lead-acid battery. Theoretical potential = 12 V, theoretical capacity = 17 Ah.

with each cell. Furthermore, Table 2 shows a data review which collects the average potential and current and the total electric charge and energy applied to each electrolytic treatment.

As expected, huge differences were found in terms of potential and current supply when different electrolyzers are powered by a lead-acid battery. Thus, the applied electric charge and the energy consumption of a particular electro-oxidation treatment depend highly on the electrolyzer resistances. As Figure 2a shows, the electrolyzers worked under a different range of potentials. At 120 minutes, the potential applied to the Si-BDD electrolyzer was almost the double than the potential supplied to Nb- and Ta-BDD electrodes. Those results are in line with the previous electrochemical characterization of each electrolyzer. As expected, the higher the ohmic

Table 2. Average potential and current, total electric charge and energy for the complete electrooxidation treatment.

Electrode material	Average potential [V]	Average current [A]	Electric charge [Ah]	Energy [Wh]
Nb-BDD	4.88	1.32	15.89	77.70
Ta-BDD	5.55	1.28	15.26	84.78
Si-BDD	9.67	1.09	13.11	126.89

ChemElectroChem
Articles
doi.org/10.1002/celc.202000550
Chemistry Europe
European Chemical Societies Publishing

resistance of the electrodes, the lower the current applied to the electro-oxidation reactor. Regardless of the applied current, in the first few minutes, the current increased until reaching a maximum value around 14.34, 13.12 and 2.06 A for Nb, Ta and Si electrode substrates, respectively. After that, the current dropped slowly until the battery was discharged. Furthermore, it can be observed that the lower the applied current, the higher the discharge time. Thus, the electrolytic treatment using Si-BDD electrodes can work for a longer time until reaching the full discharge of the battery. Conversely, Nb- and Ta-BBD electrodes showed a closer tendency in terms of current values and treatment time, which could be explained by their similar ohmic resistances. If LSV analyses and discharge current values are compared for Nb and Ta electrodes, both results follow the same tendency. The lower slope exposed by Nb electrodes at higher potential values turn into higher current as shown Figure 2b at the first time of the treatment. Conversely, its slightly higher slope at lower potential lead to lower current values after 1 h of treatment. In contrast to Si-BDD electrode, the higher current values supplied to those electrodes lead to a faster battery discharge. Regarding the current charge passed throughout the electrolyzers, again higher differences were obtained with the cell equipped with Si-BDD, which shows a more progressive passing of charge, reaching a lower value (13.1 Ah). Those results expose different battery states of charge (SOC) after twelve treatment hours. Once the electro-oxidation treatment performed with Si-BDD electrolyzer finished, the battery still had a 23% of its theoretical capacity (17 Ah), energy that could be used to attain a higher mineralization. By contrast, only a 6.53 and 10.23% of capacity remained in the battery after the electro-oxidation treatment developed with Nb and Ta electrolyzers, respectively.

Regarding the energy consumption, as expected, the huge resistances showed by the Si-BDD electrode lead to a high-power demand. Consequently, the use of a Si-BDD electrolyzer could be related with lower energy efficiency. Nevertheless, it is important to evaluate the behavior of these electrodes in terms of removal of organic compound to determine which is the best substrate material for BDD electrodes.

Figure 3 shows the changes in the clopyralid concentration over 12 h of electro-oxidation treatment for each electrolytic test (carried out with cells equipped with BDD electrodes supported on different substrate materials) as a function of reaction time and electric charge passed. The three tests attained almost the same removal of pesticide at the end of the treatment (12 h), achieving at least an 85% of removal in all cases. Nevertheless, a slightly better removal of clopyralid was attained with the Ta electrolyzer, 88.6%. Besides, it is important to note that the degradation of pesticide exposes a different tendency depending on the substrate material. Nb-BDD electrodes showed a faster removal at the first treatment hours. However, when almost a 50% of pollutant was removed, a slowly removal rate was observed. At a treatment time of 90 min, the higher removal of pesticide was attained by the BDD electrodes supported on Nb (51.8%). Conversely, 3.5 h later, the Ta-BDD electrolyzer had removed a 72.3% of pollutant in contrast to the 66.2% removed with Nb-BDD electrodes. As

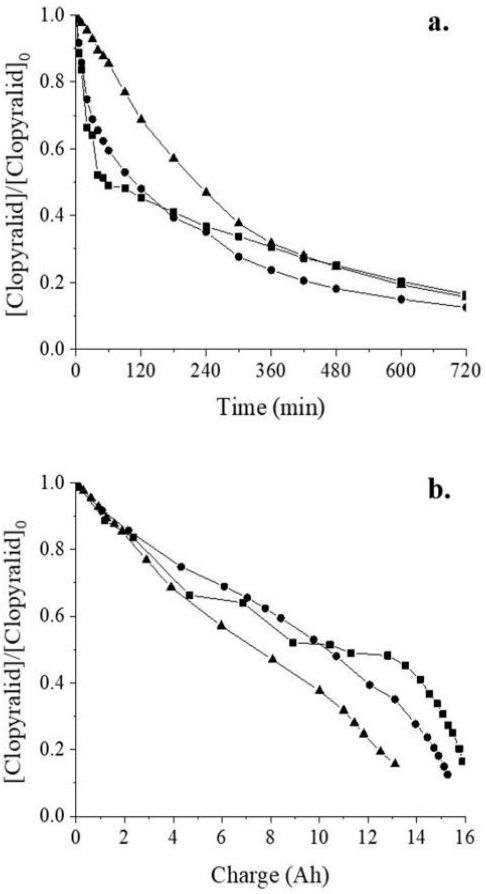

Figure 3. Clopyralid concentration profile under an electrooxidation treatment powered by a lead-acid battery. Theoretical potential = 12 V, Theoretical capacity = 17 Ah. Electrode material: Nb-BDD (■), Ta-BDD (●) and Si-BDD (▲). $[Clopyralid]_0 = 100$ ppm.

expected, the higher is the applied current density, the higher is the rate of pollutant degradation.[4c,5d,6a,7e] In this case, the lower removal rate observed by the Si-BDD electrode can be directly related to the lower current densities applied to this electro-oxidation reactor during the first hours of electrolytic treatment. The higher removal achieved by the Ta-BDD electrolyzer regarding the Nb-BDD electrolyzer could be related to the higher current applied to this electrode after 80 min of treatment. On the other hand, if the removal of clopyralid is studied in terms of applied electric charge (Figure 3b), the results release information about the efficiency of the electrolysis treatment. In this case, the higher removal of pesticide per applied electric charge was attained for the Ta-BDD electrolyzer, followed by the BDD electrodes supported on Nb and Si substrates

In order to determine the best available support for BDD electrodes, the ratio mg of removed pollutant/Wh was calcu-

ChemElectroChem
Articles
doi.org/10.1002/celc.202000550
Chemistry Europe
European Chemical Societies Publishing

lated. Si-BDD electrolyzer got the lowest removal of pesticide per energy unit, 1.95 mg removed clopyralid/Wh, while Ta-BDD electrodes showed the highest removal ratio, 2.14 mg removed clopyralid/Wh. Furthermore, it is important to evaluate the amount of total organic carbon that remained in the water effluent after 12 h of electro-oxidation treatment. In contrast to the pesticide removal results, the higher removal of TOC was achieved by the Nb-BDD electrolyzer, reaching a removal of 78.9% within the experimental time. As noted above, the electro-oxidation carried out using Si-BDD electrodes showed the lower removal of total organic carbon (67.3%).

Furthermore, the mineralization attained with Ta-BDD electrodes was slightly lower than that achieved by the electrolyzer equipped with Nb-BDD electrodes, 77.2%. The differences observed between the removal of pesticide and organic carbon are directly related to the generation of intermediate species as a result of secondary reactions between oxidants species and the pollutant in the bulk solution. Figure 4 shows the total chromatographic areas of intermediate species generated along the electro-oxidation treatment for the three studied electrolyzers.

As expected, the higher production of intermediate species corresponds to the electrolyzer that showed a lower removal of TOC, Si-BDD electrolyzer. Thereby, the total chromatographic areas of the intermediate species generated along the electro-oxidation treatment were 704.4, 1175.8 and 1940.1 a.u. (3-chloropilinic and chloropicolinic acids) for Nb-, Ta- and Si-BDD electrodes, respectively. Consequently, those results help to explain the differences observed between the removal of clopyralid and TOC for the Nb and Ta electrolyzers.

In order to clarify the difference between each substrate, the generation of oxidant species was measured throughout the electrooxidation treatments. Figure 5 shows the generation of total oxidants by each electrolyzer. Contrary to expectation according to changes observed in the organic pollutant concentration, huge differences were observed between the oxidant generation, despite attaining almost the same removal regardless of the used electrode substrate. Results are in line with previous studies that evaluated the generation of different oxidants using chloride and sulphate solutions as supporting electrolyte working at galvanostatic mode.[12] The higher oxidant generation was attained by the Ta-BDD electrode despite of the lower electric charge applied within a long treatment time regarding Nb electrolyzer. The high potential applied to the CDEO coupled with BDD-Ta after 1 h of treatment regarding the BDD-Nb could explain the higher generation of oxidant in those electrodes. Besides, those results are in line with the exposed by the LSV analyses for those electrodes. At higher current densities, Ta-BDD electrodes noticed huge overpotential values. It is worth to mention that a decomposition of oxidants could be carried out at very large cells potential values induced by the interactions of oxidants formed in the system, in particular by the action of hydroxyl radicals, which may promote the decomposition of stable

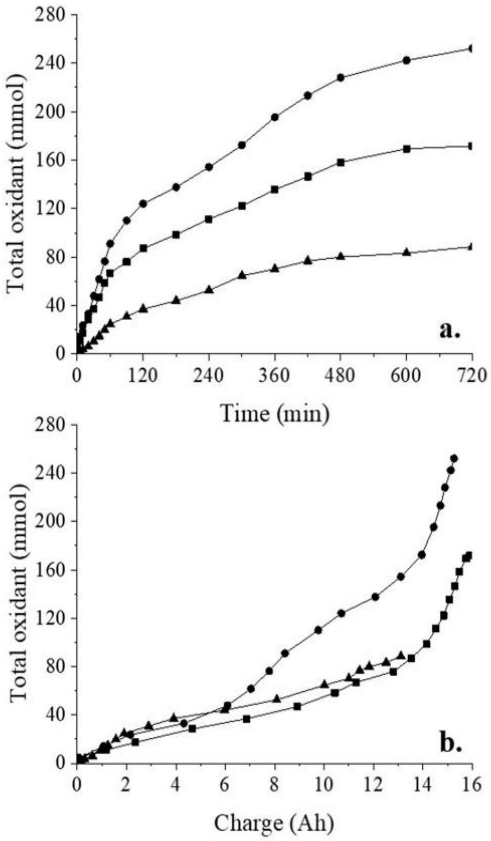

Figure 5. Total oxidants generated along an electrooxidation treatment powered by a lead-acid battery. Theoretical potential = 12 V, theoretical capacity = 17 Ah. Electrode material: Nb-BDD (■), Ta-BDD (●) and Si-BDD (▲). $[Clopyralid]_0$ = 100 ppm.

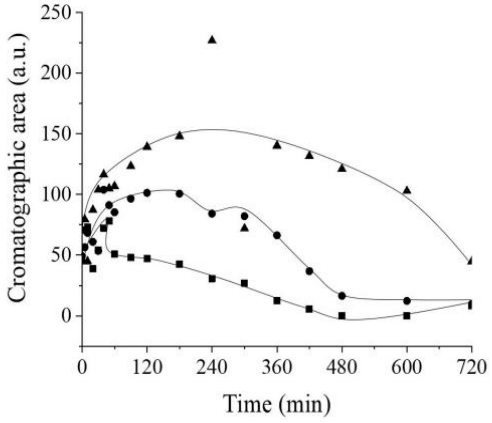

Figure 4. Total chromatographic area of intermediate species generated under an electrooxidation treatment powered by a lead-acid battery. Theoretical potential = 12 V, theoretical capacity = 17 Ah. Electrode material: Nb-BDD (■), Ta-BDD (●) and Si-BDD (▲). $[Clopyralid]_0$ = 100 ppm.

ChemElectroChem
Articles
doi.org/10.1002/celc.202000550
Chemistry Europe
European Chemical Societies Publishing

oxidants to unstable radicals. These interactions have a low probability of being generated on Nb- and Ta-BDD electrodes surface because after one treatment hours the cell potential dropped below 6 V. Nevertheless, Si-BDD electrode worked along the 12 treatment hours over 8 V which could explain its low oxidant generation.

With the aim of quantifying the performance of each system in terms of total oxidant generated, the ratio energy consumption per unit of generated oxidant was calculated. Thus, Si-BDD electrode got the higher ratio, 14.34 Wh/mmol oxidant generated, that is, the highest energy cost to generate the same amount of oxidant. On the contrary, Ta-BDD electrolyzer showed the lowest energy cost per unit of generated oxidant, 3.36 Wh/mmol oxidant. Despite the higher generation of oxidants and the lower energy consumption exposed by Ta-BDD electrode, 86.78 mmol of oxidants must be generated in order to remove a gram of pesticide. Conversely, 30.57 mmol should be generated with the Si-BDD electrode to attain the same removal. This could be explained in terms of the oxidant's strengths and the previously commented decomposition to radicals, which act immediately over the organics once formed. Some oxidants can be powerful for the oxidation of a specific pollutant, attaining higher and faster removal at lower concentrations. Among them, it is worth to mention sulphate radicals, which are one of the strongest oxidant species that can arise in the oxidation of sulphate solutions at an oxidation potential of 2.8 V, closer to the oxidation potential of hydroxyl radicals (2.7 V).[15] These sulphate radicals can generate ·OH radicals at basic pH values. Conversely, persulfate ions could generate more sulphate radicals at acid pH values.[16] Thus, the non-active persulfate ion can become in a strong oxidant agent. Besides, it is important to note that many other secondary reactions can take place in the bulk solution rising other oxidant species. ·OH radicals can be combined arising the production of H_2O_2.[6d] At same time, O_3 can be generated in the bulk solution due to secondary reaction between oxygen and hydroxyl radicals.[4a]

Regarding the relation of the electrochemical characterization of the different tested substrates and the oxidant species generation reached by each electrode, the higher oxygen evolution potential showed by the BDD electrode supported on Si substrate should be turned into a huge hydroxyl radical generation beside Nb and Ta substrates. Contrary to expectation, this electrolyzer showed the lower concentration of oxidants.

Keeping this in mind, pH and conductivity analyses were carried out over the treatment tests (Figure 6). Nb- and Ta -BDD electrodes show an increase of pH values the first hours of treatment, attaining almost constant and neutral pH at the end of the study. Conversely, the use of Si-BDD electrodes showed low pH values along the complete treatment, leaving an effluent with acid properties. These differences could be related to the intermediate and oxidant species generation and their nature. In view of the previous arguments, those results could explain the higher removal attained by the Si-BDD electrolyzer in terms of oxidant's strengths despite the lower number of oxidant species measured. Concerning conductivity, significant

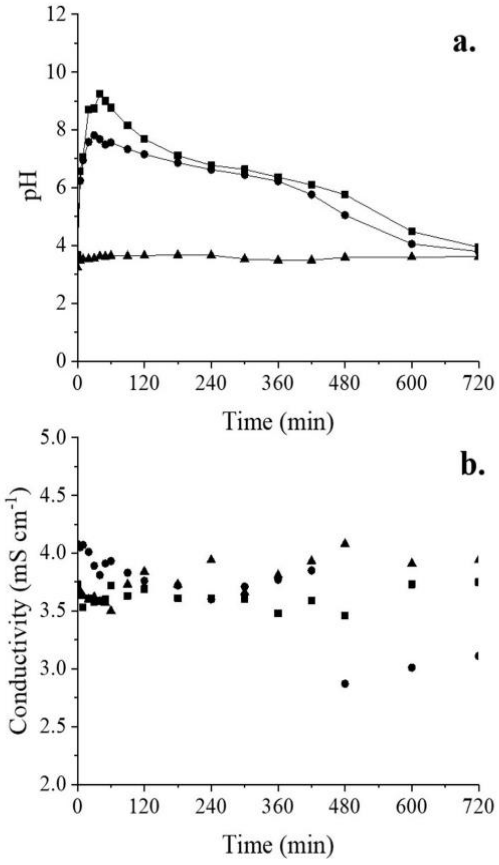

Figure 6. pH (a) and conductivity (b) profile along an electrooxidation treatment powered by a lead-acid battery. Theoretical potential = 12 V, theoretical capacity = 17 Ah. Electrode material: Nb-BDD (■), Ta-BDD (●) and Si-BDD (▲). $[Clopyralid]_0$ = 100 ppm.

differences were not observed throughout the treatment regardless of the used BDD electrode.

Once all results have been exposed, it is worth to mention that metal substrates with higher conductivity (Ta and Nb) and lower ohmic resistance were supplied by higher current density under a powering with a fully-charging battery. As a consequence, the huge current densities applied to both electrolyzers turned into faster removal rates and a higher oxidant generation, attaining huge removal efficiencies with a lower energy consumption. Furthermore, in terms of mineralization, the electrode supported on Nb substrate exposed the higher TOC removal and a lower generation of intermediate species. Thus, the huge amount of oxidant species generated during the electro-oxidation treatment performed with this electrode should be directly related to oxidized organic matter to CO_2 and the remediation efficiency of the treatment. In view of the previous results, it can be claimed that Nb and Ta substrates exposed better remediation results than the electrooxidation developed using traditional Si-BDD electrodes. Furthermore,

ChemElectroChem | Articles
doi.org/10.1002/celc.202000550
Chemistry Europe
European Chemical Societies Publishing

these results expose an important and relevant breakthrough in terms of novel substrate materials for BDD electrodes and it helps to understand better how energy has to be dosed from renewable energy devices, when the powering of the treatment technology is carried out directly from an energy storage device.

3. Conclusions

From this work, the following conclusion can be drawn. BDD electrodes supported on Silicon substrate exposed the highest ohmic resistance and consequently, the higher energy consumption for an electro-oxidation treatment powered by an energy storage system as power supply. Results suggested that BDD electrodes supported on Ta and Nb substrates showed a faster removal rate regarding the Si-BDD electrolyzer. After 12 h of treatment, the Ta-BDD electrolyzer attained a highest removal (88.56%). Nevertheless, the electrolyzer fitted with Nb-BDD electrodes exposed the higher TOC mineralization and the lower generation of intermediate species. Regarding the use of energy, around 1.98 mg of pesticide/Wh were removed in the electrolyzers equipped with anodes supported on Nb and Si, while 2.14 mg were removed using Ta-BDD electrodes. Nevertheless, a lower energy consumption must be done in order to generate a mmol of oxidant using Si-BDD electrodes (14.34 Wh $mmol^{-1}$). In terms of strength of oxidants, almost 30 mmol of oxidant must be generated in order to remove a gram of pesticide using silicon as support of BDD electrodes. Conversely, a 35% of oxidant more must be generated by the Ta-BDD electrodes to remove the same amount of pesticide.

Experimental Section

Chemicals

Clopyralid supplied by Zymit Química (Spain) was selected as organochlorinated pesticide model. A synthetic effluent was prepared with 100 mg dm^{-3} of pesticide and 3.0 g L^{-1} of Na_2SO_4 as supporting electrolyte (Panreac). Milli-Q water (Resistivity: 18.2 MΩ cm at 25 °C) was used was used to prepare the synthetic wastewater effluent.

Experimental Setup

The electro-oxidation of 4.0 L of a synthetic effluent polluted with clopyralid (an organochlorinated pesticide) was studied using a bench scale experimentation setup working in batch mode. BDD electrodes (78 cm^2) were used as anodic and cathodic electrodes. The degradation was carried out in a commercial conductive diamond electrochemical oxidation (CDEO) reactor, DiaCell® 101, provided by Adamant Technologies (Switzerland) using BDD electrodes (WaterDiam, France) consisting on the same boron doped diamond coating film supported on different materials: Niobium (Nb), Tantalum (Ta) and Silicon (Si). The three electrodes were doped with 2500 ppm of boron leading to a coating film of 7.7, 7.3 and 5.9 μm of thickness for Nb, Ta and Si -BDD electrodes, respectively. The electrooxidation was powered using a lead-acid battery (DSK, India) of 12 V and 17 Ah of capacity.

Characterization Procedures and Analytical Techniques

Each electrolyzer was characterized using lineal sweep voltammetry (LSV) and electrochemical impedance spectroscopy (EIS) measurements using an Autolab potentiostat/galvanostat (PGSTAT-302N) coupled with a FRA32M module. Clopyralid concentration, oxidants production, pH and conductivity were measured during the electrolysis. The concentration of clopyralid was measured by high performance liquid chromatography, HPLC (Agilent 1260 Infinity) as reported elsewhere.[10d] Oxidants production were quantified by an iodometric titration with thiosulfate as reported elsewhere.[17] The pH and conductivity were measured using CRISON pH25+ and CRISON CM35+ instruments.

Acknowledgements

Financial support from the Spanish Agencia Estatal de Investigación through project CTM2016-76197-R (AEI/FEDER, UE) is gratefully acknowledged. M. Millán thanks the UCLM for the predoctoral contract within the framework of the Plan Propio I+D.

Conflict of Interest

The authors declare no conflict of interest.

Keywords: boron-doped diamond electrodes · electrooxidation · environmental chemistry · energy conversion · substrate

[1] U. Nations, *Vol. 2020*, https://www.un.org/, **2020**.
[2] U. Nations, *Vol. 2020*, https://sustainabledevelopment.un.org/, **2020**.
[3] a) S. Garcia-Segura, J. D. Ocon, M. N. Chong, *Process Saf. Environ. Prot.* **2018**, *113*, 48–67; b) C. A. Damalas, I. G. Eleftherohorinos, *Int. J. Environ. Res. Public Health* **2011**, *8*, 1402–1419.
[4] a) I. Sirés, E. Brillas, M. A. Oturan, M. A. Rodrigo, M. Panizza, *Environ. Sci. Pollut. Res. Int.* **2014**, *21*, 8336–8367; b) M. A. Rodrigo, N. Oturan, M. A. Oturan, *Chem. Rev.* **2014**, *114*, 8720–8745; c) M. Panizza, G. Cerisola, *Chem. Rev.* **2009**, *109*, 6541–6569; d) C. Barrera-Diaz, P. Canizares, F. J. Fernandez, R. Natividad, M. A. Rodrigo, *J. Mex. Chem. Soc.* **2014**, *58*, 256–275.
[5] a) C. A. Martínez-Huitle, S. Ferro, *Chem. Soc. Rev.* **2006**, *35*, 1324–1340; b) C. Comninellis, I. Duo, P. A. Michaud, B. Marselli, S. M. Park, *Diam. Electrochem.* **2005**, 449–476; c) P. Canizares, M. Hernandez-Ortega, M. A. Rodrigo, C. E. Barrera-Diaz, G. Roa-Morales, C. Saez, *J. Hazard. Mater.* **2009**, *164*, 120–125; d) M. A. Rodrigo, P. Cañizares, A. Sánchez-Carretero, C. Sáez, *Catal. Today* **2010**, *151*, 173–177.
[6] a) F. C. Moreira, R. A. R. Boaventura, E. Brillas, V. J. P. Vilar, *Appl. Catal. B* **2017**, *202*, 217–261; b) M. Quiroz, S. Ferro, C. A. Martinez-Huitle, Y. Meas, *J. Braz. Chem. Soc.* **2006**, *17*, 227–236; c) C. Comninellis, G. Chen, *Electrochemistry for the Environment*, Springer New York, **2009**; d) B. Marselli, J. Garcia-Gomez, P. A. Michaud, M. A. Rodrigo, C. Comninellis, *J. Electrochem. Soc.* **2003**, *150*, D79-D83.
[7] a) C. A. Martínez-Huitle, M. A. Rodrigo, I. Sirés, O. Scialdone, *Chem. Rev.* **2015**, *115*, 13362–13407; b) E. Brillas, C. A. Martínez-Huitle, *Appl. Catal. B* **2015**, *166–167*, 603–643; c) P. V. Nidheesh, M. Zhou, M. A. Oturan, *Chemosphere* **2018**, *197*, 210–227; d) A. K. Abdessalem, M. A. Oturan, N. Oturan, N. Bellakhal, M. Dachraoui, *Int. J. Environ. Anal. Chem.* **2010**, *90*, 468—477; e) M. A. Oturan, J.-J. Aaron, *Crit. Rev. Environ. Sci. Technol.* **2014**, *44*, 2577–2641.
[8] M. Panizza, G. Cerisola, *Electrochim. Acta* **2005**, *51*, 191–199.
[9] a) C. A. Martínez-Huitle, M. A. Rodrigo, O. Scialdone, *Electrochemical Water and Wastewater Treatment*, Elsevier Science, **2018**; b) W. T. Mook,

ChemElectroChem | Articles doi.org/10.1002/celc.202000550 | Chemistry Europe European Chemical Societies Publishing

M. K. Aroua, G. Issabayeva, *Renewable Sustainable Energy Rev.* **2014**, *38*, 36–46.
[10] a) R. López-Vizcaíno, E. Mena, M. Millán, M. A. Rodrigo, J. Lobato, *Renewable Energy* **2017**, *114*, 1123–1133; b) E. Mena, R. Lopez-Vizcaino, M. Millan, P. Canizares, J. Lobato, M. A. Rodrigo, *Int. J. Energy Res.* **2018**, *42*, 720–730; c) M. Millán, M. A. Rodrigo, C. M. Fernández-Marchante, S. Díaz-Abad, M. C. Peláez, P. Cañizares, J. Lobato, *Electrochim. Acta* **2018**, *270*, 14–21; d) M. Millán, M. A. Rodrigo, C. M. Fernández-Marchante, P. Cañizares, J. Lobato, *ACS Sustainable Chem. Eng.* **2019**, *7*, 8303–8309.
[11] a) J. M. de Melo Henrique, D. C. de Andrade, E. L. Barros Neto, D. R. da Silva, E. V. dos Santos, *J. Chem. Technol. Biotechnol.* **2019**, *94*, 2999–3006; b) S. O. Ganiyu, L. R. D. Brito, E. C. T. De Araújo Costa, E. V. Dos Santos, C. A. Martínez-Huitle, *J. Environ. Chem. Eng.* **2019**, *7*.
[12] I. Moraleda, S. Cotillas, J. Llanos, C. Sáez, P. Cañizares, L. Pupunat, M. A. Rodrigo, *J. Electroanal. Chem.* **2019**, *850*, 113416.
[13] L. Zhang, L. Xu, J. He, J. Zhang, *Electrochim. Acta* **2014**, *117*, 192–201.
[14] G. Santos, K. Eguiluz, G. Salazar Banda, C. Saez, M. Rodrigo, *J. Electroanal. Chem.* **2020**, 113756.
[15] J. G. Speight, *Reaction Mechanisms in Environmental Engineering: Analysis and Prediction*, Elsevier Science, **2018**.
[16] C. M. Galanakis, E. Agrafioti, *Sustainable Water and Wastewater Processing*, Elsevier Science, **2019**.
[17] a) M. Rodríguez, M. Muñoz-Morales, J. F. Perez, C. Saez, P. Cañizares, C. E. Barrera-Díaz, M. A. Rodrigo, *Ind. Eng. Chem. Res.* **2018**, *57*, 10709–10717; b) P. Cañizares, C. Sáez, A. Sánchez-Carretero, M. A. Rodrigo, *J. Appl. Electrochem.* **2009**, *39*, 2143.

Manuscript received: April 15, 2020
Revised manuscript received: May 23, 2020
Accepted manuscript online: June 16, 2020

ARTICLES

Removal company: Conductive diamond electro-oxidation (CDEO) treatments powered by a fully charged battery and equipped with boron-doped diamond (BDD) electrodes supported on different substrates showed different performances. The Si-BDD electrolyzer shows a higher resistance and higher overpotential. Despite the excellent efficiency shown by the Si-BDD electrodes, the CDEO reactor assembled with Ta-BDD electrodes exposes the highest removal per unit of energy.

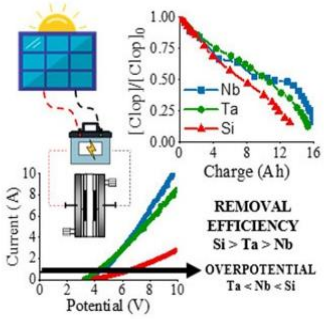

*V. M. García-Orozco, M. Millán, Prof. J. Lobato, Dr. C. M. Fernández-Marchante, Dr. G. Roa-Morales, Dr. I. Linares-Hernández, Dr. R. Natividad, Dr. M. A. Rodrigo**

1 – 9

Importance of Electrode Tailoring in the Coupling of Electrolysis with Renewable Energy

SPACE RESERVED FOR IMAGE AND LINK

Share your work on social media! *ChemElectroChem* has added Twitter as a means to promote your article. Twitter is an online microblogging service that enables its users to send and read short messages and media, known as tweets. Please check the pre-written tweet in the galley proofs for accuracy. If you, your team, or institution have a Twitter account, please include its handle @username. Please use hashtags only for the most important keywords, such as #catalysis, #nanoparticles, or #proteindesign. The ToC picture and a link to your article will be added automatically, so the **tweet text must not exceed 250 characters**. This tweet will be posted on the journal's Twitter account (follow us @ChemElectroChem) upon publication of your article in its final (possibly unpaginated) form. We recommend you to re-tweet it to alert more researchers about your publication, or to point it out to your institution's social media team.

ORCID (Open Researcher and Contributor ID)

Please check that the ORCID identifiers listed below are correct. We encourage all authors to provide an ORCID identifier for each coauthor. ORCID is a registry that provides researchers with a unique digital identifier. Some funding agencies recommend or even require the inclusion of ORCID IDs in all published articles, and authors should consult their funding agency guidelines for details. Registration is easy and free; for further information, see http://orcid.org/.

Dr. Carmen M. Fernández-Marchante
Dr. Gabriela Roa-Morales
Prof. Justo Lobato
Maria Millán
Dr. Reyna Natividad
Violeta M. García-Orozco
Dr. Ivonne Linares-Hernández
Dr. Manuel A. Rodrigo http://orcid.org/0000-0003-2518-8436

4.4. Resultados no publicados y discusión general

En esta sección se colocaron los resultados que no fueron publicados en el artículo.

4.4.1. Caracterización fisicoquímica

En el mes de marzo del 2017 se realizó una caracterización previa, antes de empezar el set de experimentos de EC, para conocer las características de la muestra del agua residual mostradas en la Tabla 10.

Tabla 10. Caracterización fisicoquímica previa realizada en marzo del 2017

Parámetro	Unidades	Valor	Parámetro	Unidades	Valor
pH	-	4.52	*CE*	µS/cm	785.8
Color	Pt-Co	870	Coliformes totales	CFU/100mL	54000000
Sulfato	SO_4^{2-}mg/L	0	Coliformes fecales	CFU/100mL	<2000000
DQO	mg/L	4993	Cloruros	Cl^- mg/L	238.44
DBO_5	mg/L	1526	Fe	mg/L	3.32
DBO_5/DQO		0.31	Cu	mg/L	0.11
TOC	mg/L	560	Na	mg/L	67.14
Nitrógeno Amoniacal	NH_4^+ mg/L	16	K	mg/L	17.52
Nitritos	$N\text{-}NO_2^-$ mg/L	0.79	Mg	mg/L	12.48
Fosforo total	P mg/L	11.57	Al	mg/L	0.48
Turbiedad	NTU	1323	Ca	mg/L	26.86

4.4.2. Análisis de Fluorescencia de los electrodos de trabajo

Este análisis fue realizado para los electrodos que se usaron en la EC, antes y después del tratamiento con sus mejores condiciones, para conocer que se encuentra en la superficie de los electrodos.

En la Tabla 11 el electrodo de aluminio muestra una superficie irregular, pues presenta predominantemente aglomerados o estructuras granulares intercaladas con las marcas de maquinado (estrías longitudinales a lo largo del electrodo). En el caso de los electrodos de Cu y Zn, la superficie presenta estrías longitudinales de manera homogénea a lo largo de todo el electrodo, siendo más definidas y profundas en el electrodo de Zn.

Una vez realizado el proceso de electrocoagulación, tanto el ánodo como cátodo de Al y Zn, se observa la presencia de depósitos de lodo (incremento considerable de fluorescencia) en la superficie de estos:

- Para el Al, el ánodo presenta rastros de degradación debido a la perdida de los aglomerados y/o estructuras granulares que presentaba inicialmente, observándose de forma más definida las estrías de maquinado, propias de la fabricación de los electrodos. Por el contrario, en el caso del cátodo, se forma una capa más gruesa en la superficie de electrodo. Esto se observa, ya que se rellenan por completo los surcos de las estrías del cátodo y además se presentan dos tipos de texturas, distribuidas de forma aleatoria y alternada. Una textura suave y algodonosa que recubre la mayor parte del electrodo, la cual se intercala en menor proporción con una textura organizada de forma semicircular con aspecto rugoso y áspero la cual cuenta con una señal de fluorescencia de mayor intensidad.

- Para el Zn, el ánodo donde se observa una mayor cantidad de depósitos de lodo en la superficie. Estos depósitos se organizan como puntos de nucleación, los cuales presentan una mayor intensidad de emisión de fluorescencia, distribuidos de manera homogénea a lo largo del electrodo y aparentemente tienen preferencia por acumularse en las regiones profundas de las estrías, ya que estas siguen siendo claramente visibles. En el cátodo

también se observa el depósito de los lodos recubriendo por completo el electrodo con presencia de aglomerados con una distribución heterogénea y en mucha menor proporción que en el ánodo correspondiente.

- En el caso del Cu, se observa la presencia de un recubrimiento en la superficie de los electrodos, mostrándose en mayor cantidad en el cátodo que en el ánodo, sin embargo, la fluorescencia de estas capas distan por completo de las características de florescencia presentes en los electrodos de Al y Zn, lo cual sugiere que el depósito tiene una composición diferente a los otros electrodos pues presenta señales de fluorescencia específica en longitudes correspondientes a 425 nm y 590 nm (azul y rojo respectivamente), estas señales se emiten de estructuras pequeñas, posiblemente trazas de metales y/o estructuras semi-cristalinas. Otra característica del depósito es que no se está incorporando el material que compone principalmente a los lodos ya que la fluorescencia en la longitud de 515 nm (verde) característica de estos (Tabla 12) es prácticamente nula.

Respecto a los lodos, en la Tabla 12, se muestra una comparativa en campo claro, por microscopía de fluorescencia y por microscopía confocal, a los mismos aumentos. Aquí se observa que los lodos con electrodos de Al y Zn poseen mayor índice de fluorescencia, que los obtenidos con electrodos de Cu.

Los lodos de Al y Zn están organizados en su mayoría por estructuras granulares de tamaño homogéneo, mientras que los obtenidos con Cu tienen forma de hojuelas de tamaño variable, ya que presentan bordes irregulares, son planas y de mayor superficie.

En el caso de la muestra de lodos de Cu, se presenta un mayor número de fibras y sobre todo gránulos o estructuras semi-cristalinas, con una marcada emisión de fluorescencia distinta a la verde.

Con las imágenes de confocal de los mismos lodos (es en las mismas zonas que las imágenes tomadas para fluorescencia y campo claro) se confirma la baja señal de fluorescencia de los lodos obtenidos con los electrodos de Cu.

Tabla 11. Superficie de los Electrodos por microscopía de Fluorescencia con longitudes de onda de 405, 488, 532 y 635 nm.

Muestra	Blanco		Ánodo	Cátodo
			Experimental	Experimental
Al	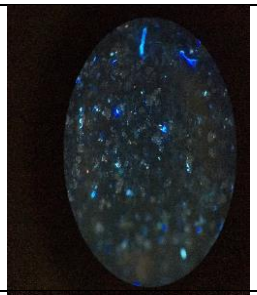	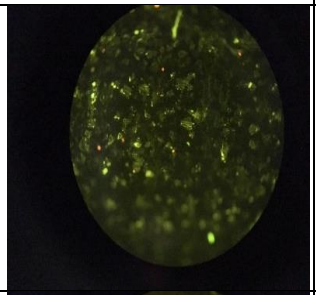	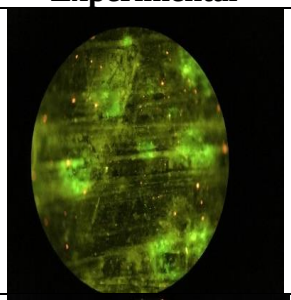	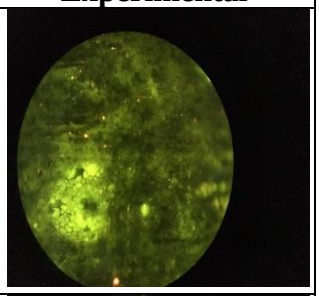
Cu		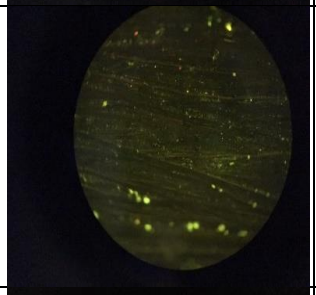	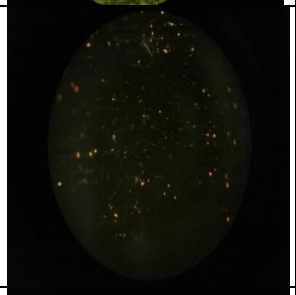	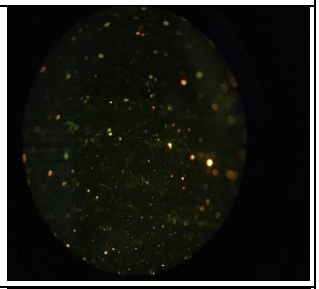
Zn		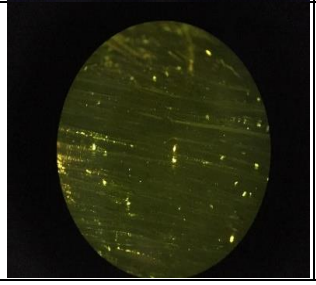	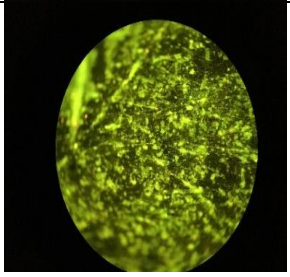	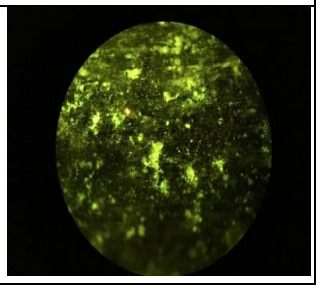

Tabla 12. Micrografías por microscopía de Fluorescencia de muestras de Lodos con longitudes de onda de 405, 488, 532 y 635 nm.

Muestra	Campo Claro	Fluorescencia	Confocal
Al 10X	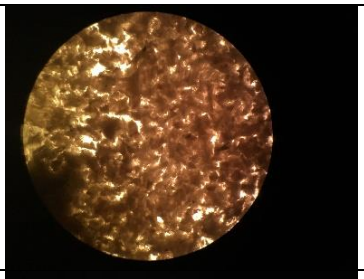	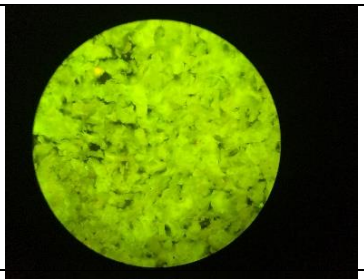	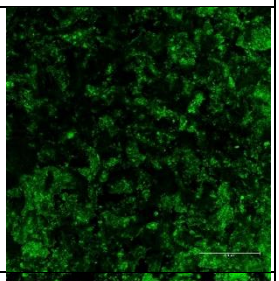
Al 40X	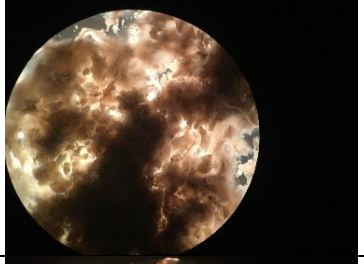	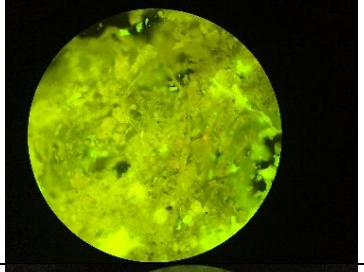	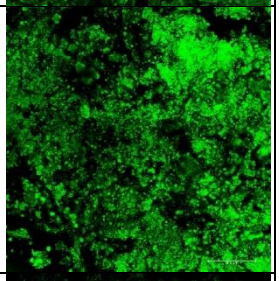
Cu 10X	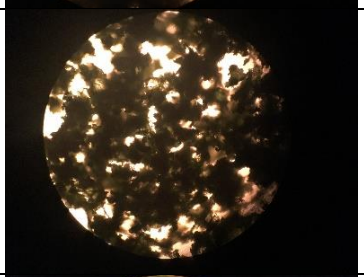	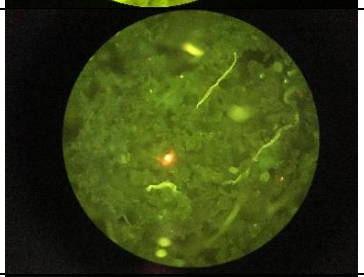	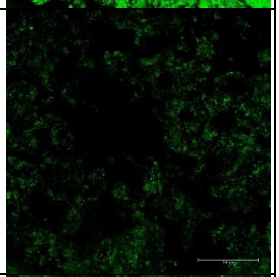
Cu 40X		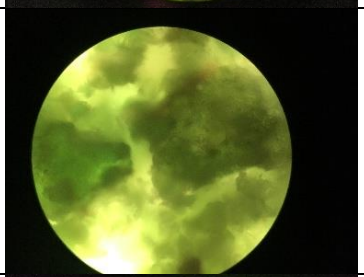	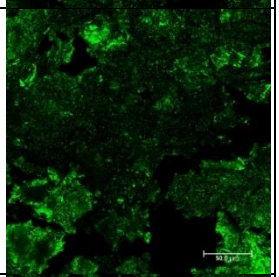
Zn 10X	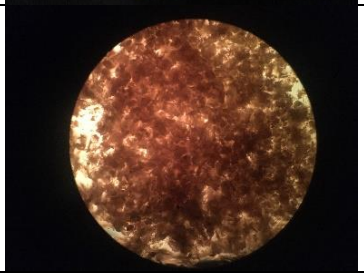	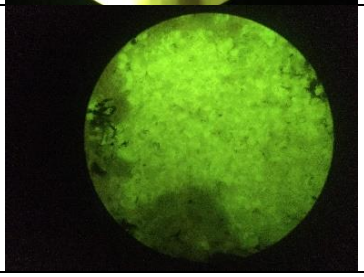	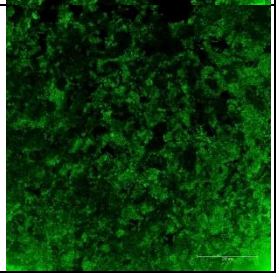

Zn 40X		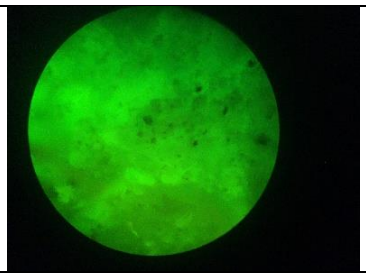	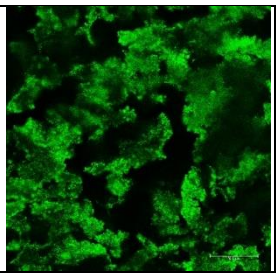

Los lodos resultantes de la electrocoagulación con electrodos de Al y de Zn genera una mayor fluorescencia, lo que podría ser resultado de una mayor precipitación de elementos orgánicos (desechos orgánicos, bacterianos entre otros), considerando que son producto de aguas residuales y que usualmente presentan índices altos de autofluorescencia. En el caso del proceso realizado con el cobre, la precipitación de estos elementos es mucho menor, debido a la baja presencia de fluorescencia verde, característica del lodo correspondiente, sin embargo, se observa que incorpora otros materiales, probablemente semi-cristalinos (por la señal intensa y definida), ya que estos emiten en longitudes diferentes a 515 nm (verde) y la señal es muy puntual.

Los electrodos de Al y Zn presentan una mayor captación de lodos en su superficie, a diferencia del Cu donde se observa que tanto el ánodo como el cátodo presentan un recubrimiento homogéneo con una fluorescencia en verde notablemente inferior.

En los electrodos de Al, se observa un importante desgaste del electrodo y también pequeños depósitos de lodo a lo largo del mismo, y en el cátodo se observa la generación de un recubrimiento homogéneo y grueso formado por los lodos resultantes. Se menciona que la capa es gruesa, debido a que dejan de observarse las estrías de pulido mecánico del electrodo, por lo que se asume que tanto las regiones profundas de las estrías como los valles, han sido recubiertos en su totalidad, incluso generando puntos de alta densidad de material que destacan por el incremento de la fluorescencia y que le dan un aspecto áspero o craquelado.

En los electrodos de Zn, se observa que, contrario a lo que se espera de un proceso electroquímico, el ánodo, además de presentar señales de incremento de corrosión, también cuenta con depósitos más densos de lodo distribuidos en el electrodo homogéneamente, mientras que en el cátodo la capa es fina, ya que pueden observarse las estrías naturales del electrodo.

4.4.3. Efecto del electrolito soporte en la EC: Sulfato de Sodio y Cloruro de Sodio

La *CE* de la muestra es muy pequeña (785.8 µS/cm) para introducirle corrientes altas a los electrodos por eso se le suministró sulfato y cloruro de sodio 1M para subir la *CE* hasta 1680 µS/cm, a esta *CE* se puedo llevar cabo la EC con corrientes altas. Se realizó la EC con los tres diferentes materiales de electrodos con una corriente de 1A. En al Figuras 11-13 se realizó una comparación con respecto al Sulfato de Sodio y Cloruro de Sodio.

Cuando se realizaron los tratamientos con esas características no existió ninguna diferencia con los electrodos de Al y Cu para los diferentes medios electrolíticos (Figura 11-12).

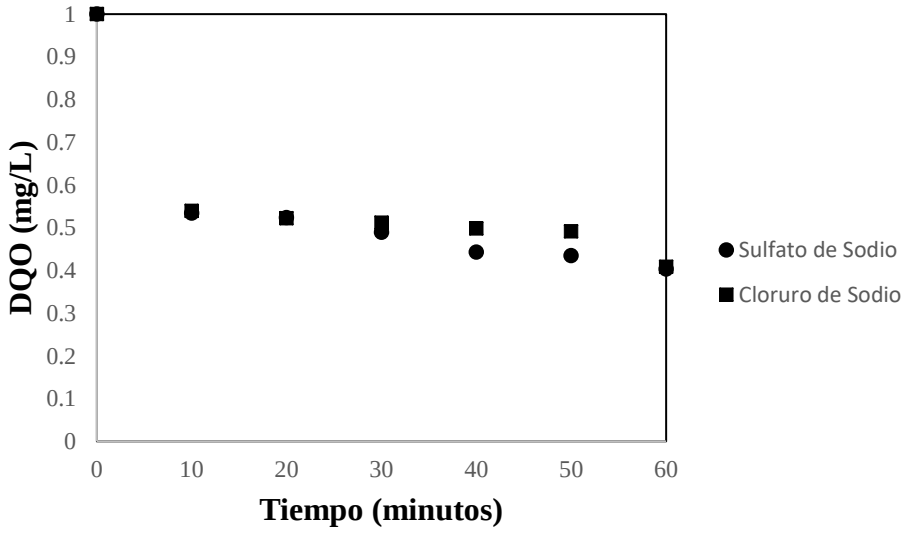

Figura 11. EC con electrodos de Cu implementando un 1A con diferente medio conductor

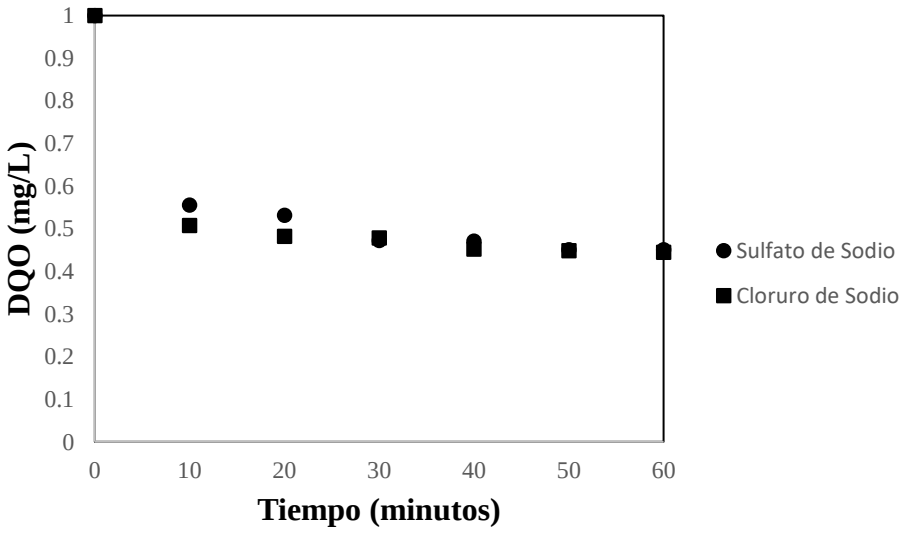

Figura 12. EC con electrodos de Al implementando un 1A con diferente medio conductor

Con respecto a los electrodos de zinc (figura 13), se ve una diferencia significativa entre usar sulfato sodio y cloruro Sodio.

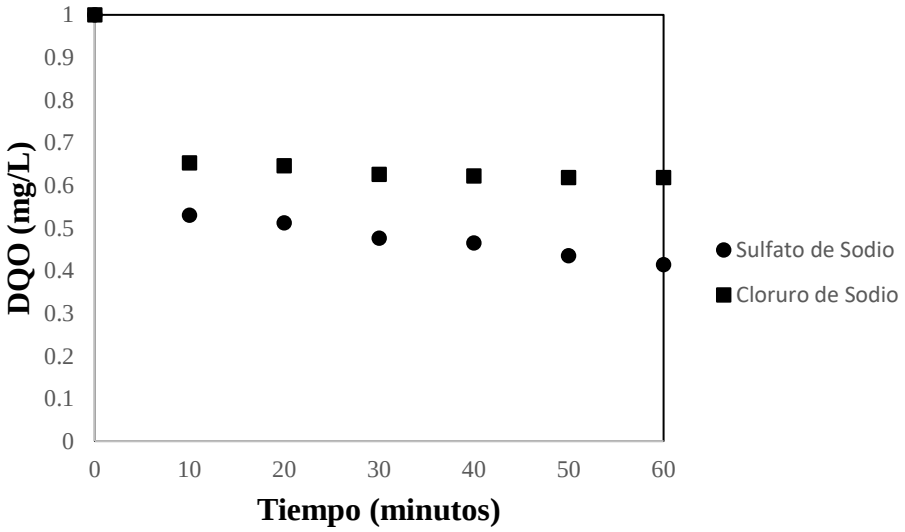

Figura 13. EC con electrodos de Zn implementando un 1A con diferente medio conductor

4.4.4. Electrocoagulación en continúo

El tratamiento se realizó en continúo durante 10 minutos, a un Q_L igual 0.06 L/s, 6 L y 3.16 A, debido a que fueron las mejores condiciones en el tratamiento en batch con recirculación.

Donde todos los parámetros analizados (tabla 13) tiene una remoción por que la materia orgánica e inorgánica de esta removiendo por el coagulante que se forma en este proceso.

El único parámetro analizado que no disminuyó fue la concentración de Al en la solución por esa razón se aumentó el pH a 9 para promover su precipitación. La remoción de la DQO fue únicamente del 25% mediante el sistema en flujo continúo.

Tabla 13. Caracterización antes del tratamiento y después del tratamiento en continúo

Parámetros	**Unidades**	**Antes EC**	**Después de la EC en Continúo**	**% remoción**
pH	-	6.4	7.1	-
Turbidez	NTU	512.4	90	82.4
Color	Pt-Co	1560	1030	34.0
Coliformes Totales	MPN/100mL	$1.7x10^6$	700	-
Colifomes Fecales	MPN/100mL	$1.4x10^6$	<200	-
DQO	mg/L	1732	1299	25
DBO_5	mg/L	1399.8	330.9	76.4
CE	µS/cm	1680	1600	4.8
Sulfatos	SO_4^{2-}mg/L	711.4	683.8	3.9
Nitritos	$N\text{-}NO_2^-$ mg/L	0.9	0.5	47.2
Nitratos	$N\text{-}NO_3^-$ mg/L	1.4	1.2	14.3
Nitrógeno Amonical	$N\text{-}NH_3$ mg/L	10	2	80
Fosfato	PO_4^{3-} mg/L	26.9	19.5	27.5
Fluoruro	F^- mg/L	0.3	0.1	66.7
Choruros	Cl^- mg/L	169.7	141.4	16.6

Fe	mg/L	1.4	0.7	50
Cu	mg/L	0.6	0.6	0
Na	mg/L	251.2	210.6	16.2
K	mg/L	10.4	10.2	1.9
Mg	mg/L	14.7	11.6	21.1
Al	mg/L	1.6	23.7 a pH 9 (1.13)	-
Ca	mg/L	30.3	25.0	17.5

CONCLUSIONES

Una muestra de aguas residuales industriales de la industria del chocolate se caracterizó de acuerdo con las normas mexicanas. Se identificaron altos contenidos de nitrógeno y fósforo, esto podría causar eutrofización si tales aguas residuales se vierten sin un tratamiento previo. Se propuso un sistema de electrocoagulación solar fotovoltaica para su tratamiento, utilizando Al, Cu y Zn como materiales anódicos. Se estudió el efecto del pH (4.38 y 7), la densidad de corriente (1.781 mA / cm^2 y 0.356 mA / cm^2) a los 60 minutos de tratamiento. El sistema de aluminio exhibió los mejores resultados para parámetros orgánicos. La eliminación de DQO máxima alcanzada fue del 50% y la DBO_5 se redujo un 39%. El IB se incrementó considerablemente de 0.49 a 0.59. El COT se redujo solo 26.65%. El sistema de cobre también mostró un comportamiento prometedor en la eliminación de compuestos orgánicos: 43% de DQO, 53% de DBO_5, 30.7% de COT y el IB fue de 0.4. Se descubrió que el sistema de zinc es ligeramente menos eficiente que los sistemas de Cu y Al. La eliminación lograda fue 39% DQO, 30% DBO_5, 19% COT. El IB muestra un aumento de 0.49 a 0.56, mejorando la biodegradabilidad de las aguas residuales. El color y la turbidez presentaron una reducción de 89.5% y 73.86%, respectivamente. El consumo de energía de los tres tratamientos es bajo, si se utilizara la red eléctrica. En este caso, el costo real con respecto al consumo de electricidad es nulo porque se utilizó energía solar.

Teniendo en cuenta que se obtiene una mayor remoción con los electrodos de Al, se realizó el tratamiento de la misma muestra con un volumen de 6L, en un reactor electroquímico mediante una columna de flujo descendente con recirculación. La electricidad con la que se energizaron los electrodos provenía de paneles solares. Se concluyó que las variables que tienen el mayor impacto en la DQO y la eliminación del color son la corriente eléctrica y el caudal volumétrico del líquido. El primero debido a la dosis de aluminio, mientras que el segundo determina el tiempo de contacto de los electrodos y la efectividad del contacto entre las especies de Al generadas y los contaminantes. La materia inorgánica y orgánica se eliminó mediante el coagulante producido, y simultáneamente se produjo y acumuló hidrógeno en la parte superior de la columna. En las condiciones estudiadas y después de un tiempo de tratamiento de 30 minutos, la eliminación de DQO fue del 63% y 96.9% del color, cuando el caudal volumétrico de recirculación (QL) fue de 0.06 L/s, la corriente eléctrica fue de 3.16 A a pH 6.4. El costo de este tratamiento se analizó tomando en cuenta la energía consumida (la bomba y el electrodo), el lodo generado y el desgaste

de los electrodos dio un consumo de 4.01 USD/m^3. El efluente tratado cumple con el estándar mexicano NOM-02-SEMARNAT-1996. Los datos resultantes se ajustaron a un modelo Behnajady-Modirshahla-Ghanbery (BMG).

Con el trabajo realizado en la estancia, se concluye lo siguiente, que los electrodos de DDB soportados en sustrato de silicio expusieron la mayor resistencia óhmica y en consecuencia, el mayor consumo de energía para un tratamiento de electrooxidación alimentado por un sistema de almacenamiento de energía que se usó como fuente de alimentación. Los resultados sugirieron que los electrodos DDB soportados en sustratos de Ta y Nb mostraron una tasa de eliminación más rápida con respecto al electrolizador Si-DDB. Después de 12 h de tratamiento, el electrolizador Ta-DDB alcanzó la mayor remoción (88.56%). Sin embargo, el electrolizador equipado con electrodos Nb-DDB expuso la mayor mineralización de COT y la menor generación de especies intermedias. Con respecto al uso de energía, se eliminaron alrededor de 1.98 mg de pesticida/Wh en los electrolizadores equipados con ánodos soportados en Nb y Si, mientras que 2.14 mg se eliminaron usando electrodos Ta-DDB. Sin embargo, se debe hacer un menor consumo de energía para generar un mmol de oxidante usando electrodos Si-DDB (14.34 Wh/mmol). En términos de resistencia de los oxidantes, se deben generar casi 30 mmol de oxidante para eliminar un gramo de pesticida utilizando silicio como soporte de los electrodos DDB.

Por el contrario, los electrodos Ta-DDB deben generar un 35% más de oxidante para eliminar la misma cantidad de plaguicida.

PRODUCTIVIDAD ACADÉMICA

En la tabla 14 se muestran los congresos, coloquios, curso y estancia de investigación que se realizaron en el periodo del doctorado

Tabla 14. Productividad académica

	Fecha
Congreso	
XXIII Congreso de la sociedad Iberoamericana de Electroquímica- SIBAE Nombre del trabajo presentado: Análisis comparativo de cobre contra aluminio, como ánodo y cátodo para el tratamiento de electrocoagulación hacia la industria chocolatera	3 al 8 de junio 2018
XXXIV Congreso Nacional de la Sociedad Mexicana de Electroquímica y el 12th Meeting of the Mexican Selectión of Electrochemical Society Nombre del trabajo presentado: Electrocoagulación en un reactor batch con recirculación para aguas residuales de una industria chocolatera	2 al 6 de junio 2019
Coloquios	
1er Coloquio de Investigación en Ingeniería y el 10º Curso-Taller "Temas Actuales en Ciencias del Agua". Nombre del trabajo presentado: Energía fotovoltaica como fuente alternativa de suministro para sistemas de electrocoagulación	24 al 26 de octubre del 2018
Cursos	
Electrosíntesis orgánica, una herramienta ecológicamente compatible de la Química Orgánica	8 al 12 de octubre del 2018
Taller de Microscopía Confocal: Fundamentos y aplicaciones.	20 al 23 de noviembre del 2018
Espectrometría de Masas: Fundamentos e Interpretación.	9 al 30 de octubre del 2018
Espectroscopía de infrarrojo: fundamentos e interpretación	24 al 28 de septiembre del 2018
Análisis de Datos por Statgraphics Centurion	21 al 25 de enero de 2019

Capítulo de libro

Tópicos en Ciencias Ambientales 2020 Nombre del capítulo: Oxidación de fenolftaleína por un sistema electroquímico acoplado con ozono	Aceptado el 21 de enero del 2020

Estancia de investigación

Lugar: Laboratorio de Ingeniería Electroquímica y Medioambiental, Universidad de Castilla-La Mancha, Cuidad Real, España. Investigador: Dr. Manuel Andrés Rodrigo Rodrigo Proyecto: "Tratamiento electroquímico de aguas contaminadas con compuestos organoclorados"	1 de septiembre del 2019 al 31 de enero del 2020

FINANCIAMIENTO

Este proyecto se financio por la Universidad Autónoma del Estado de México con el apoyo a los proyectos 4986 / 2020CIB y 4967/2020 CIB.

Agradecemos el apoyo financiero brindado por el CONACYT beca alimenticia con el CVU 626446 y por el apoyo de movilidad a España.

LITERATURA

ACNUR, U. (2019) *Escasez de agua en el mundo: causas y consecuencias*. Available at: https://eacnur.org/blog/escasez-agua-en-el-mundo-tc_alt45664n_o_pstn_o_pst/.

AlJaberi, F. Y. (2019) 'Operating cost analysis of a concentric aluminum tubes electrodes electrocoagulation reactor', *Heliyon*. Elsevier Ltd, 5(8), p. e02307. doi: 10.1016/j.heliyon.2019.e02307.

Ameta, S. C. (2018) 'Introduction', *Advanced Oxidation Processes for Wastewater Treatment: Emerging Green Chemical Technology*, pp. 1–12. doi: 10.1016/B978-0-12-810499-6.00001-2.

APHA/AWWA/WEF (2012) *Standard Methods for the Examination of Water and Wastewater. Stand Methods 541*.

Babu, D. S. *et al.* (2019) 'Detoxification of water and wastewater by advanced oxidation processes', *Science of the Total Environment*. Elsevier B.V., 696, p. 133961. doi: 10.1016/j.scitotenv.2019.133961.

Bani, K. and Smith, E. (2012) 'Grey water treatment by a continuous process of an electrocoagulation unit and a submerged membrane bioreactor system', *Chemical Engineering Journal*. Elsevier B.V., 198–199, pp. 201–210. doi: 10.1016/j.cej.2012.05.065.

Barrera, C. E., Balderas, P. and Bilyeu, B. (2018) 'Electrocoagulation: Fundamentals and prospectives', *Electrochemical Water and Wastewater Treatment*, pp. 61–76. doi: 10.1016/B978-0-12-813160-2.00003-1.

Brillas, E. (2020) 'A review on the photoelectro-Fenton process as efficient electrochemical advanced oxidation for wastewater remediation. Treatment with UV light, sunlight, and coupling with conventional and other photo-assisted advanced technologies', *Chemosphere*. Elsevier Ltd,

250, p. 126198. doi: 10.1016/j.chemosphere.2020.126198.
Cai, Q. Q. *et al.* (2020) 'Potential of combined advanced oxidation – Biological process for cost-effective organic matters removal in reverse osmosis concentrate produced from industrial wastewater reclamation: Screening of AOP pre-treatment technologies', *Chemical Engineering Journal*, 389. doi: 10.1016/j.cej.2019.123419.
Chen, B. Y., Wu, L. and Hong, J. (2020) 'Kinetics of bisphenol a degradation by advanced oxidation processes: Asymptotic approximation of singular perturbation', *Journal of the Taiwan Institute of Chemical Engineers*. Elsevier B.V., 0, pp. 1–7. doi: 10.1016/j.jtice.2020.02.004.
Chen, W. J., Su, W. T. and Hsu, H. Y. (2012) 'Continuous flow electrocoagulation for MSG wastewater treatment using polymer coagulants via mixture-process design and response-surface methods', *Journal of the Taiwan Institute of Chemical Engineers*. Taiwan Institute of Chemical Engineers, 43(2), pp. 246–255. doi: 10.1016/j.jtice.2011.10.003.
Conagua (2018a) 'Calidad del agua en México'. Available at: https://www.gob.mx/conagua/es/articulos/calidad-del-agua?idiom=es.
Conagua (2018b) *Si no puedes reusarlo, rehúsalo*. Available at: https://www.gob.mx/conagua/es/articulos/si-no-puedes-reusarlo-rehusalo?idiom=es.
Contigiani, C. C., González, O. and Bisang, J. M. (2018) 'Local mass-transfer study in a decaying swirling flow electrochemical reactor under single-phase and two-phase (gas-liquid) flow', *Chemical Engineering Journal*. Elsevier, 350(May), pp. 233–239. doi: 10.1016/j.cej.2018.05.181.
Cornejo, O. M. *et al.* (2020) 'Characterization of the reaction environment in flow reactors fitted with BDD electrodes for use in electrochemical advanced oxidation processes: A critical review', *Electrochimica Acta*, 331. doi: 10.1016/j.electacta.2019.135373.
Dermentzis, K. *et al.* (2015) 'Photovoltaic electrocoagulation process for remediation of chromium plating wastewaters', *Desalination and Water Treatment*, 56(5), pp. 1413–1418. doi: 10.1080/19443994.2014.950992.
Dermentzis, K. *et al.* (2016) 'Removal of copper and COD from electroplating effluents by photovoltaic electrocoagulation / electrooxidation process', 2, pp. 55–62.
Dia, O. *et al.* (2017) 'Electrocoagulation of bio-filtrated landfill leachate: Fractionation of organic matter and influence of anode materials', *Chemosphere*, 168, pp. 1136–1141. doi: 10.1016/j.chemosphere.2016.10.092.

Dura, A. and Breslin, C. B. (2019) 'The removal of phosphates using electrocoagulation with Al−Mg anodes', *Journal of Electroanalytical Chemistry*. Elsevier, 846(May), p. 113161. doi: 10.1016/j.jelechem.2019.05.043.

Elnakar, H. and Buchanan, I. (2020) 'Soluble chemical oxygen demand removal from bypass wastewater using iron electrocoagulation', *Science of the Total Environment*. Elsevier B.V, 706, p. 136076. doi: 10.1016/j.scitotenv.2019.136076.

Elnenay, A. M. H. *et al.* (2017) 'Treatment of drilling fluids wastewater by electrocoagulation', *Egyptian Journal of Petroleum*. Egyptian Petroleum Research Institute, 26(1), pp. 203–208. doi: 10.1016/j.ejpe.2016.03.005.

Esparza-Soto, M. *et al.* (2019) 'Anaerobic treatment of chocolate-processing industry wastewater at different organic loading rates and temperatures', *Water Science and Technology*, 79(12), pp. 2251–2259. doi: 10.2166/wst.2019.225.

EXCELSIOR (2020) *Los municipios y la crisis del agua; persiste desigualdad*. Available at: https://www.excelsior.com.mx/nacional/los-municipios-y-la-crisis-del-agua-persiste-desigualdad/1368849.

Fayad, N. *et al.* (2017) 'Preliminary purification of volatile fatty acids in a digestate from acidogenic fermentation by electrocoagulation', *Separation and Purification Technology*, 184, pp. 220–230. doi: 10.1016/j.seppur.2017.04.041.

FOA, O. de las N. U. para la A. y la A. (2019) *Escasez de agua: Uno de los mayores retos de nuestro tiempo*. Available at: http://www.fao.org/fao-stories/article/es/c/1185408/.

Francis, F. P. and Ramalingam, C. (2019) 'Hybrid hydrogel dispersed low fat and heat resistant chocolate', *Journal of Food Engineering*. Elsevier Ltd. doi: 10.1016/j.jfoodeng.2019.03.012.

García-García, A. *et al.* (2015) 'Industrial wastewater treatment by electrocoagulation-electrooxidation processes powered by solar cells', *Fuel*, 149(October), pp. 46–54. doi: 10.1016/j.fuel.2014.09.080.

Gautam, P., Kumar, S. and Lokhandwala, S. (2019) 'Advanced oxidation processes for treatment of leachate from hazardous waste landfill: A critical review', *Journal of Cleaner Production*. Elsevier Ltd, 237, p. 117639. doi: 10.1016/j.jclepro.2019.117639.

Gerba, C. P. and Pepper, I. L. (2019) *Municipal Wastewater Treatment*. 3rd edn, *Environmental Microbiology: Third Edition*. 3rd edn. Elsevier Inc. doi: https://doi.org/10.1016/B978-0-12-814719-1.00022-7.

González, T., Dominguez, J. R. and Correia, S. (2020) 'Neonicotinoids removal by associated binary, tertiary and quaternary advanced oxidation processes: Synergistic effects, kinetics and mineralization', *Journal of Environmental Management*, 261(January). doi: 10.1016/j.jenvman.2020.110156.

Hama Aziz, K. H. (2019) 'Application of different advanced oxidation processes for the removal of chloroacetic acids using a planar falling film reactor', *Chemosphere*. Elsevier Ltd, 228, pp. 377–383. doi: 10.1016/j.chemosphere.2019.04.160.

Hu, C. *et al.* (2017) 'Enhanced efficiency in HA removal by electrocoagulation through optimizing flocs properties: Role of current density and pH', *Separation and Purification Technology*, 175, pp. 248–254. doi: 10.1016/j.seppur.2016.11.036.

Hussin, F. *et al.* (2017) 'Removal of lead by solar-photovoltaic electrocoagulation using novel perforated zinc electrode', *Journal of Cleaner Production*. Elsevier Ltd, 147, pp. 206–216. doi: 10.1016/j.jclepro.2017.01.096.

Iluz, D. and Abu-Ghosh, S. (2016) 'A novel photobioreactor creating fluctuating light from solar energy for a higher light-to-biomass conversion efficiency', *Energy Conversion and Management*. Elsevier Ltd, 126, pp. 767–773. doi: 10.1016/j.enconman.2016.08.045.

INEGI, I. N. de E. y G. (2015) *Agua*. Available at: https://www.inegi.org.mx/temas/agua/.

Jin, Y. *et al.* (2017) 'Calorie reduction of chocolate ganache through substitution of whipped cream', *Journal of Ethnic Foods*. Elsevier Ltd, 4(1), pp. 51–57. doi: 10.1016/j.jef.2017.02.002.

Kannan, N. and Vakeesan, D. (2016) 'Solar energy for future world: - A review', *Renewable and Sustainable Energy Reviews*, 62, pp. 1092–1105. doi: 10.1016/j.rser.2016.05.022.

Khemila, B. *et al.* (2018) 'Removal of a textile dye using photovoltaic electrocoagulation', *Sustainable Chemistry and Pharmacy*. Elsevier, 7(November 2017), pp. 27–35. doi: 10.1016/j.scp.2017.11.004.

Khuntia, H. K., Janardhana, N. and Chanakya, H. N. (2020) 'Fractionation of FOG (fat, oil, grease), wastewater and particulate solids based on low-temperature solidification and stirring', *Journal of Water Process Engineering*. Elsevier, 34(July 2019), p. 101167. doi: 10.1016/j.jwpe.2020.101167.

Kim, M., Nakhla, G. and Keleman, M. (2019) 'Modeling the impact of food wastes on wastewater treatment plants', *Journal of Environmental Management*. Elsevier, 237(February), pp. 344–358. doi: 10.1016/j.jenvman.2019.02.065.

Kim, Y. J. *et al.* (2017) 'Calorie reduction of chocolate ganache through substitution of whipped cream', *Journal of Ethnic Foods*. Elsevier B.V. doi: 10.1016/j.jef.2017.02.002.

Kindlein, M., Elts, E. and Briesen, H. (2018) 'Phospholipids in chocolate: Structural insights and mechanistic explanations of rheological behavior by coarse-grained molecular dynamics simulations', *Journal of Food Engineering*. Elsevier Ltd. doi: 10.1016/j.jfoodeng.2018.02.014.

Kiumarsi, M. *et al.* (2020) 'Comparative study of instrumental properties and sensory profiling of low-calorie chocolate containing hydrophobically modified inulin. Part 1: Rheological, thermal, structural and external preference mapping', *Food Hydrocolloids*. Elsevier Ltd, 104, p. 105698. doi: 10.1016/j.foodhyd.2020.105698.

Konstantas, A. *et al.* (2018) 'Environmental impacts of chocolate production and consumption in the UK', *Food Research International*. Elsevier Ltd, 106(2017), pp. 1012–1025. doi: 10.1016/j.foodres.2018.02.042.

Kruszewski, B. and Obiedziński, M. W. (2018) 'Multivariate analysis of essential elements in raw cocoa and processed chocolate mass materials from three different manufacturers', *LWT - Food Science and Technology*. Elsevier Ltd. doi: 10.1016/j.lwt.2018.08.030.

Kumar, N. S. and Goel, S. (2010) 'Factors influencing arsenic and nitrate removal from drinking water in a continuous flow electrocoagulation (EC) process', *Journal of Hazardous Materials*, 173(1–3), pp. 528–533. doi: 10.1016/j.jhazmat.2009.08.117.

Kyzas, G. Z. and Matis, K. A. (2016) 'Electroflotation process: A review', *Journal of Molecular Liquids*, 220, pp. 657–664. doi: 10.1016/j.molliq.2016.04.128.

Li, J. *et al.* (2019) 'The electrochemical advanced oxidation processes coupling of oxidants for organic pollutants degradation: A mini-review', *Chinese Chemical Letters*. Chinese Chemical Society, 30(12), pp. 2139–2146. doi: 10.1016/j.cclet.2019.04.057.

Liu, S. X. (2014) *Food and agricultural wastewater utilization and treatment*. Second Edi.

Ma, P. *et al.* (2018) 'Electrochemical treatment of real wastewater. Part 1: Effluents with low conductivity', *Chemical Engineering Journal*, 336, pp. 133–140. doi: 10.1016/j.cej.2017.11.046.

Ma, S. *et al.* (2020) 'Plasma-assisted advanced oxidation process by a multi-hole dielectric barrier discharge in water and its application to wastewater treatment', *Chemosphere*. Elsevier Ltd, 243, p. 125377. doi: 10.1016/j.chemosphere.2019.125377.

Magalhães, I. *et al.* (2018) 'Volatile compounds and protein profiles analyses of fermented cocoa beans and chocolates from different hybrids cultivated in Brazil', *Food Research International*.

Elsevier Ltd, (2017). doi: 10.1016/j.foodres.2018.04.012.

Mareddy, A. R. (2017) *Technology in EIA, Environmental Impact Assessment*. doi: 10.1016/b978-0-12-811139-0.00012-8.

Mazivila, S. J. *et al.* (2019) 'A review on advanced oxidation processes: From classical to new perspectives coupled to two- and multi-way calibration strategies to monitor degradation of contaminants in environmental samples', *Trends in Environmental Analytical Chemistry*, 24, pp. 1–10. doi: 10.1016/j.teac.2019.e00072.

Michel, B., Mazet, N. and Neveu, P. (2016) 'Experimental investigation of an open thermochemical process operating with a hydrate salt for thermal storage of solar energy: Local reactive bed evolution', *Applied Energy*. Elsevier Ltd, 180, pp. 234–244. doi: 10.1016/j.apenergy.2016.07.108.

Millán, M. *et al.* (2018) 'Towards the sustainable powering of the electrocoagulation of wastewater through the use of solar-vanadium redox flow battery: A first approach', *Electrochimica Acta*. Elsevier Ltd, 270, pp. 14–21. doi: 10.1016/j.electacta.2018.03.055.

Mohamed, D. K. B. *et al.* (2016) 'Reaction screening in continuous flow reactors', *Tetrahedron Letters*, 57(36), pp. 3965–3977. doi: 10.1016/j.tetlet.2016.07.072.

Mores, R. *et al.* (2016) 'Remove of phosphorous and turbidity of swine wastewater using electrocoagulation under continuous flow', *Separation and Purification Technology*, 171, pp. 112–117. doi: 10.1016/j.seppur.2016.07.016.

Moussa, D. T. *et al.* (2017) 'A comprehensive review of electrocoagulation for water treatment: Potentials and challenges', *Journal of Environmental Management*. Elsevier Ltd, 186, pp. 24–41. doi: 10.1016/j.jenvman.2016.10.032.

Muralikrishna, I. V. and Manickam, V. (2017) *Wastewater treatment technologies*, *Pollution Engineering*. doi: https://doi.org/10.1016/B978-0-12-811989-1.00012-9.

Naje, A. S. *et al.* (2016) 'Electrocoagulation by solar energy feed for textile wastewater treatment including mechanism and hydrogen production using a novel reactor design with a rotating anode', *RSC Adv.* Royal Society of Chemistry, 6(12), pp. 10192–10204. doi: 10.1039/C5RA26032A.

OMS, O. M. d ela salud (2019) *Agua*. Available at: https://www.who.int/es/news-room/fact-sheets/detail/drinking-water.

Omwene, P. I., Kobya, M. and Can, O. T. (2018) 'Phosphorus removal from domestic

wastewater in electrocoagulation reactor using aluminium and iron plate hybrid anodes', *Ecological Engineering*. Elsevier, 123(September), pp. 65–73. doi: 10.1016/j.ecoleng.2018.08.025.

ONU-OMS (2018) *Progresos en Materia de agua potable, saneamiento e higiene, Organización Mundial de la Salud*. Available at: http://apps.who.int/iris/bitstream/handle/10665/260291/9789243512891-spa.pdf?sequence=1.

Oswald, Ú. (2018) *La seguridad del agua en México*.

Ozlu, S. and Dincer, I. (2016) 'Performance assessment of a new solar energy-based multigeneration system', *Energy*. Elsevier Ltd, 112, pp. 164–178. doi: 10.1016/j.energy.2016.06.040.

Patil, S. A. *et al.* (2009) 'Electricity generation using chocolate industry wastewater and its treatment in activated sludge based microbial fuel cell and analysis of developed microbial community in the anode chamber', *Bioresource Technology*. Elsevier Ltd, 100(21), pp. 5132–5139. doi: 10.1016/j.biortech.2009.05.041.

Pavón-silva, T. B. *et al.* (2018) 'Photovoltaic Energy-Assisted Electrocoagulation of a Synthetic Textile Effluent', 2018. Available at: https://doi.org/10.1155/2018/7978901%0AResearch.

Pirsaheb, M., Hossaini, H. and Janjani, H. (2020) 'Reclamation of hospital secondary treatment effluent by sulfate radicals based–advanced oxidation processes (SR-AOPs) for removal of antibiotics', *Microchemical Journal*. Elsevier B.V., 153, p. 104430. doi: 10.1016/j.microc.2019.104430.

Prajapati, A. K. *et al.* (2016) 'Electrocoagulation treatment of rice grain based distillery effluent using copper electrode', *Journal of Water Process Engineering*. Elsevier Ltd, 11, pp. 1–7. doi: 10.1016/j.jwpe.2016.03.008.

Programa de las Naciones Unidas para el Medio Ambiente (2017) *ONU-Estrategia sobre el agua dulce 2017-2021*.

Qasim, S. R. and Zhu, G. (2017) *Wastewater Treatment and Reuse, Theory and design Examples, Taylor and Franis group*. Available at: http://tylorandfranicis.com.

Qi, Z., You, S. and Ren, N. (2017) 'Wireless Electrocoagulation in Water Treatment Based on Bipolar Electrochemistry', *Electrochimica Acta*. Elsevier Ltd, 229, pp. 96–101. doi: 10.1016/j.electacta.2017.01.151.

Radha, K. V. and Sirisha, K. (2018) 'Electrochemical Oxidation Processes', *Advanced Oxidation*

Processes for Wastewater Treatment: Emerging Green Chemical Technology, pp. 359–373. doi: 10.1016/B978-0-12-810499-6.00011-5.

Rahmatmand, A., Harrison, S. J. and Oosthuizen, P. H. (2018) 'An experimental investigation of snow removal from photovoltaic solar panels by electrical heating', *Solar Energy*. Elsevier, 171(July), pp. 811–826. doi: 10.1016/j.solener.2018.07.015.

Ramalho, R. S. (2013) *Introduction to Wastewater Treatment Processes, Introduction to Wastewater Treatment Processes*. doi: 10.1016/0043-1354(85)90110-1.

Ramos Osorio, S. (2010) *Normatividad y Tratamiento de Aguas Residuales SEMARNAT*. Available at: ftp://ftp.conagua.gob.mx/PlayasLimpias/Memorias/Memorias6/Panel 3-Normatividad y Fomento/1. Lic. Sergio Ramos Osorio.pdf (Accessed: 22 March 2015).

Recanati, F., Marveggio, D. and Dotelli, G. (2018) 'From beans to bar: A life cycle assessment towards sustainable chocolate supply chain', *Science of the Total Environment*. Elsevier B.V., 613–614, pp. 1013–1023. doi: 10.1016/j.scitotenv.2017.09.187.

Rosales, M., Coreño, O. and Nava, J. L. (2018) 'Removal of hydrated silica, fluoride and arsenic from groundwater by electrocoagulation using a continuous reactor with a twelve-cell stack', *Chemosphere*. Elsevier Ltd, 211, pp. 149–155. doi: 10.1016/j.chemosphere.2018.07.113.

Safwat, S. M. (2020) 'Treatment of real printing wastewater using electrocoagulation process with titanium and zinc electrodes', *Journal of Water Process Engineering*. Elsevier, 34(January), p. 101137. doi: 10.1016/j.jwpe.2020.101137.

Sandhwar, V. K. and Prasad, B. (2017) 'Terephthalic acid removal from aqueous solution by electrocoagulation and electro-Fenton methods: Process optimization through response surface methodology', *Process Safety and Environmental Protection*. Institution of Chemical Engineers, 107, pp. 269–280. doi: 10.1016/j.psep.2017.02.014.

Santana Martínez, G. (2019) *Tesis de doctoral 'ELECTRO-OXIDACIÓN DE FENOL EN UNA COLUMNA DE BURBUJEO DE FLUJO PARALELO DESCENDENTE'*. Toluca, México.

Santiago, G. O. *et al.* (2018) *Electroflotation, Electrochemical Water and Wastewater Treatment*. doi: 10.1016/B978-0-12-813160-2.00004-3.

SEMARNAT, (La Secretaría de Medio Ambiente y Recursos Naturales) (1996a) *NOM-001-SEMARNAT-1996*. Available at: http://www.ceajalisco.gob.mx/sia/pdf/nom-001-semarnat.pdf (Accessed: 20 May 2016).

SEMARNAT, (La Secretaría de Medio Ambiente y Recursos Naturales) (1996b) *NOM-002-*

SEMARNAT -1996. Available at: http://vatten-corporate-s-a-de-c-v.webnode.mx/news/norma-oficial-mexicana-nom-002-semarnat-1996-que-establece-los-limites-maximos-permisibles-de-contaminantes-en-las-descargas-de-aguas-residuales-a-los-sistemas-de-alcantarillado-urbano-o-municipal/ (Accessed: 20 May 2016).

SEMARNAT, (La Secretaría de Medio Ambiente y Recursos Naturales) (1997) *NOM-003-SEMARNAT -1997*. Available at: http://www.sedema.df.gob.mx/sedema/images/archivos/sedema/leyes-reglamentos/normas/federales/NOM-003-SEMARNAT-1997.pdf (Accessed: 20 May 2016).

Shimadzu (2020) *TOC-L*. Available at: https://www.shimadzu.com/an/toc/lab/toc-l/features.html (Accessed: 2 June 2020).

Skoog, D. A., West, D. M. and Holler, F. J. (2005) *Fundamentos de química analítica*. 8th ed. Thomson.

Sun, D. *et al.* (2020) 'Simultaneous removal of ammonia and phosphate by electro-oxidation and electrocoagulation using RuO2–IrO2/Ti and microscale zero-valent iron composite electrode', *Water Research*. Elsevier Ltd, 169, p. 115239. doi: 10.1016/j.watres.2019.115239.

Tanner, A. *et al.* (2018) 'Electrocoagulation of raw wastewater using aluminum, iron, and magnesium electrodes', *Journal of Hazardous Materials*. Elsevier B.V. doi: 10.1016/j.jhazmat.2018.10.017.

Tejocote-pérez, M. *et al.* (2010) 'Bioresource Technology Treatment of industrial effluents by a continuous system : Electrocoagulation – Activated sludge', 101, pp. 7761–7766. doi: 10.1016/j.biortech.2010.05.027.

Toker, O. S. *et al.* (2018) 'Formulation of Dark Chocolate as a Carrier to Deliver Eicosapentaenoic and Docosahexaenoic acids: Effects on Product Quality', *Food Chemistry*. doi: 10.1016/j.foodchem.2018.02.019.

UNESCO (2018) *UNESCO_2018_Informe mundial Naciones Unidas desarrollo recursos hídricos 2018, Interciencia*. Available at: https://www.ecuadorencifras.gob.ec/documentos/web-inec/Bibliotecas/Libros/AGUA,_SANEAMIENTO_e_HIGIENE.pdf.

Urban, F., Geall, S. and Wang, Y. (2016) 'Solar PV and solar water heaters in China: Different pathways to low carbon energy', *Renewable and Sustainable Energy Reviews*. Elsevier, 64, pp. 531–542. doi: 10.1016/j.rser.2016.06.023.

Valero, D. *et al.* (2008) 'Electrocoagulation of a synthetic textile effluent powered by

photovoltaic energy without batteries: Direct connection behaviour', *Solar Energy Materials and Solar Cells*, 92(3), pp. 291–297. doi: 10.1016/j.solmat.2007.09.006.

Wang, J. and Zhuan, R. (2020) 'Degradation of antibiotics by advanced oxidation processes: An overview', *Science of the Total Environment*. Elsevier B.V., 701, p. 135023. doi: 10.1016/j.scitotenv.2019.135023.

Wayne, R. P. (1991) *Principles and applications of photochemistry*. Oxford Uni.

Xu, Y. *et al.* (2018) 'Global status of recycling waste solar panels : A review', *Waste Management*. Elsevier Ltd. doi: 10.1016/j.wasman.2018.01.036.

Yenneti, K., Day, R. and Golubchikov, O. (2016) 'Geoforum Spatial justice and the land politics of renewables : Dispossessing vulnerable communities through solar energy mega-projects', *Geoforum*. Elsevier Ltd, 76, pp. 90–99. doi: 10.1016/j.geoforum.2016.09.004.

Zhang, S. *et al.* (2013) 'Removal of phosphate from landscape water using an electrocoagulation process powered directly by photovoltaic solar modules', *Solar Energy Materials and Solar Cells*. Elsevier, 117, pp. 73–80. doi: 10.1016/j.solmat.2013.05.027.

Zhang, X. *et al.* (2020) *Journal Pre-proof*. doi: 10.1016/j.chemosphere.2020.126360.